Politechnika Wrocławska

FIELD OF SCIENCE: Exact and Natural Sciences

DISCIPLINE OF SCIENCE: Chemical sciences

DOCTORAL DISSERTATION

Cyanobacterial biomass in biocatalysis and bioaccumulation processes

Sunday Ocholi Samson

Supervisor:
Prof. dr hab. inż. Ewa Żymańczyk-Duda

Assistant supervisor:
Dr. inż. Monika Serafin-Lewańczuk

Keywords: Bioaccumulation; Bioconversion; Circular bioeconomy; Cyanobacteria; Ecotoxicity screening; High value-added compounds; Substrates; Photobiocatalysis.

WROCŁAW 2025

Table of contents

Title page ……. i

Table of contents …….…..... ii

List of abbreviations ……. vii

List of tables …….…… x

List of figures ……...…… xi

Acknowledgements ……...…. xii

Scientific achievements ……...…xiv

Conference presentations ……..… xvii

Patent applications ……..… xix

Grants and awards ……..… xx

Abstract (English)……... xxi

Streszczenie (Polski) ……...……... xxiii

CHAPTER ONE: Introduction

1.1. Background …….…… 1

1.2. Rationale for the study …...…….…… 2

1.3. Research objectives …….…… 2

1.4. Hypotheses …….…… 3

1.5. Significance of the study …….……... 4

1.6. Limitations and future perspective …….…… 5

CHAPTER TWO: Literature Review

2.1. Conceptual basis of biocatalysis and biotransformation **……...……**6

2.2. Classes and modes of operation of biocatalysts …….…….... 9

2.2.1. Purified enzymes …….…… 10

2.2.2. Cell-free lysates (crude extracts) …….……... 11

2.2.3. Whole-cell biological systems in biocatalysis …….……. 11

2.3. Advantages of biocatalysis over chemical catalysis …….…. 17

2.3.1. Selectivity: chemo-, regio-, and stereoselectivity …….……... 17

2.3.2. Mild reaction conditions and functional group tolerance …… 18

2.3.3. Environmental and economic sustainability 18
2.3.4. Process integration and multistep cascade reactions 19
2.3.5. Safety and regulatory advantages 19
2.4. Limitations of biocatalysis and mitigation strategies 21
2.4.1. Narrow substrate scope and enzyme specificity 21
2.4.2. Enzyme instability under industrial conditions 22
2.4.3. Cofactor dependence and regeneration challenges 22
2.4.4. Product inhibition and substrate overload 23
2.4.5. Mass transfer limitations in whole-cell systems 23
2.4.6. Scalability and regulatory constraints 24
2.5. Biocatalytic approaches to isomer synthesis 25
2.5.1. Enzymatic racemization and deracemization 25
2.5.2. Asymmetric isomerization: alkene and ketone systems 27
2.5.3. Epimerization and diastereomer interconversion 27
2.5.4. Enzymatic synthesis of chiral isomers via transaminases and Ketoreductases 28
2.5.5. Photobiocatalytic isomerization and emerging trends 29
2.6. Biocatalytic reduction and hydrolysis reactions 31
2.6.1. Alcohol dehydrogenases (ADHs) and ketoreductases (KREDs) 31
2.6.2. Ene-reductases and the old yellow enzyme (OYE) family 32
2.6.3. Cofactor regeneration in reduction reactions 33
2.6.4. Lipases and esterases 33
2.6.5. Amidases and proteases 34
2.7. Microbial cell factories for biocatalysis 35
2.7.1. Applications of microbial cell factories 36
2.7.2. Challenges in microbial cell factory engineering 37
2.8. Metabolic diversity and biotechnological potential of cyanobacterial metabolites 38
2.9. Rare earth elements (REE) and their bioaccumulation mechanisms in cyanobacteria 40

2.10. Synthetic biology tools, research gaps and prospects ……...43

CHAPTER THREE: Materials and Methods

3.1. Reagents ……45

3.2. Microorganisms ……..... 50

3.3. Analyses ……52

3.3.1. Instrumental analysis ……....52

3.3.1.1. Nuclear Magnetic Resonance (NMR) Spectroscopy …… 52

3.3.1.2. High-Performance Liquid Chromatography (HPLC) ……...…52

3.3.1.3. Gas Chromatography (GC) ……... 53

3.3.1.4. Mass Spectrometry (MS) ……....53

3.3.1.5. Product (DMHPP) purification ……..... 53

3.3.1.6. UV-Visible Spectrophotometry ……..……... 54

3.3.1.7. Inductively Coupled Plasma Mass Spectrometry (ICP-MS) …… 54

3.3.1.8. Optical Microscopy …… 54

3.3.2. Statistical analysis …… 54

3.3.2.1. Quantification of biotransformation efficiency via GC ……..……... 55

3.3.2.2. Evaluation of enantioselectivity via chiral gas chromatography …… 55

3.3.2.3. Conversion degree assessment using ^{31}P NMR spectroscopy ……55

3.3.2.4. Calibration-based quantification of inorganic phosphate using malachite green assay …… 56

3.3.2.5. Quantitative yield determination of DMHPP via internal standardized ^{31}P NMR ……56

3.4. Cyanobacterial media preparation …… 57

3.4.1. Spirulina medium …… 57

3.4.2. BG-11/BG-11$_0$ medium …… 59

3.5. Media modification for *Limnospira* sp.: balancing growth promotion with epoxymethyl dimethylphosphonate stability ……61

3.6. Substrate stability analysis …… 63

3.7. Culturing of cyanobacterial strains ……63

3.8. Biotransformation process …… 63

3.8.1. Product purification and analysis 65
3.8.2. *In-vitro* chemical synthesis of dimethyl (1*E*)-3-hydroxyprop-1-enylphosphonate 66
3.8.3. Malachite Green Phosphate Assay 67
3.8.4. Antimicrobial susceptibility testing using disk and agar well diffusion methods 68
3.8.5. Scaling-up process 70
3.8.6. Product yield 70
3.9. Bioaccumulation process 71
3.9.1. Ecotoxicological screening 72
3.9.2. Dry mass determination 73
3.9.3. Rare earth element quantification by ICP-MS 73

CHAPTER FOUR: Results and Discussion

4.1. Substrate stability and medium composition effects 75
4.1.1. Unsaturated fatty acids stability 75
4.1.2. Phosphonates stability 76
4.2. Bioconversions with cyanobacteria 78
4.2.1 Unsaturated fatty acid bioconversion 79
4.2.2. Vinyl phosphonates bioconversion 82
4.2.3. Bioconversion of 1-phenylethyl acetate 87
4.2.4. Bioconversion of epoxymethyl dimethyl phosphonate 95
4.2.5. DMHPP–membrane interactions as a factor in apparent yield discrepancy 102
4.2.6. Antibacterial plate test 104
4.3. Bioaccumulation 106
4.3.1. Microscopic examination of pre- and post- bioconversion biomass 106
4.3.2. Ecotoxicity assessment 108
4.3.3. Dry mass analysis of bioaccumulated REEs 111
4.3.4. Inductively coupled plasma mass spectrometry (ICP-MS) analysis of bioaccumulated REEs 111

CHAPTER FIVE: Conclusion

5.1. Summary of major findings 116

5.2. Validation of research hypotheses 117

5.3. Scientific and technological implications 118

References 119

List of abbreviations

ABC-type – ATP-Binding Cassette transporter type

ADHs – Alcohol Dehydrogenases

ATCC – American Type Culture Collection

BG-11 – Blue-Green Medium 11

CALB – *Candida antarctica* Lipase B

CCALA – Culture Collection of Autotrophic Organisms

CFU – Colony Forming Units

COSY – Correlation Spectroscopy

CRISPR – Clustered Regularly Interspaced Short Palindromic Repeats

DEVP – Diethyl Vinylphosphonate

DKR – Dynamic Kinetic Resolution

DMF – Dimethylformamide

DMHP – Dimethyl (1*E*)-3-hydroxyprop-1-enylphosphonate

DMSO – Dimethyl Sulfoxide

DMVP – Dimethyl Vinylphosphonate

DNA – Deoxyribonucleic Acid

EDTA – Ethylenediaminetetraacetic Acid

EMDP – Epoxymethyl Dimethyl Phosphonate

EPS – Exopolysaccharide

ERs – Ene-Reductases

ESI – Electrospray Ionization

Eu – Europium

FAD – Flavin Adenine Dinucleotide

$FADH_2$ – Flavin Adenine Dinucleotide (Reduced form)

FDH – Formate Dehydrogenase

FID – Flame Ionization Detector

GC – Gas Chromatography

GDH – Glucose Dehydrogenase

Gd – Gadolinium

GMP – Good Manufacturing Practice

HMBC – Heteronuclear Multiple Bond Correlation

HMQC – Heteronuclear Multiple Quantum Coherence

HPLC – High-Performance Liquid Chromatography

HRMS – High-Resolution Mass Spectrometry

ICP-MS – Inductively Coupled Plasma Mass Spectrometry

ICP-OES – Inductively Coupled Plasma Optical Emission Spectrometry

IREDs – Imine Reductases

JEOL – Japan Electron Optics Laboratory

KREDs – Ketoreductases

LC-MS/MS – Liquid Chromatography Tandem Mass Spectrometry

LOD – Limit of Detection

LOQ – Limit of Quantification

MDR – Multi-Drug Resistant

MEP – Methylerythritol 4-Phosphate

MIC – Minimum Inhibitory Concentration

MS – Mass Spectrometry

NADH – Nicotinamide Adenine Dinucleotide (Reduced)

NADPH – Nicotinamide Adenine Dinucleotide Phosphate (Reduced)

N.b – Nutrient broth

NMR – Nuclear Magnetic Resonance

NSAIDs – Non-Steroidal Anti-Inflammatory Drugs

OYE – Old Yellow Enzyme

PBS – Phosphate-Buffered Saline

PCC – Pasteur Culture Collection

PhnCDE – Phosphonate Transport System (ABC-type)

PTDH – Phosphite Dehydrogenase

REE – Rare Earth Elements

RNA – Ribonucleic Acid

ROS – Reactive Oxygen Species

SM – Spirulina Medium

TAs – Transaminases

TFA – Trifluoroacetic Acid

TPP – Triphenyl Phosphate

UDP-galactose – Uridine Diphosphate Galactose

UDP-glucose – Uridine Diphosphate Glucose

UV-Vis – Ultraviolet–Visible Spectrophotometry

VOCs – Volatile Organic Compounds

WUST – Wrocław University of Science and Technology

List of tables

Table 1. Comparison of biocatalyst classes and their characteristics ……...16

Table 2. Comparison of biocatalysis and chemical catalysis ……..... 20

Table 3. Summary of selected enzymatic reaction types for stereoselective isomer synthesis and applications …….... 30

Table 4. Cyanobacterial metabolites and their applications ……...…...39

Table 5. Chemical reagents ……..…. …..45

Table 6. Microbial strains ……51

Table 7. Spirulina medium composition and it's modification ……58

Table 8. BG-11/BG-11_0 medium composition and it's modification …… …..59

Table 9. Trace element composition in spirulina and BG-11 media ……..……. …..60

Table 10. Substrate-specific bioconversion by cyanobacterial strains ….……... 64

Table 11. Unsaturated fatty acids stability test in growth media (7 days). ……..... 76

Table 12. Biotransformation of unsaturated fatty acids …….……..….. 81

Table 13. Concentration (mM) of inorganic phosphonate in the test samples (A_{620}) ……..…… 86

Table 14. Bioconversion of 1-phenylethyl acetate (7 days culture) in phytotron ...91

Table 15. Bioconversion of 1-phenylethyl acetate (14 days culture) in phytotron..92

Table 16. Comparative bioconversion by *Leptolyngbya* sp. (14 days culture) in phytotron vs. manual chamber ……...…. 93

Table 17. Percentage yield of DMHPP from EMDP by *Synechococcus* sp. and *Limnospira* sp. at different substrate concentrations (mM) ……...…… 103

Table 18. Antimicrobial activity of EMDP and DMHPP using the disk diffusion method ……105

Table 19. Antimicrobial activity of EMDP and DMHPP using the agar well diffusion method ……...……106

Table 20. Analysis of bioaccumulated REEs by *Limnospira indica* ..……...…… 112

Table 21. Analysis of bioaccumulated REEs by *Limnospira maxima* ..……..... 112

Table 22. Analysis of bioaccumulated REEs by *Synechococcus* sp. ...…… 112

Table 23. Analysis of bioaccumulated REEs by *Leptolyngbya* sp. …….. 112

List of figures

Figure 1. Schematic representation of a combined bioconversion and bioaccumulation process ……4
Figure 2. Schematic overview of biocatalysis …… 9
Figure 3. Chemoselective reduction of cinnamaldehyde by *Synechocystis* sp. PCC 6803 ……32
Figure 4. Selected substrates for photobiocatalysis and bioaccumulation with cyanobacterial strains ……49
Figure 5. Comparative stability of EMDP and biomass growth of *Limnospira* sp. in modified media over 7 days ……77
Figure 6. Malachite Green Assay Standard curve …… 86
Figure 7. GC analysis of 1-phenylethyl acetate bioconversion ……94
Figure 8. Possible two-step bioconversion of epoxymethyl dimethyl phosphonate by biocatalysts (*Synechococcus* sp and *Limnospira* sp.) …... 97
Figure 9. Spectral analysis of the biotransformation process ……99
Figure 10. Comparative analysis of the bioconversion percentages by cyanobacterial biocatalysts …… 100
Figure 11. Antimicrobial susceptibility testing using disk diffusion and agar well diffusion …… 104
Figure 12. Light microscope images of pre- and post-bioconversion biomass ….. 107
Figure 13. Growth inhibition (%) of four cyanobacterial strains exposed to REEs.109
Figure 14. Determination of optimal concentrations of REEs……..…. 110
Figure 15. Dry mass assessment of pre- and post- bioconversion biomass …….... 111
Figure 16. Graphical illustration of ICP-MS analysis of bioaccumulated REEs 114

Acknowledgement

I would like to express my deepest and most sincere gratitude to my principal supervisor, Prof. dr hab. inż. Ewa Żymańczyk-Duda, Professor and Deputy Head of the Department of Biochemistry, Molecular Biology, and Biotechnology, as well as Head of the Biotechnology Laboratory at the Faculty of Chemistry, Wrocław University of Science and Technology. I am profoundly thankful for the opportunity to pursue my doctoral research under her expert guidance. Her unwavering support, insightful supervision, and constructive feedback have been instrumental to the successful execution and completion of this thesis. I am particularly grateful for her generosity, patience, and encouragement throughout every phase of my doctoral journey.

I am also sincerely grateful to my auxiliary supervisor, Dr. inż. Monika Serafin-Lewańczuk, for her valuable scientific oversight and thoughtful advice throughout the course of my research. Her contributions were crucial in enhancing the scientific depth and methodological rigor of this work.

I extend my heartfelt thanks to Dr. Agnieszka Śliżewska for her selfless support, valuable time, and scientific guidance, especially during the early stages of this project. Her mentorship and kind introduction to the research topic provided a strong foundation for my academic development.

My deep appreciation goes to Prof. Milada Vítová, Dr. Mária Čížková, and Dr. Mahleh Eghbalinejad of the Department of Phycology, Institute of Botany of the Czech Academy of Sciences, Třeboň, Czechia. Their remarkable support during my international research internship, undertaken within the framework of the COST Action, greatly enriched both the scientific scope and international dimension of my doctoral work. Their mentorship, collaboration, and warm hospitality made my stay both academically rewarding and personally memorable.

I also wish to acknowledge Dr. Cornelius Arome Omatola of the Department of Microbiology, Kogi State University, Anyigba, Nigeria, for his steadfast academic encouragement, motivation, and active collaboration on international research and

publications. His guidance has been a valuable source of inspiration and support throughout my academic journey.

A very special thanks goes to Liza Ines Samson, whose unwavering support, patience, and understanding have sustained me throughout this demanding journey. Her quiet strength, constant encouragement, and enduring presence have made an immeasurable difference during the most challenging moments of this pursuit. I also extend my heartfelt gratitude to all my well-wishers, who have played vital roles in the realization of this academic milestone. Their steadfast support, sincere encouragement, and unceasing prayers have provided a strong foundation of reassurance and strength, uplifting me through both the demanding and rewarding phases of this journey.

Finally, I express my sincere appreciation to all faculty members, colleagues, collaborators, and administrative staff who, in various ways, contributed to the successful realization of this Ph.D. project. Your support and goodwill will always be remembered with gratitude.

Scientific achievements

Publications

Publications directly related to doctoral dissertation

1. Żymańczyk-Duda, E., **Samson, S.O.**, Brzezińska-Rodak, M., Klimek-Ochab, M. (2022). Versatile applications of cyanobacteria in biotechnology. *Microorganisms 10*, 2318. https://doi.org/10.3390/microorganisms10122318
2. **Samson, S.O.**, Serafin-Lewańczuk, M., Brzezińska-Rodak, M., Klimek-Ochab, M., Żymańczyk-Duda, E. (2024). Complete epoxy phosphonate conversion to dimethyl (1*E*)-3-hydroxyprop-1-enylphosphonate with photobiocatalysts' assistance. *Symmetry 16*, 1676. https://doi.org/10.3390/sym16121676
3. **Samson, S.O.**, Serafin-Lewańczuk, M., Żymańczyk-Duda, E., Brzezińska-Rodak, M., Klimek-Ochab, M, Vítová, M., Čížková, M., Eghbalinejad, M. (2025). Photobiotransformation of xenobiotics by cyanobacterial biomass and its further valorization as bioaccumulator of rare earth elements. *Submitted for publication; currently under editorial review (Manuscript ID: ALGAL-D-25-01633).*

Publications from other international collaborations related to the discipline

4. Omatola, C.A., Mshelbwala, P.P., Okolo, M.L.O., Onoja, A.B., Abraham, J.O., Adaji, D.M., **Samson, S.O.**, Okeme, T.O., Aminu, R.F., Akor, M.E. (2024). Noroviruses: evolutionary dynamics, epidemiology, pathogenesis, and vaccine advances—a comprehensive review. *Vaccines 12*, 590. https://doi.org/10.3c390/vaccines12060590
5. Omatola, C.A., Ogunsakin, R.E., Onoja, A.B., Okolo, M.L.O., Abraham-Oyiguh, J., **Samson, S.O.**, Mofolorunsho, K.C., Akoh, P.Q., Adejo, O.P., Idakwo, J., Okeme, T.O. (2024). Enteropathogenic viruses associated with acute gastroenteritis among African children under 5 years of age: a systematic review and meta-analysis. *Journal of Infection 88*, 106169. https://doi.org/10.1016/j.jinf.2024.106169
6. **Samson, S.O.**, Emmanuel, E., Cornelius, A.O. (2021). In-vitro assessment of antibacterial activity of crude methanolic and aqueous extracts of *Mitracarpus*

villosus. *African Journal of Microbiology Research 15*, 62–68. https://doi.org/10.5897/ajmr2020.9416

7. Emurotu, O.M., Anyanwu, C., Omatola, C.A., Aminu, R.F., Abraham, J.O., Nfor, G.K., **Samson, S.O.**, Gumbi, S.T. (2024). Detection and molecular characterization of *Escherichia coli* from wastewater environments in two university campuses in Nigeria. *Frontiers in Bioscience (Elite Edition) 16*, 38. https://doi.org/10.31083/j.fbe1604038
8. Omatola, C.A., Okolo, M.L.O., Adaji, D.M., Mofolorunsho, C.K., Oyiguh, J.A., Zige, D.V., Akpala, N.S., **Samson, S.O.** (2020). Coinfection of human immunodeficiency virus-infected patients with hepatitis B virus in Lokoja, North Central Nigeria. *Viral Immunology 33*, 391–395. https://doi.org/10.1089/vim.2019.0157
9. Okolo, M.L.O., Alaba, A.Z., **Samson, S.O.**, Omatola, C.A., Mudi, I.B., Omatola, J.A., Okolo, U.E. (2023). Microbiological and molecular investigation of *Candida* spp. infection among women accessing antenatal care at Prince Abubakar Audu University Teaching Hospital Anyigba, North-Central Nigeria. *Microbes and Infectious Diseases 4*, 1435–1445. https://doi.org/10.21608/mid.2023.187584.1452
10. Okolo, M.L.O., Omatola, C.A., **Samson, S.O.**, Idache, B.M. (2022). Evidence of hepatitis B infection and co-infection with enteric fever among febrile patients in a primary health facility in Kogi State, Nigeria. *Journal of Immunoassay and Immunochemistry 43*, 516–525. https://doi.org/10.1080/15321819.2022.2071127
11. Edegbo, E., Okolo, M.L., Adegoke, A.S., Omatola, C.A., Onoko, P.O., **Samson, S.O.**, Abraham, J.O., Alaba, Z., Okeme, T.O., Joseph, C.J., Zakari, D.A. (2025). Evaluation of phytochemical properties and antifungal activity of *Ocimum gratissimum* crude leaf extracts towards dermatophytes. *Journal of Medicinal Plants Research 19*, 13–19. https://academicjournals.org/journal/JMPR/article-abstract/3A4E32F72962
12. Abraham, J.O., Omatola, C.A., Egbunu, Z.K., Iyanda, M.O., Okolo, M.L.O., Aminu, R.F., Edegbo, E., Emurotu, O.M., **Samson, S.O.**, Muhammed, D., Chock, J.J. (2024). Occurrence and seroprevalence of infectious viral, bacterial, and protozoal diseases among patients attending the Ore General Hospital in Southwestern Nigeria. *Microbes and Immunity 1*, 57–69. https://doi.org/10.36922/mi.3283

13. Lateef, O.M., Akintubosun, M.O., Olaoba, O.T., **Samson, S.O.**, Adamczyk, M. (2022). Making sense of "nonsense" and more: challenges and opportunities in the genetic code expansion, in the world of tRNA modifications. *International Journal of Molecular Sciences 23*, 938. https://doi.org/10.3390/ijms23020938

Conference presentations

1. **Samson, Sunday Ocholi**, Serafin-Lewańczuk, Monika, Żymańczyk-Duda, Ewa. "Cyanobacterial biomass in biocatalysis processes." Poster presented at the *Third Key to Sustainability Symposium*, Wrocław University of Science and Technology, 29–30 April 2025, Wrocław, Poland. https://keytosustainability.com/
2. **Samson, Sunday Ocholi**, Serafin-Lewańczuk, Monika, Żymańczyk-Duda, Ewa, Vítová, Milada, Čížková, Mária, Eghbalinejad, Mahleh. "Photobiocatalytic conversion of epoxymethyl dimethylphosphonate and 1-phenylethyl acetate using cyanobacterial systems: advanced applications in high-value product synthesis and rare earth element bioaccumulation." Oral presentation at the *VII Ogólnopolska Konferencja "Biotechnologia niejedno ma imię" / 2nd International Conference "The Many Faces of Biotechnology"*, Uniwersytet Medyczny im. Karola Marcinkowskiego w Poznaniu, 23–24 November 2024, Poznań, Poland. https://kbib.up.poznan.pl/?q=node%2F253
3. **Samson, Sunday Ocholi**, Serafin-Lewańczuk, Monika, Żymańczyk-Duda, Ewa. "Biocatalysis in the synthesis of valuable substances from cyanobacterial cells." Oral presentation at the *6th Symposium on Biotransformations for Pharmaceutical and Cosmetic Industry*, Institute of Catalysis and Surface Chemistry, Polish Academy of Sciences, Kraków, 17–19 June 2024. https://ikifp.edu.pl/ ; https://ikifp.edu.pl/wp-content/uploads/2024/01/6thSymposium-A4-3kopie.pdf
4. **Samson, Sunday Ocholi**, Serafin-Lewańczuk, Monika, Żymańczyk-Duda, Ewa. "Biocatalysis in the synthesis of valuable substances from cyanobacterial cells." Poster presented at *PANIC 2024: PhoBiA Annual Nanophotonics International Conference*, 16–17 May 2024, Wrocław, Poland. https://panic.pwr.edu.pl/ ; https://dbc.wroc.pl/Content/126538/PANIC_2024_Book_of_Abstracts_e-book.pdf
5. **Samson, Sunday Ocholi**, Śliżewska, Agnieszka, Żymańczyk-Duda, Ewa. "Biological synthesis of high-added-value compounds (using selected cyanobacteria strains)." Poster presented at *PANIC Summer School 2022: PhoBiA*

Annual Nanophotonics International Conference, 30 May–3 June 2022, Wrocław, Poland. https://panic.pwr.edu.pl/ ; https://www.dbc.wroc.pl/dlibra/publication/154989/edition/115413/content

6. Brzezińska-Rodak, Małgorzata, Serafin-Lewańczuk, Monika A., Raczyńska, Agnieszka, **Samson, Sunday Ocholi**, Lubiak, Katarzyna D., Pieła, Aleksandra, Śliżewska, Agnieszka, Klimek-Ochab, Magdalena, Żymańczyk-Duda, Ewa. "Biocatalysis in the synthesis of high-added-value compounds." Presented at the *5th Symposium on Biotransformations for Pharmaceutical and Cosmetic Industry*, 13–15 June 2022, Kraków-Częstochowa Upland, Poland. https://books.google.com/books/about/The_5rd_Symposium_on_Biotransformations.html?id=_O9NzwEACAAJ

Patent applications

1. Biokatalityczny sposób otrzymywania (1*E*)-3-hydroksyprop-1-enylofosfonianu dimetylu z wykorzystaniem szczepu *Synechococcus bigranulatus* CCALA 187. Sunday Ocholi Samson, Monika Serafin-Lewańczuk, Ewa Żymańczyk-Duda, Małgorzata Brzezińska-Rodak, Magdalena Klimek-Ochab.
2. Biokatalityczny sposób otrzymywania (1*E*)-3-hydroksyprop-1-enylofosfonianu dimetylu z wykorzystaniem szczepu *Nodularia moravica* CCALA 797. Monika Serafin-Lewańczuk, Ewa Żymańczyk-Duda, Sunday Ocholi Samson, Małgorzata Brzezińska-Rodak, Magdalena Klimek-Ochab.
3. Biokatalityczny sposób otrzymywania (1*E*)-3-hydroksyprop-1-enylofosfonianu dimetylu z wykorzystaniem szczepu *Leptolyngbya foveolarum* CCALA 76. Monika Serafin-Lewańczuk, Ewa Żymańczyk-Duda, Sunday Ocholi Samson, Małgorzata Brzezińska-Rodak, Magdalena Klimek-Ochab.

Grants and awards

- **Quartus Program Award (2025)** – Received in recognition of the patent application titled *"Biokatalityczny sposób otrzymywania (1E)-3-hydroksyprop-1-enylofosfonianu dimetylu z wykorzystaniem szczepu Synechococcus bigranulatus* CCALA 187."
- **Increased Doctoral Scholarship (2024/2025)** – Awarded in recognition of academic performance and research progress.
- **COST Action CA19116 – Short-Term Scientific Mission (STSM)** – Funded research visit to the Institute of Botany, Czech Academy of Sciences, Třeboň, Czech Republic (19 August – 30 September 2024).
- **NAWA STER award (2022/2023)** – Granted under the Polish National Agency for Academic Exchange for domestic and international researchers on scientific achievements under the InterDoc school.
- **Increased Doctoral Scholarship (2022/2023)** – Awarded based on academic merit and research contributions.

Abstract (English)

The growing demand for solutions in the economy that align with the principles of sustainable development is an important driver for the advancement of biotechnology, both in the field of chemical synthesis using biological tools and in environmental bioremediation. Cyanobacteria are useful organisms in this regard, as they can be employed both as photobiocatalysts and as tools for improving environmental quality. This dissertation addresses the potential of selected cyanobacterial strains, *Synechococcus bigranulatus* CCALA 187, *Nostoc cf-muscorum* CCALA 129, *Limnospira indica* PCC 8005, *Limnospira maxima* CCALA 27, *Leptolyngbya foveolarum* CCALA 76, *Kamptonema animale* CCALA 138, and *Nodularia moravica* CCALA 114 as whole-cell biocatalysts and bioaccumulators that could serve as elements in bioremediation and resource recovery strategies.

A series of photobiocatalytic tests were conducted under controlled conditions to assess the efficiency of transforming unsaturated fatty acids, acetic acid esters, and organophosphonates such as epoxymethyl dimethylphosphonate (EMDPP). Analytical techniques including GC, HPLC, NMR, IR and ICP-MS were used for quantitative analysis of biotransformation, evaluation of stereoselectivity, and determination of rare earth element (REE) accumulation, particularly gadolinium (Gd) and europium (Eu).

The study demonstrated significant catalytic activity of the cyanobacteria. In the case of *Synechococcus bigranulatus* CCALA 187 and *Limnospira* sp. (PCC 8005 and CCALA 27), almost complete bioconversion of EMDPP was achieved within 72 and 24 hours, respectively, resulting in the formation of the product, dimethyl (1*E*)-3-hydroxyprop-1-enylphosphonate (DMHPP). Enantioselective hydrolysis of 1-phenylethyl acetate was also observed, with the use of *Leptolyngbya foveolarum* CCALA 76 yielding an enantiomeric excess exceeding 70%. Parallel bioaccumulation experiments showed that cyanobacterial biomass, especially after bioconversion, exhibits a high affinity for REEs, confirming its applicability in bioremediation and resource recovery strategies.

This work demonstrates that cyanobacterial biomass can be utilized in the design of processes aligned with the development of a circular economy, where microalgae act as photobiocatalysts enabling the synthesis of valuable products, and the recovered biomass is valorized for its bioaccumulation capabilities, which in turn enables, for example, the recovery of critical elements. It provides a foundation for future applications in synthetic biology, pharmaceutical synthesis, and environmentally sustainable REE extraction.

Streszczenie (Polski)

Rosnące zapotrzebowanie na stosowanie w gospodarce rozwiązań zgodnych z zasadami zrównoważonego rozwoju jest ważną przesłanką dla rozwoju biotechnologii w zakresie syntezy chemicznej z wykorzystaniem narzędzi biologicznych oraz w zakresie bioremediacji środowiskowej. Cyjanobakterie są w tym przypadku użytecznymi organizmami, które można wykorzystać zarówno jako fotobiokatalizatory jak i narzędzie poprawiające jakość środowiska. Niniejsza rozprawa odpowiada na pytanie jaki jest potencjał wybranych szczepów cyjanobakterii, *Synechococcus bigranulatus* CCALA 187, *Nostoc cf-muscorum* CCALA 129, *Limnospira indica* PCC 8005, *Limnospira maxima* CCALA 27, *Leptolyngbya foveolarum* CCALA 76, *Kamptonema animale* CCALA 138, oraz *Nodularia moravica* CCALA 114, jako całokomórkowych biokatalizatorów oraz bioakumulatorów, które mogą być elementem strategii bioremediacji i odzysku zasobów. Przeprowadzono serię testów fotobiokatalitycznych w kontrolowanych warunkach, aby ocenić efektywność transformacji nienasyconych kwasów tłuszczowych, estrów kwasu octowego oraz organofosfonianów, takich jak epoksymetylo-dimetylofosfonian (EMDPP). Do ilościowej analizy biotransformacji, oceny stereoselektywności i oznaczenia akumulacji pierwiastków ziem rzadkich (REE), szczególnie gadolinu (Gd) i europu (Eu), zastosowano techniki analityczne takie jak GC, HPLC, NMR, IR i ICP-MS.

Badania wykazały istotną aktywność katalityczną sinic. W przypadku *Synechococcus bigranulatus* CCALA 187 and *Limnospira* sp. (PCC 8005 and CCALA 27) uzyskano niemal całkowitą biokonwersję EMDPP odpowiednio w ciągu 72 i 24 godzin i otrzymano produkt, dimetylowy (1*E*)-3-hydroksypropeno-1-ylowy fosfonian (DMHPP). Zaobserwowano także enantioselektywną hydrolizę octanu 1-fenyloetanolu, przy czym użycie szczepu *Leptolyngbya foveolarum* CCALA 76 pozwoliło na uzyskanie nadmiaru enancjomerycznego przekraczającego 70%. Równoległe eksperymenty bioakumulacyjne wykazały, że biomasa cyjanobakterii, zwłaszcza po biokonwersji, wykazuje wysokie powinowactwo do REE, co potwierdza jej przydatność w bioremediacji i strategiach odzysku zasobów.

Praca ta wskazuje, że biomasa cyjanobakterii może być wykorzystana do planowania procesów wpisujących się w rozwój gospodarki o obiegu zamkniętym, gdzie mikroalgi są fotokatalizatorami pozwalającymi na syntezę wartościowych produktów, a następnie, odzyskana biomasa jest waloryzowana pod kątem zdolności do bioakumulacji, co z kolei umożliwia np. odzysk pierwiastków krytycznych. Wyniki badań stanowić mogą podstawę dla przyszłych zastosowań w biologii syntetycznej, syntezie farmaceutycznej oraz zrównoważonym środowiskowo pozyskiwaniu REE.

CHAPTER ONE

Introduction

1.1. Background

The connection between biotechnology and environmental chemistry has witnessed rapid advances in recent decades, particularly in the development of microbial systems for sustainable catalysis and metal recovery. Cyanobacteria, a group of oxygenic photoautotrophic prokaryotes, have emerged as potent biological agents capable of not only driving complex enzymatic transformations but also accumulating metals (such as rare earth elements) through biosorption, intracellular sequestration, and biomineralization. Their unique physiological and metabolic attributes, including photosynthetic capability, rapid growth, and rich cell wall chemistry, render them highly attractive for applications in green biocatalysis and bioaccumulation.

Biocatalysis refers to the use of biological catalysts, enzymes or whole cells, to mediate chemical transformations under environmentally benign conditions. Traditionally, microbial biocatalysis has been dominated by heterotrophic organisms, particularly bacteria and fungi. However, cyanobacteria offer the added advantage of phototrophic growth, enabling the direct harnessing of solar energy to drive metabolic processes. This feature has fostered growing interest in their deployment for photobiocatalysis, light-driven biotransformations involving complex substrates such as fatty acids, esters, and organophosphonates.

Simultaneously, increasing concerns over the environmental and geopolitical constraints of rare earth element (REE) extraction have catalyzed the search for sustainable recovery technologies. Rare earths such as gadolinium (Gd) and europium (Eu) are critical to diverse technologies including medical imaging, clean energy, and electronics, yet conventional mining practices are often associated with ecological degradation. Cyanobacteria have been increasingly recognized for their metal-binding potential, attributed to the abundance of functional groups (e.g., hydroxyl, carboxyl,

phosphate) on their extracellular polymeric substances (EPS) and cell surfaces, as well as their capacity for intracellular uptake under regulated metabolic states.

1.2. Rationale for the study

While several studies have documented enzymatic activities and heavy metal tolerance in cyanobacteria, few have comprehensively explored their dual functionality in both biocatalytic conversions and metal bioaccumulation under controlled photoautotrophic conditions. Moreover, there is a paucity of research addressing the integration of these functions within a single experimental framework, especially under scalable, reproducible conditions.

The use of cyanobacterial strains such as *Synechococcus bigranulatus* CCALA 187, *Nostoc cf-muscorum* CCALA 129, *Kamptonema animale* CCALA 138, *Limnospira indica* PCC 8005, *Limnospira maxima* CCALA 27, *Nodularia moravica* CCALA 114 *and Leptolyngbya foveolarum* CCALA 76 in the current study provides a valuable opportunity to examine a diverse set of physiological and enzymatic traits. These strains were evaluated not only for their ability to convert organic compounds into value-added products, but also for their REE uptake potential in pre- and post-biotransformation states (Figure 1).

1.3. Research objectives

This doctoral research is guided by the following objectives:

- To assess the capacity of selected cyanobacterial strains to catalyze photobiotransformation reactions involving fatty acids, phosphonates, and ester substrates.
- To evaluate the stability of substrates and optimize growth media to balance biomass productivity and substrate integrity.
- To determine the stereoselectivity and conversion efficiency by cyanobacteria during enantioselective transformations using analytical techniques such as HPLC, GC, MS, NMR and IR.

- To explore the bioaccumulation potential of cyanobacterial biomass, before and after biotransformation, for the recovery of REEs (Gd^{3+} and Eu^{3+}), using ICP-MS.
- To investigate the antimicrobial activity of bioconversion products and evaluate their potential as precursor in biomedical or environmental applications.
- To identify the most promising cyanobacterial candidates for downstream scale-up studies based on catalytic performance, tolerance to elevated substrate loads, and REE accumulation efficiency.

1.4. Hypotheses

1. *Cyanobacteria possess photobiocatalytic activity:*

   Cyanobacterial strains can catalyze the biotransformation of selected organic compounds, including epoxymethyl dimethyl phosphonate, vinyl phosphonates, unsaturated fatty acids, and 1-phenylethyl acetate, under controlled photoautotrophic conditions.
2. *Growth medium influences substrate stability and metabolism:*

   The composition of the cyanobacterial growth medium affects both the chemical stability of substrates and the metabolic efficiency of the strains during photobiocatalytic reactions.
3. *Cyanobacteria exhibit enantioselective catalytic potential:*

   Certain cyanobacterial strains can catalyze the enantioselective hydrolysis of prochiral substrates such as 1-phenylethyl acetate.
4. *Controlled environmental conditions affect catalytic performance:*

   Photobiocatalytic performance and enantioselectivity could differ between cyanobacteria cultivated in phytotron-controlled environments and those grown in manually regulated conditions.
5. *Biotransformation affects bioaccumulation potential:*

   Cyanobacterial biomass retains or enhances its capacity for rare earth element (REE) bioaccumulation following biotransformation processes.
6. *Strain-specific suitability for biotechnological scale-up:*

Some cyanobacterial strains exhibit superior biocatalytic and biosorptive characteristics that make them suitable candidates for scale-up in biotechnological applications.

1.5. Significance of the study

This research represents a novel convergence of two biotechnologically important processes, biocatalysis and bioaccumulation, within a single phototrophic microbial platform. By integrating substrate transformation and elemental uptake, it opens pathways for simultaneous bioproduct synthesis and environmental remediation. Additionally, the project aligns with global goals of sustainable chemistry and circular bioeconomy, wherein biological systems are harnessed for both value generation and waste minimization.

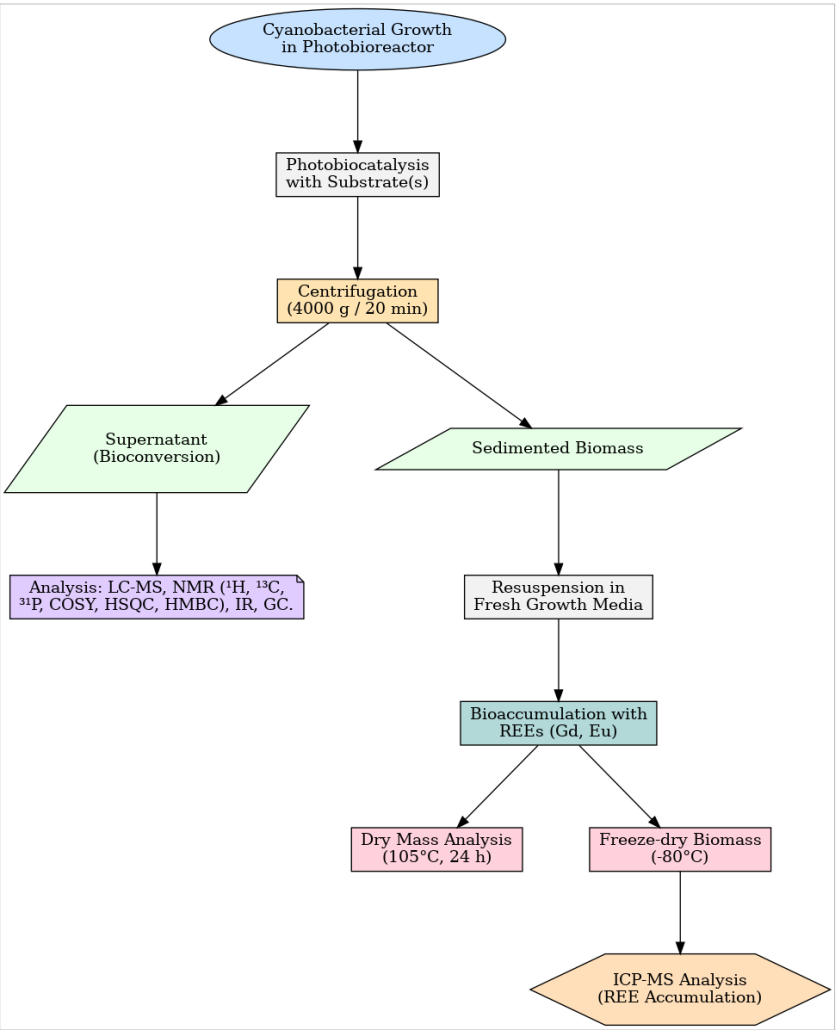

Figure 1. Schematic representation of a combined bioconversion and bioaccumulation processes (*sketched by the author*).

The biotransformation of organophosphonates into hydroxyphosphonates, particularly the synthesis of dimethyl (1*E*)-3-hydroxyprop-1-enylphosphonate (DMHPP), illustrates the potential for cyanobacteria in stereoselective reactions with biomedical implications, since pure enantiomers of phosphonates derivatives are common motives in the drug structures. Furthermore, the use of modified and unmodified cyanobacterial media to tune substrate stability while maintaining organism viability emphasizes a key methodological advancement for future research.

Finally, the application of cyanobacterial biomass for rare earth element recovery not only mitigates environmental pollution but also offers a bioresource pathway for strategic material supply. The capacity to recover REEs using a biological chassis that previously facilitated catalysis offers efficiency, modularity, and sustainability not achievable via conventional processes.

1.6. Limitations and future perspective

This study focuses on a limited number of organic substrates and cyanobacterial strains cultured under laboratory conditions. While the selected strains represent diverse morphophysiological types, the findings may not fully capture the performance spectrum of naturally occurring or genetically modified cyanobacteria. Additionally, while the analytical framework employed ensures high sensitivity and specificity, limitations in yield scalability, product purification, and long-term bioreactor stability remain to be addressed in future studies. Future research will also focus on optimizing the bioaccumulation processes for these strains by extending the acclimation period for post-bioconversion biomass, which could enhance their resilience and bioaccumulation efficiency. Exploring a broader range of REEs and cyanobacterial species will as well deepen understanding of these processes and their potential applications.

CHAPTER TWO

Literature Review

2.1. Conceptual basis of biocatalysis and biotransformation

Biocatalysis refers to the use of biological molecules, primarily enzymes or whole microbial cells, to catalyze chemical reactions. It offers high specificity, efficiency under mild conditions, and reduced environmental impact compared to traditional chemical catalysis [1]. Through selective transformation of substrates, biocatalysis plays a central role in biotransformation processes, enabling the synthesis of enantiomerically pure compounds, complex natural products, and industrial intermediates [2,3], as demonstrated in Figure 2. Biotransformation is broadly described as the enzymatic or microbially mediated alteration of chemical compounds, yielding structurally distinct products under environmentally benign and mild operational conditions. This approach influences the catalytic power of biological systems, ranging from purified enzymes to whole microbial cells, to conduct transformations that are often infeasible or inefficient under conventional chemical catalysis [2,4]. Unlike chemical synthesis, which typically relies on extreme pH, high temperatures, and toxic solvents, biotransformations proceed under aqueous, near-physiological conditions, aligning with the principles of green chemistry [5].

The foundational scope of biotransformations encompasses a diverse array of reaction types. These include oxidation and reduction, hydrolysis, esterification, amino-transfer, C–C and C–X bond formations, and even more complex cleavages such as C–P and C–N bonds [5,6]. Such versatility is not merely theoretical, numerous studies have demonstrated the feasibility and efficiency of these transformations across various industrial settings. For instance, Sheldon and Brady [6] critically reviewed the boundaries of biocatalysis and emphasized its application in challenging bond-forming and -breaking processes. Their work expands on the catalytic flexibility of evolved enzymes, demonstrating that with the right engineering, enzymes can be pushed beyond their native substrate and reaction scope.

A particularly impactful area is the use of oxidoreductases in the asymmetric reduction of prochiral ketones, a process widely adopted in pharmaceutical synthesis [7]. Wu *et al*. [7] showed that ketoreductases (KREDs) and alcohol dehydrogenases (ADHs) could catalyze these reductions with >99% enantiomeric excess (ee) using renewable cofactors. This exemplifies not only the selectivity of biocatalysis but also its inherent compatibility with green cofactor recycling strategies. Such processes are effective compared to metal-catalyzed equivalents, which often require toxic or precious metals like rhodium or palladium and generate hazardous waste streams.

The biological systems used for biotransformations (as expatiated in section 2.2) are generally categorized into three: purified enzymes, cell-free lysates (crude enzyme mixtures), and whole-cell systems. Each has unique advantages and operational contexts. Purified enzymes provide high specificity, kinetic simplicity, and reduced side-product formation, but often suffer from cofactor dependency and limited robustness [8,9]. In contrast, whole-cell systems offer metabolic self-sufficiency, including in situ regeneration of expensive cofactors like NAD(P)H or ATP [10]. Zhao and van der Donk [10] reviewed various cofactor regeneration strategies and concluded that intracellular pathways provide a cost-effective advantage in large-scale operations, especially in redox chemistry.

Recent studies also highlight the importance of choosing the right biocatalyst system based on the complexity of the desired transformation. For example, Liese *et al*. [5] and Singh *et al*. [8] both advocate for whole-cell systems in multistep cascade reactions, where endogenous enzymes and transport mechanisms facilitate product conversion through intermediate stages. These observations are particularly pertinent in industrial biotechnology, where reaction efficiency and scalability dictate process viability.

The sustainability credentials of biotransformations further reinforces their industrial relevance. Enzymes and microbial systems are derived from renewable resources, function in aqueous or non-toxic solvents, and often eliminate the need for hazardous

reagents [11,12]. These aspects translate directly to improved E-factors (mass of waste per mass of product) and process mass intensity (PMI), both critical metrics in sustainable process engineering. Sheldon [11] emphasized the role of biocatalysis in advancing resource efficiency, especially in pharmaceutical manufacturing where process waste is tightly regulated.

One illustrative example of the transformative potential of biocatalysis is the development of an engineered transaminase for the synthesis of sitagliptin, a DPP-4 inhibitor used in diabetes management. Savile *et al*. [13] documented how a single biocatalytic step, replacing a six-step metal-catalyzed route, led to a 19% reduction in waste, improved atom economy, and enhanced yield. Moreover, the reach of biotransformation has been dramatically extended through enzyme engineering techniques such as directed evolution and rational design [14]. Arnold [14] demonstrated that enzyme functionality could be tuned not only for increased activity or altered substrate specificity but also for stability in non-natural environments such as organic solvents or elevated temperatures. This expansion of biocatalyst utility has allowed chemists to exploit novel reaction chemistries, including carbene and nitrene insertions, once the exclusive domain of synthetic organometallic chemistry [15].

Integration with synthetic biology further supports the diversification and scalability of biotransformations. Cravens *et al*. [16] outlined microbial chassis engineering strategies for the overproduction of plant-derived natural products, highlighting how gene editing and pathway balancing can be used to drive efficient biosynthetic transformations. This development synergizes well with the push toward decentralized, bio-based chemical manufacturing platforms.

Of particular interest in modern biocatalysis is the emergence of photobiocatalysis, where phototrophic organisms or photoactivated enzymes facilitate light-driven chemical conversions. Cyanobacteria have attracted attention in this regard due to their oxygenic photosynthetic machinery and metabolic versatility. These organisms possess the unique capacity to couple solar energy capture with enzymatic redox

reactions, thereby offering a sustainable platform for solar-to-chemical energy transduction [17]. Cyanobacteria also harbor numerous oxidoreductases, hydrolases, and transferases that can be exploited in situ for value-added compound production without external cofactors, a significant advantage in bioprocess economics [18].

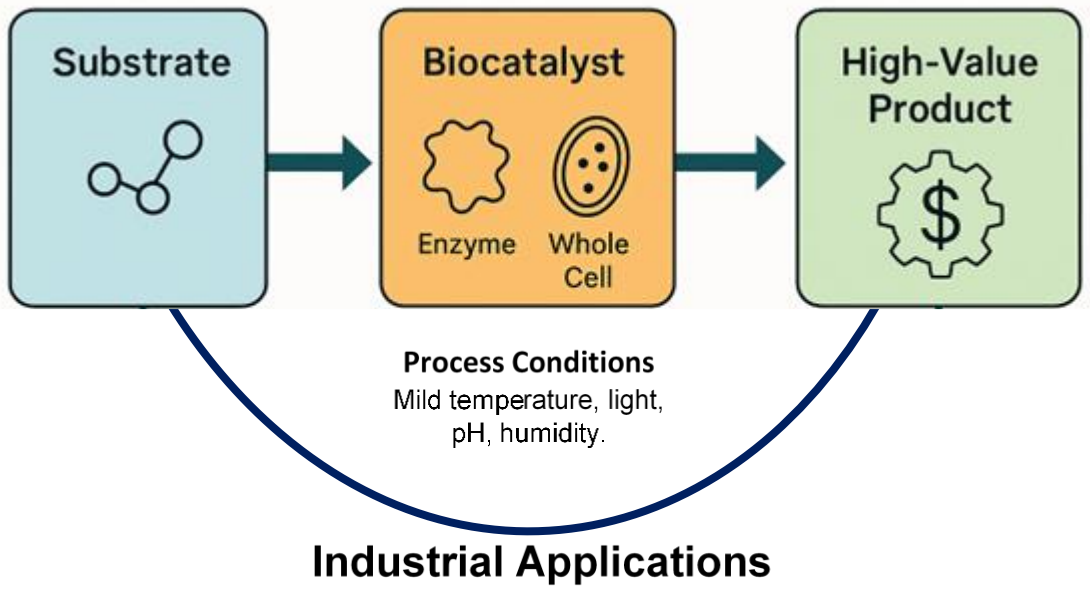

Figure 2. Schematic overview of biocatalysis *(designed by the author)*.

Finally, the translation of biotransformations from lab to industrial scale has been facilitated by innovations in reactor design and process intensification. Continuous flow systems and immobilized enzyme technologies now enable long-term operational stability and enzyme reusability, making biocatalytic production economically viable [19]. These systems allow for seamless integration of multistep reactions in a single setup, reducing residence time, solvent usage, and operational footprint.

2.2. Classes and modes of operation of biocatalysts

Biocatalysts, the functional agents in biotransformations, can be operationally categorized into three main systems: (1) purified enzymes, (2) cell-free extracts or lysates, and (3) whole-cell systems. Each of these systems offers distinct catalytic characteristics, operational advantages, and limitations, depending on the complexity of the reaction, substrate specificity, cofactor requirements, economic viability, and scalability [5,8,9].

2.2.1. Purified enzymes

Purified enzymes represent the most refined form of biocatalysts. They are typically isolated from microbial, plant, or recombinant sources and exhibit high catalytic efficiency and substrate specificity. These enzymes provide excellent stereo-, chemo-, and regioselectivity, which is critical in fine chemical and pharmaceutical synthesis [1,4,7]. Their defined kinetic behavior allows detailed mechanistic studies and straightforward reaction modeling.

One of the primary benefits of using purified enzymes is the elimination of cellular barriers and transport limitations that may impede substrate access in whole-cell systems. For example, ketoreductases, lipases, transaminases, and esterases have been widely applied in enantioselective reductions, hydrolyses, and amination reactions due to their broad substrate scope and catalytic precision [4]. The immobilization of purified enzymes on solid supports further enhances their industrial utility. For example, immobilized *Candida antarctica* lipase B (CALB), often marketed as Novozym 435, has become a benchmark biocatalyst for esterification, transesterification, and kinetic resolution of racemic alcohols and amines [20]. Lish *et al*. [20] recently demonstrated that the immobilization protocol significantly influences catalytic performance in biodiesel production, emphasizing the critical role of matrix selection and enzyme orientation.

Despite their advantages, purified enzymes suffer from several operational constraints. Some enzymes utilize redox cofactors such as the oxidized forms NAD^+ and FAD, or their reduced counterparts NADH and $FADH_2$, depending on the specific redox requirement for catalytic turnover, which are prohibitively expensive for large-scale use unless an effective cofactor regeneration system is integrated [10,21]. In addition, they are often sensitive to industrial process conditions such as temperature extremes, pH variation, and organic solvents [22]. To mitigate this, enzyme engineering strategies, such as mutagenesis or fusion to stabilizing protein partners, have been used to enhance solvent tolerance and thermal stability [22].

2.2.2. Cell-free lysates (crude extracts)

Cell-free lysates occupy a middle ground between purified enzymes and whole-cell systems. They are typically derived from disrupted microbial cells and contain a complex mixture of enzymes, cofactors, metabolites, and structural proteins. These lysates retain the endogenous cofactors and metabolite pools necessary for catalysis and offer a cost-effective alternative for multienzyme reactions where in situ cofactor regeneration is required [4,23,24]. Alissandratos [24] demonstrated the potential of recombinant *E. coli* lysates in assembling in vitro enzymatic cascades. These systems allow simultaneous expression of multiple enzymatic activities, facilitating multi-step transformations in a single pot. Such systems are particularly advantageous when substrate channeling and intermediate stabilization are needed, as is often the case in redox transformations or chiral amine synthesis.

However, the main limitation of cell-free lysates lies in their compositional complexity and variability. The presence of proteases, side reactions catalyzed by contaminant enzymes, and loss of activity during storage or freeze-thaw cycles are recurring challenges [25]. Moreover, due to the lack of cellular membrane barriers, sensitive enzymes or unstable intermediates may be quickly degraded, affecting overall yield and reproducibility. Nonetheless, these systems remain a valuable tool for pilot-scale biotransformations, enzyme screening, and academic applications, especially when process economy is a concern and substrate tolerance is moderate [26].

2.2.3. Whole-cell biological systems in biocatalysis

Whole-cell biocatalysts are living or non-viable microbial systems (e.g., bacteria, yeast, cyanobacteria) used to catalyze reactions via their native or engineered metabolic pathways. These systems are self-sufficient in cofactor recycling and are ideal for complex biotransformations involving multiple enzymatic steps or high-energy cofactor dependency [8,27,28]. The whole-cell catalysis has several intrinsic advantages. First, cofactors such as NADH, NADPH, and ATP are regenerated in situ via primary metabolism, eliminating the need for costly external supplementation.

Second, enzymes are naturally compartmentalized and protected by the cellular environment, which often increases stability and tolerance toward mildly toxic substrates or solvents [19,27]. Guo *et al*. [29], for example, engineered *E. coli* strains for sequential biotransformation of glucose into 2-phenylethanol and its ester derivative, leveraging intracellular redox cycling and endogenous metabolic flux.

Beyond bacterial biocatalysts, a growing body of research has demonstrated the value of fungi, yeasts, plant-derived systems, and cyanobacteria in mediating complex biotransformations under mild, sustainable conditions. These platforms expand the biochemical diversity available to industrial biotechnology, offering robust enzyme systems, increased solvent tolerance, and the ability to process structurally diverse or recalcitrant substrates.

Fungal biocatalysts, particularly those derived from filamentous species such as *Aspergillus* sp. and *Penicillium* sp. are notable for their ability to produce extracellular oxidative and hydrolytic enzymes. These include laccases, peroxidases, and monooxygenases, which catalyze the oxidation of phenols, aromatic amines, lignin derivatives, and industrial pollutants. Filamentous fungi have shown remarkable utility in transforming hydrophobic or high-molecular-weight substrates, often under biphasic or solvent-rich conditions. In an exemplary study, marine *Penicillium citrinum* was used to reduce chalcones to dihydrochalcones with high enantioselectivity and process stability, demonstrating significant potential in asymmetric reduction reactions relevant to pharmaceutical synthesis [30,31]. In a related development, previous investigations showed that nutrient-starved *Aspergillus niger* cultures could stereoselectively resolve heterocyclic phosphonates, including thienyl-, imidazolyl-, and pyrazolyl-substituted derivatives, into optically pure (*S*)-enantiomers with enantiomeric excess exceeding 98% and yields approaching 100% [32,33]. These results suggested that specific enzymatic pathways involved in stereoselective redox transformations are activated in response to nutrient limitation, likely through secondary metabolic mechanisms that are not constitutively expressed under standard growth conditions.

Concurrently, anaerobic fungi from the *Neocallimastigomycota* phylum have emerged as promising sources of novel lignocellulolytic enzymes. These strictly anaerobic species inhabit herbivore gastrointestinal tracts and express a range of cellulases and hemicellulases capable of degrading lignin-rich biomass. Unlike the aerobic molds such as *Penicillium* sp. and *Aspergillus* sp., which belong to the phylum *Ascomycota*, *Neocallimastigomycota* represent a phylogenetically and ecologically distinct lineage of early-diverging fungi. While their role in traditional biotransformations remains underexplored, early genomic and enzymatic characterizations suggest a valuable future contribution to biorefineries and enzymatic pretreatment of biomass for biofuels [34–36].

Yeasts also represent a versatile group of biocatalysts. Species such as *Saccharomyces cerevisiae*, *Pichia pastoris*, and *Yarrowia lipolytica* have been extensively used in whole cell biocatalysis, largely due to their eukaryotic expression systems, capacity for recombinant enzyme production, and intrinsic redox capabilities. Żymańczyk-Duda *et al*. demonstrated that baker's yeast, *S. cerevisiae*, can be applied in the stereoselective reduction of diethyl 2-oxoalkylphosphonates, leading to the production of optically pure (*S*)-alcohols with high selectivity. This transformation, mediated by endogenous alcohol dehydrogenase activity, exemplifies how yeast systems may complement bacterial biocatalysis in handling polar, non-natural substrates [37]. Similarly, *Y. lipolytica* has been genetically engineered to express surface-bound lipases for biodiesel production from hydrophobic triglyceride substrates, enabling catalysis in non-aqueous media with superior reusability and operational stability [38]. In the beverage industry, brewing yeasts have been exploited for their ability to release thiols and terpenes from non-volatile precursors during fermentation. This biotransformation is largely driven by β-glucosidase and β-lyase enzymes, which hydrolyze glycosidic and thiol-bound aroma precursors, thus enhancing the flavor profile of hoppy beers [39,40]. These cases underline the potential of yeast strains not only as hosts for metabolic engineering but also as biocatalysts in their native form for specialty chemical and flavor production.

Plant-derived biocatalysis, though less industrialized, offers unique functionalities. Plant enzymes such as peroxidases, polyphenol oxidases, and glycosyltransferases are capable of catalyzing regioselective oxidation, hydroxylation, and glycosylation reactions relevant to pharmaceutical and nutraceutical chemistry. Suspension cultures from *Catharanthus roseus* and *Nicotiana tabacum* have been applied in the biosynthesis of alkaloids and hydroxylated flavonoids, though scalability and culture stability remain challenges. These systems are particularly valuable for mimicking native plant biosynthetic routes and for functionalizing complex natural product scaffolds [41–43].

Cyanobacteria present another emerging platform for biocatalysis. These phototrophic organisms can perform both primary and secondary biotransformations under carbon-neutral conditions due to their photosynthetic metabolism. Strains such as *Nostoc cf-muscorum*, *Nodularia sphaerocarpa*, and *Arthrospira maxima* have been investigated for the asymmetric reduction of oxophosphonate esters, with high conversion efficiencies and enantiomeric excess exceeding 95% [44]. In contrast to heterotrophic systems, cyanobacteria can carry out these transformations using CO_2 and light as primary energy and carbon sources, providing a model for sustainable, light-driven biocatalysis. Furthermore, phosphate-limited conditions were shown to induce enhanced enzymatic reduction in cyanobacteria, further supporting the strategic application of nutrient stress to modulate catalytic performance, as previously observed in fungi.

The success of these whole-cell biocatalysts relies not only on their inherent catalytic potential but also on the application of innovative engineering strategies. Immobilization techniques have been widely applied to fungal and yeast biocatalysts to enhance reusability, maintain stability in organic solvents, and facilitate integration into continuous flow reactors. Matrix supports such as alginate, chitosan, or cotton-based carriers have been employed with success, particularly in the asymmetric reduction of hydrophobic substrates by *Penicillium citrinum* and *S. cerevisiae* [31,37]. Additionally, advances in synthetic biology have enabled surface display of enzymes in *Y. lipolytica*, facilitating direct substrate access and reducing mass transfer

limitations. The application of nutrient starvation or stress-induced activation also offers a valuable regulatory mechanism to induce cryptic or secondary pathways responsible for stereoselective redox activity [32].

Furthermore, cyanobacteria like *Synechococcus elongatus* and *Synechocystis sp.* have been engineered as photoautotrophic whole-cell biocatalysts capable of converting CO_2 and light into industrial platform chemicals and chiral alcohols, offering an unparalleled model of carbon-neutral chemical manufacturing [45,46].

Generally, fungi and yeasts, through stress-induced or recombinant systems, offer unique access to redox chemistry and asymmetric synthesis. Plant-based systems provide functional group modifications that are often unachievable by microbial routes, and cyanobacteria bridge the gap between environmental sustainability and catalytic efficiency. Despite these strengths, whole-cell systems present their own set of challenges. These include transport barriers across membranes, side reactions from competing metabolic activities, limited tolerance to high substrate/product concentrations, and difficulties in downstream product isolation [47]. However, as the field evolves, the combination of metabolic engineering, immobilization, and bioprocess optimization will be key to unlocking the full potential of these alternative biological systems in industrial biocatalysis [28,47]. In industrial contexts, the productivity of whole-cell systems has been further improved by process intensification tools. For instance, flow bioreactors and enzyme immobilization strategies have been successfully employed to increase space-time yield, reduce mass transfer limitations, and enhance catalyst reusability [26,48].

Table 1. Comparison of biocatalyst classes and their characteristics

Feature	Purified enzyme	Cell-free lysate	Whole-cell catalyst	Reference
Substrate Specificity	Very High	Moderate to High	Moderate	[23,25,49]
Cofactor Requirement	High (external)	Moderate (endogenous)	Low (internal recycling)	[4,21,25]
Operational Stability	Moderate	Moderate	High	[4,49,50]
Tolerance to Harsh Conditions	Low	Moderate	High	[19,49,50]
Cost of Implementation	High	Moderate	Low	[4,23,25]
Genetic Modifiability	Not Applicable	Not Applicable	High	[4,47]
Multi-Step Conversion	Low	Moderate	Very High	[4,24,51]
Industrial Examples	CALB, KREDs	*E. coli* transaminase lysate	Recombinant *E. coli*, *S. elongatus*	[24,29,45,46,49]

The decision to use a particular biocatalyst system should be guided by the balance of cost, operational feasibility, reaction complexity, cofactor dependency, and environmental constraints (Table 1). While purified enzymes are ideal for precision chemistry in high-value sectors, whole-cell catalysts dominate in large-scale and cofactor-intensive transformations. Cell-free lysates offer a valuable compromise in early-phase development or proof-of-concept studies.

As enzyme engineering, metabolic design, and bioprocess intensification technologies advance, the boundaries between these systems continue to blur. Hybrid systems, such as semi-purified enzyme cocktails within permeabilized cells, are now being explored to harness the best of both specificity and self-sufficiency [26]. This convergence opens new pathways for flexible, scalable, and environmentally sustainable biocatalytic platforms.

2.3. Advantages of biocatalysis over chemical catalysis

Biocatalysis has emerged as a transformative methodology in chemical synthesis, providing clear advantages over traditional chemical catalysis in terms of selectivity, sustainability, safety, and process integration. Unlike conventional catalysis, which often relies on high temperatures, extreme pH, and toxic reagents, biocatalysis offers a platform for performing complex chemical transformations under mild, aqueous, and physiologically relevant conditions. This not only improves the sustainability of the process but also enhances reaction efficiency and product specificity [1]. These advantages are particularly significant in industries such as pharmaceuticals, agrochemicals, and fine chemicals, where the demand for precise, eco-friendly, and economically viable synthetic methods continues to grow [4,6,7].

2.3.1. Selectivity: chemo-, regio-, and stereoselectivity

One of the most compelling advantages of biocatalysis lies in the unmatched selectivity offered by enzymes. These biomolecules are inherently evolved to recognize and act upon specific substrates with remarkable precision, displaying high levels of chemo-, regio-, and stereoselectivity [4,5]. This feature is critical in the synthesis of chiral compounds, where the configuration of the final product determines its biological activity, toxicity, and pharmacokinetics.

For example, ketoreductases (KREDs) have been widely used to reduce prochiral ketones into chiral alcohols with enantiomeric excesses often exceeding 99%, far surpassing what is achievable using traditional metal-based catalysts without complex chiral ligands [7]. In the synthesis of sitagliptin, a prominent DPP-4 inhibitor, a single-step biocatalytic process using an engineered transaminase replaced a multi-step rhodium-catalyzed hydrogenation. This not only enhanced yield but also eliminated the need for chiral auxiliaries and expensive metals [13].

Chemical catalysis, by contrast, often requires multistep synthesis, chiral directing groups, or specialized ligands to achieve comparable enantioselectivity. These

additions increase cost, introduce environmental hazards, and necessitate additional purification steps, making the overall process less sustainable [52].

2.3.2. Mild reaction conditions and functional group tolerance

Biocatalytic reactions typically occur under mild conditions, neutral pH, atmospheric pressure, and temperatures between 20–45 °C, which is highly beneficial for preserving sensitive functional groups and minimizing side reactions [1,7]. This tolerance enables selective transformations of multifunctional molecules, a significant advantage when dealing with complex intermediates such as active pharmaceutical ingredients (APIs) or bioactive natural products.

Enzymes also perform well in aqueous environments or biphasic systems, reducing the reliance on hazardous organic solvents. The ability to operate in such benign conditions is particularly advantageous for reactions involving unstable or reactive intermediates, which may degrade under the harsh conditions required by traditional chemical catalysts [11].

Stepankova *et al*. [22] reported that although native enzymes often lose activity in organic solvents, enzyme stabilization strategies such as immobilization, directed evolution, and protein fusion can extend their performance even under non-aqueous conditions. These enhancements allow broader substrate ranges while retaining the inherent selectivity of the enzyme.

2.3.3. Environmental and economic sustainability

Biocatalysis strongly aligns with the principles of green chemistry. Enzymes are renewable, biodegradable catalysts that function in non-toxic solvents, generate fewer by-products, and require lower energy input [11,53]. The substitution of heavy metal catalysts and toxic oxidants with enzyme systems dramatically reduces the environmental burden of chemical manufacturing.

Sheldon [11] emphasized that enzymatic processes typically yield lower E-factors, defined as the ratio of waste to product mass, than analogous chemical routes. In pharmaceutical production, where the average E-factor may reach 25–100 for chemical processes, biocatalytic routes often achieve E-factors as low as 5–10 [11]. These improvements are not only environmentally desirable but also cost-effective due to reduced waste treatment and resource input.

Anastas and Warner [54] further emphasized that biocatalysis enables safer reaction pathways with inherently less hazardous reaction profiles, contributing to sustainability on both ecological and occupational health levels.

2.3.4. Process integration and multistep cascade reactions

Enzymes can be organized into cascade reactions, where multiple enzymatic steps occur in one vessel without intermediate isolation, thus improving atom economy, shortening production timelines, and simplifying purification [55]. Such "one-pot" systems are difficult to achieve using chemical catalysis due to compatibility issues between different catalysts, solvents, and reagents.

A notable example is the multi-enzyme cascade reported by Huffman *et al*. [56] for the synthesis of islatravir, an antiviral compound. The process combined five enzymes in a sequential transformation from simple substrates to the final product with near-quantitative yield and high stereochemical purity. The cascade design avoided intermediate workups, solvent swaps, or reagent incompatibilities, challenges commonly encountered in purely chemical routes. This level of integration makes biocatalysis especially attractive in continuous manufacturing and flow reactor systems, where enzymes can be immobilized and reused across extended operation periods [26,48]

2.3.5. Safety and regulatory advantages

From a safety perspective, biocatalysts are non-toxic, non-flammable, and non-corrosive. Their use in water-based systems reduces the risk of fires, explosions, and

exposure to volatile organic compounds (VOCs), aligning well with occupational safety standards [26]. This also lowers the infrastructure and insurance costs associated with hazardous chemical storage, transportation, and reaction monitoring.

In contrast, chemical catalysis often involves pressurized gases (e.g., hydrogen in metal hydrogenations), strong acids or bases, and reactive organometallic intermediates, all of which require complex containment, waste management, and environmental risk assessments [6].

Moreover, biocatalysis facilitates regulatory compliance, especially in pharmaceutical manufacturing where residual metal contamination is tightly controlled. Biocatalysts leave no metal traces and are thus preferable in late-stage functionalization or API synthesis where purity standards are stringent [13,52].

Table 2. Comparison of biocatalysis and chemical catalysis

Feature	Biocatalysis	Chemical catalysis	Reference
Selectivity	Very high chemo-, regio-, and stereoselectivity	Moderate; often requires chiral ligands	[4,13,52]
Reaction conditions	Mild (ambient temperature, aqueous solvents)	Harsh (high temperature, extreme pH, organics)	[1,7]
Environmental impact	Low; biodegradable, low waste	High; toxic metals, large solvent volumes	[11,53,54]
Catalyst toxicity	Non-toxic, biodegradable	Often toxic (e.g., heavy metals)	[53,54]
Energy requirement	Low	Moderate to high	[1,7]
Compatibility with cascades	High (one-pot multi-step feasible)	Low (cross-reactivity of catalysts)	[56,57]
Safety and regulatory profile	High (safe solvents, minimal hazards)	Low (flammable/toxic reagents)	[26]

Biocatalysis offers a set of advantages that position it as a sustainable and highly effective tool in modern chemical synthesis (Table 2). Its superior selectivity, operational simplicity, and environmental compatibility provide compelling reasons for its growing adoption across industries. Furthermore, the ability to engineer enzymes and design integrated cascade reactions continues to expand the frontier of what is synthetically possible through biocatalysis.

2.4. Limitations of biocatalysis and mitigation strategies

While biocatalysis offers compelling advantages in modern chemical synthesis, it is not without limitations. These constraints, ranging from substrate specificity and enzyme instability to cofactor dependency, product inhibition, mass transfer issues, and scalability, can impact the broader industrial adoption of enzyme-based systems. Understanding these limitations is essential for overcoming them through enzyme engineering, process optimization, and integration with synthetic biology tools.

2.4.1. Narrow substrate scope and enzyme specificity

One of the most significant challenges in biocatalysis is the narrow substrate range of many native enzymes. Enzymes are inherently selective for their physiological substrates and may show little to no activity toward synthetic or structurally diverse compounds [3,58]. This limitation restricts their applicability in chemical industries, particularly where feedstock diversity is critical.

For example, natural alcohol dehydrogenases readily reduce simple aliphatic ketones but display poor activity toward bulky or heterocyclic analogs, compounds that are commonly encountered in pharmaceutical intermediates [7]. As a result, the applicability of wild-type enzymes is often constrained unless modified.

To address this, protein engineering approaches such as directed evolution and rational design have been successfully employed to broaden substrate compatibility [14,27]. Arnold [14] demonstrated that iterative rounds of mutagenesis and selection could significantly enhance an enzyme's substrate range and catalytic efficiency.

Similarly, Bornscheuer *et al*. [3] referred to this expansion of substrate scope as the "third wave of biocatalysis," emphasizing the routine use of design tools to tailor biocatalysts for synthetic needs. However, these strategies are resource-intensive and may not be economically viable in early development stages.

2.4.2. Enzyme instability under industrial conditions

Another critical limitation is the operational instability of many enzymes under industrial process conditions. Enzymes evolved for function in aqueous environments at physiological temperature and pH (~37 °C, pH 7.0), and they often denature when exposed to extremes of pH, temperature, organic solvents, or mechanical shear stress [1,22].

For instance, lipases, which are widely used in ester hydrolysis and biodiesel synthesis, may lose catalytic activity in solvents such as acetonitrile or under oxidizing environments [59]. This issue is particularly relevant in pharmaceutical synthesis, where substrates are often hydrophobic or poorly soluble in water. Stabilization techniques such as enzyme immobilization, crosslinking, and introduction of disulfide bonds have shown promise in enhancing enzyme robustness [22,50]. Immobilization also facilitates enzyme recovery and reuse, improving the economic viability of the process. However, these modifications can also reduce catalytic turnover and substrate diffusion, creating a new set of trade-offs.

2.4.3. Cofactor dependence and regeneration challenges

A major bottleneck in redox biocatalysis is the dependence on costly cofactors like NADH, NADPH, ATP, and FAD, which are required in stoichiometric or catalytic amounts for oxidoreductase and ligase-catalyzed reactions [10,21]. Without efficient in situ regeneration, these cofactors make enzymatic reactions economically impractical at scale. Whole-cell systems can regenerate cofactors internally through metabolism, but this often introduces side reactions and regulatory complexity. Alternatively, enzymatic cofactor regeneration systems, such as glucose dehydrogenase (GDH),

formate dehydrogenase (FDH), or phosphite dehydrogenase (PTDH), have been developed to recycle NAD(P)H from inexpensive sacrificial substrates like glucose or formate [60,61]. These systems are effective but require precise matching of kinetic parameters and careful control of by-products.

Bachosz *et al*. [60] emphasized the need to evaluate cofactor regeneration systems not only in terms of turnover efficiency but also integration potential with downstream processes. In many cases, unbalanced rates between the primary enzyme and the recycling system led to accumulation of intermediate or unproductive consumption of cofactors.

2.4.4. Product inhibition and substrate overload

Product inhibition is another common challenge that can severely impact the performance of biocatalysts, especially in batch reactions. Many enzymes exhibit feedback inhibition by their own products or experience substrate inhibition at higher concentrations, reducing the overall reaction rate and volumetric productivity [47,62].

For instance, hydrolases have been reported to experience substrate inhibition at concentrations above 50 mM, a level often necessary in industrial production for achieving acceptable space-time yields [62]. This constraint limits process intensification and may necessitate continuous removal of the product or in situ extraction strategies, increasing process complexity and cost.

Enzyme engineering can sometimes alleviate product inhibition by modifying binding site interactions. However, such changes may compromise substrate affinity or alter selectivity, requiring extensive re-optimization of reaction conditions [63].

2.4.5. Mass transfer limitations in whole-cell systems

Whole-cell biocatalysts, while metabolically self-sufficient, are often limited by mass transfer barriers. Substrates must traverse the cellular membrane to reach intracellular enzymes, and hydrophobic or bulky molecules frequently show poor permeability

[64]. Similarly, product export can be rate-limiting and may result in intracellular accumulation, leading to product low yield, cytotoxicity or metabolic feedback.

Additionally, native metabolic pathways could compete with the desired biotransformation, diverting flux toward by-products and reducing overall yield. Wachtmeister and Rother [64] noted that this is particularly problematic in the case of aldehydes, which are rapidly oxidized or reduced by multiple endogenous enzymes in most hosts. Mitigation strategies include permeabilization of the cell membrane, heterologous expression of transport proteins, or switching to cell-free systems [65]. However, these modifications add to upstream and downstream processing burdens and can affect catalyst longevity.

2.4.6. Scalability and regulatory constraints

Despite successful laboratory-scale demonstrations, many biocatalytic processes face challenges in scale-up due to enzyme supply, stability during storage and transport, and regulatory compliance. In the pharmaceutical sector, enzymes used for GMP manufacturing must be produced under validated and consistent conditions, and any changes to the enzyme production methods such as a new expression host or purification process, can trigger costly re-approval procedures [26,66].

Moreover, enzyme production at industrial scale requires robust fermentation, downstream processing, and quality control systems. Schmid *et al*. [67] emphasized that biocatalysis, though attractive at gram-to-kilogram scale, often encounters bottlenecks when scaled to metric tons, due to low enzyme expression yields, proteolytic degradation, or instability during shipping and storage. Cost-effective large-scale implementation therefore demands optimization across the entire value chain, from strain selection and enzyme formulation to reactor design and process control.

While biocatalysis holds immense promises for sustainable synthesis, its widespread adoption depends on overcoming technical and regulatory challenges. Continued

innovation in enzyme engineering, bioprocess design, and synthetic biology is essential for expanding the operational boundaries of biocatalysts. With appropriate strategies, many of these limitations are surmountable, paving the way for broader integration of biocatalysis into mainstream chemical manufacturing.

2.5. Biocatalytic approaches to isomer synthesis

Isomer synthesis, particularly the preparation of structural, geometric, and stereoisomers, is a critical step in the production of fine chemicals, agrochemicals, and especially pharmaceuticals. Many bioactive compounds exist in chiral or stereospecific forms, with only one isomer exhibiting the desired biological function, while others may be inactive or toxic. Traditional chemical methods for isomer synthesis often involve multistep procedures, chiral auxiliaries, and metal-based catalysts, which are resource-intensive and environmentally problematic. Biocatalysis offers an efficient, selective, and sustainable alternative for synthesizing specific isomeric forms with high yield and purity [1,4,7,52].

2.5.1. Enzymatic racemization and deracemization

Enzymatic racemization refers to the interconversion of enantiomers, which is often used in dynamic kinetic resolution (DKR) processes. This strategy allows one enantiomer of a racemic mixture to be selectively converted into a desired product while the undesired enantiomer is continuously racemized, thus enabling full conversion of racemic substrates [68]. An illustrative example is the use of racemases and epimerases in conjunction with stereoselective hydrolases or transaminases. This approach has been applied in the synthesis of optically pure amino acids and secondary alcohols. Kroutil *et al*. [69] described a DKR process where mandelate racemase was combined with a stereoselective oxidoreductase to obtain enantiopure (*S*)-mandelic acid in high yield and optical purity. This method avoids the 50% yield limitation of conventional kinetic resolution and aligns with green chemistry principles by minimizing waste. Unlike chemical racemization methods, enzymatic

systems avoid harsh conditions, thus preserving sensitive functional groups and reducing undesired by-products.

Deracemization refers to the conversion of a racemic mixture into a single, optically pure enantiomer. Unlike classical resolution, which discards one enantiomer, deracemization theoretically allows full conversion of both enantiomers into the desired form, making it more atom-economical. For instance, monoamine oxidase (MAO-N) has been used for oxidative deracemization of racemic amines, followed by stereoselective reduction to yield enantiopure products [70]. These cascade processes are efficient, environmentally benign, and amenable to scaling. There are multiple biocatalytic strategies for achieving deracemization, with dynamic kinetic resolution (DKR), stereoinversion, and cyclic deracemization being the most common.

In DKR, a racemization catalyst and an enantioselective catalyst operate simultaneously. The racemase converts the unwanted enantiomer to the desired configuration, while the enantioselective catalyst selectively transforms one enantiomer into a product. This has been effectively applied using combinations such as amino acid racemases with lipases or transaminases [71,72]. For example, the resolution of racemic 1-phenylethanol can be achieved through lipase-mediated acylation of the (*R*)-enantiomer while a racemase converts the (*S*)-enantiomer into (*R*), thus enabling complete transformation to optically active (*R*)-acetate [73,74]. Stereoinversion involves the selective conversion of one enantiomer into its mirror image, typically via a two-step oxidation-reduction sequence. For example, the (*S*)-enantiomer of alcohol can be oxidized to a ketone intermediate and then reduced back to the (*R*)-enantiomer using a stereoselective reductase [75,76]. Enzymes such as alcohol dehydrogenases (ADHs) and Baeyer–Villiger monooxygenases have been engineered or combined in tandem for this purpose. This process is particularly attractive for deracemizing substrates with labile stereocenters or those difficult to resolve via classical methods. While cyclic deracemization involves enzymatic cycles that convert both enantiomers of a racemic mixture into a single product through parallel pathways. An example is the use of oxidase and reductase pairs in which one

enantiomer is oxidized and then reduced stereoselectively to the desired isomer. Whole-cell systems are especially suited for such processes due to the presence of multiple cofactor-recycling enzymes and redox mediators that enhance turnover and maintain reaction balance [77,78].

2.5.2. Asymmetric isomerization: alkene and ketone systems

Enzymes also catalyze geometric isomerization reactions, such as cis–trans conversion in alkenes or keto–enol tautomerism. Isomerases like maleate isomerase have been explored for the synthesis of defined geometric isomers of unsaturated acids, which serve as precursors for polymers and surfactants [79]. Of relevance is the biocatalytic transformation of α, β-unsaturated ketones into optically enriched allylic alcohols or saturated ketones. These reactions are commonly mediated by ene-reductases (ERs), which catalyze the stereoselective hydrogenation of activated double bonds [80]. The Old Yellow Enzyme (OYE) family of flavin-dependent ERs has been extensively characterized and engineered for this purpose. These enzymes operate under mild conditions, require only NAD(P)H, as a reductant, and display exquisite stereoselectivity.

For example, Müller *et al*. [80] demonstrated that ERs from *Thermus scotoductus* and *Lactobacillus kefir* could selectively reduce chalcone derivatives to (*S*)- or (*R*)-configured dihydrochalcones, depending on enzyme variant. These products are key intermediates in flavor and pharmaceutical industries.

2.5.3. Epimerization and diastereomer interconversion

Epimerases and mutases are enzymes that catalyze the inversion of stereocenters at specific positions of a molecule, enabling the interconversion of epimers or diastereomers. Such transformations are especially valuable in carbohydrate and sugar acid chemistry. For instance, UDP-glucose 4-epimerase catalyzes the reversible conversion between UDP-glucose and UDP-galactose, facilitating the synthesis of rare sugars [81].

Likewise, epimerases have been employed in the transformation of hydroxy acids and α-amino acids into their less common isomers. These isomers often possess distinct pharmacokinetic properties or serve as precursors for semi-synthetic antibiotics and enzyme inhibitors. However, most epimerases are substrate-specific and reversible, posing challenges in achieving high conversions without equilibrium shifting strategies [82].

Recent work has focused on coupling epimerases with selective downstream enzymes or in situ trapping of products to drive the equilibrium toward desired isomers. For example, combining D-tagatose epimerase with a selective aldolase has allowed the stereoselective synthesis of rare C7 sugars from glyceraldehyde and D-fructose, opening routes to high-value specialty carbohydrates [83].

2.5.4. Enzymatic synthesis of chiral isomers via transaminases and ketoreductases

Transaminases (TAs) and ketoreductases (KREDs) are among the most versatile biocatalysts for the synthesis of stereoisomers. These enzymes catalyze reversible transfer of amino or hydride groups, generating optically active amines and alcohols from prochiral ketones or aldehydes [1,7,13]. Transaminase-catalyzed synthesis has been extensively exploited in the pharmaceutical industry. The engineering of (*R*)-selective TAs enabled the one-step synthesis of sitagliptin, replacing a six-step metal-catalyzed route and reducing waste and cost significantly [13]. Similarly, KREDs have been applied in the industrial production of chiral alcohols such as (*S*)-1-phenylethanol and (*R*)-pantolactone, which serve as key building blocks in drug and vitamin synthesis.

Advanced KRED libraries now allow selection of enzyme variants with complementary enantioselectivity, thermostability, and solvent tolerance. Sheldon and Woodley [1] highlighted how combinatorial screening and computational modeling are accelerating the discovery of KREDs with tailored specificity and improved kinetics, facilitating gram-to-tonne scale synthesis of stereoisomers.

2.5.5. Photobiocatalytic isomerization and emerging trends

Recent advances have extended isomer synthesis into the realm of photobiocatalysis. Here, light energy is used to activate or enhance enzyme-catalyzed transformations, often through photosensitizer-mediated electron transfer [84]. Cyanobacterial and algal enzymes involved in light-driven redox cycles have shown potential in driving isomerization reactions using CO_2 and water as feedstocks.

For instance, studies on engineered *Synechococcus elongatus* and *Synechocystis sp.* demonstrated their capacity to use light and atmospheric carbon to generate chiral alcohols and fatty acid derivatives with high stereoselectivity [45,46]. These systems represent a convergence of carbon fixation and asymmetric synthesis, with far-reaching implications for renewable chemical manufacturing.

Other innovations involve coupling light-activated flavin or heme enzymes with isomerization reactions. Such hybrid systems have enabled the isomerization of non-activated alkenes, opening new routes to stereodefined olefins under mild, aqueous conditions [84].

Biocatalytic approaches to isomer synthesis offer unprecedented levels of stereoselectivity and efficiency under mild conditions. From racemization and asymmetric reduction to photobiocatalytic isomerization, enzymes provide powerful tools to generate structurally and stereochemically defined molecules at scale. As enzyme engineering and synthetic biology continue to advance, the scope of isomer synthesis is broadening further, reinforcing the central role of biocatalysis in modern asymmetric synthesis.

Table 3. Summary of selected enzymatic reaction types for stereoselective isomer synthesis and applications.

Reaction type	Enzyme class	Representative product	Application
Asymmetric reduction	Alcohol dehydrogenases (ADHs), Ketoreductases (KREDs), Imine reductases (IREDs)	Chiral alcohols, chiral amines	• Engineered transaminase for sitagliptin precursor amination, replacing rhodium catalysis
			• KRED-catalyzed reduction of acetophenone to (*S*)-1-phenylethanol with NADH regeneration
Hydrolytic resolution	Lipases (e.g., CALB), Esterases, Epoxide hydrolases	Enantiopure esters, alcohols, diols	• CALB-mediated resolution of β-amino acid esters with >99% ee
			• *A. radiobacter* epoxide hydrolase desymmetrizing racemic styrene oxides
Racemization / Epimerization	Racemases, Epimerases	α-Amino acids, secondary alcohols	• Mandelate racemase enabling DKR of phenylethylamine via transaminase coupling
			• DKR of N-acylated amino acids using racemase/acylase system
Isomerization	Isomerases (e.g., glucose isomerase), Prenyltransferases	Fructose, lactulose, geometric olefins	• Glucose to fructose conversion in high-fructose corn syrup (HFCS) production
			• Stereoselective olefin rearrangement by engineered double bond isomerases

These enzymatic strategies offer scalable, efficient, and stereoselective routes to isomers that are otherwise challenging to access using classical synthetic chemistry.

The diversity of reaction types and enzyme classes (Table 3) highlights the flexibility of biocatalysis in asymmetric synthesis, with ongoing innovations in enzyme engineering and high-throughput screening further expanding this biochemical toolkit.

2.6. Biocatalytic reduction and hydrolysis reactions

Reduction and hydrolysis reactions constitute two of the most fundamental transformations in organic chemistry. In traditional chemical processes, these reactions often rely on harsh conditions, stoichiometric reagents, and toxic catalysts such as metal hydrides or strong acids/bases. In contrast, biocatalytic reduction and hydrolysis reactions offer highly selective, mild, and environmentally benign alternatives that are increasingly used in industrial processes, particularly in the synthesis of pharmaceuticals, agrochemicals, and fine chemicals [1,4,7,11].

2.6.1. Alcohol dehydrogenases (ADHs) and ketoreductases (KREDs)

Alcohol dehydrogenases and ketoreductases are pivotal biocatalysts in asymmetric reduction of ketones and aldehydes to their corresponding alcohols. These enzymes utilize NADH or NADPH as hydride donors to deliver highly enantioselective reductions under aqueous conditions at ambient temperatures [1,7]. Their ability to catalyze the conversion of prochiral ketones into chiral alcohols (Figure 3) has been widely exploited in the manufacture of active pharmaceutical ingredients (APIs), including intermediates for β-blockers, statins, and anti-HIV agents.

One of the most cited applications is the production of (*S*)-1-phenylethanol and (*R*)-pantolactone using engineered ADHs and KREDs with enantiomeric excesses exceeding 99% [1,7,85]. The advantage of these enzymes lies in their ability to produce single enantiomers with high yield and minimal side reactions, eliminating the need for chiral resolution steps and reducing solvent and reagent use. Engineered libraries of KREDs have been developed to expand substrate scope, increase thermostability, and allow operation in organic cosolvents. Savile *et al*. [13] described the successful

deployment of an evolved transaminase–KRED system for sitagliptin synthesis, replacing a six-step metal-catalyzed process with a one-step biotransformation, thereby significantly improving environmental performance and cost-efficiency.

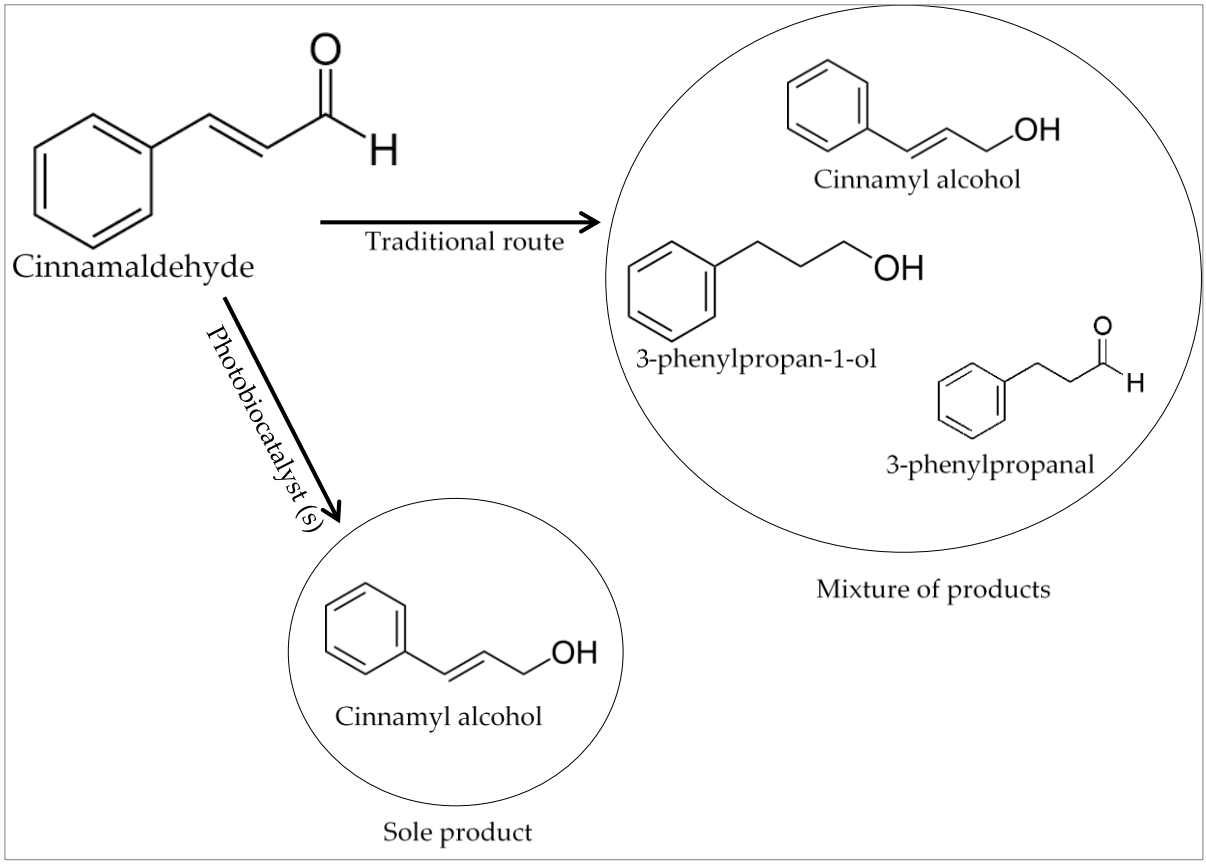

Figure 3. Chemoselective reduction of cinnamaldehyde to cinnamyl alcohol by *Synechocystis* sp. PCC 6803 under light conditions with photosynthetic NADPH regeneration [86] *(sketched by the author)*.

2.6.2. Ene-reductases and the old yellow enzyme (OYE) family

Ene-reductases, particularly from the OYE family, catalyze the asymmetric reduction of activated carbon-carbon double bonds, typically in α,β-unsaturated carbonyl compounds [80]. These enzymes perform 1,4-reductions with high stereoselectivity and are used in the synthesis of flavoring agents, pharmaceuticals, and chiral building blocks. The OYE enzymes are flavin-dependent and utilize NAD(P)H for hydride transfer.

Müller *et al*. [80] demonstrated selective reduction of chalcones and cinnamic acid derivatives into optically active dihydrochalcones using OYE variants from *Thermus scotoductus* and *Lactobacillus kefir*. These biocatalysts have broad substrate ranges and tolerate several functional groups including halogens, hydroxyls, and esters. Directed evolution and rational design have been successfully applied to tune substrate specificity and invert enantioselectivity in these systems, expanding their applicability in complex synthesis pathways [14,27].

2.6.3. Cofactor regeneration in reduction reactions

Reductive biocatalysis depends heavily on the availability of nicotinamide cofactors (NADH/NADPH). Since these cofactors are expensive, their efficiency in situ regeneration is critical. Enzymatic regeneration systems, such as glucose dehydrogenase (GDH), formate dehydrogenase (FDH), and phosphite dehydrogenase (PTDH), are widely used to maintain redox balance during large-scale reductions [10,60].

Zhao and van der Donk [10] provided a comprehensive overview of cofactor regeneration systems and highlighted the economic and kinetic advantages of coupling such systems with high-efficiency reductases. More recent strategies involve whole-cell systems that naturally recycle cofactors or electrochemical systems that regenerate cofactors at the electrode surface.

Biocatalytic hydrolysis reactions involve the cleavage of chemical bonds via the addition of water and are one of the most widely applied reactions in enzyme catalysis. Hydrolases, including lipases, esterases, amidases, and proteases, are responsible for such reactions and have become indispensable in both aqueous and non-aqueous biotransformations [1,4,11].

2.6.4. Lipases and esterases

Lipases (EC 3.1.1.3) and esterases (EC 3.1.1.1) catalyze the hydrolysis of ester bonds, producing alcohol and acids. They are among the most robust and widely used

enzymes in industrial catalysis, owing to their broad substrate range, high stability, and functionality in organic solvents and biphasic systems [20,50]. A classic industrial example is the resolution of racemic esters using lipases to obtain enantiopure alcohols or acids. CALB (*Candida antarctica* lipase B), immobilized on acrylic resin (e.g., Novozym 435), is a gold standard in such kinetic resolutions [20]. Lish *et al*. [20] reported the application of CALB in biodiesel synthesis and in resolving racemic ibuprofen esters under mild, environmentally friendly conditions.

Moreover, lipases are commonly used in non-hydrolytic reactions such as esterification and transesterification in water-restricted systems, further expanding their industrial role in biolubricants, surfactants, and pharmaceuticals.

2.6.5. Amidases and proteases

Amidases catalyze the hydrolysis of amide bonds to yield carboxylic acids and amines. They are widely employed in the synthesis of β-lactam antibiotics, chiral amides, and agrochemicals. For instance, amidase-mediated hydrolysis of mandelic acid amides provides enantiomerically pure mandelic acid, a key intermediate in semi-synthetic penicillins and cephalosporins [87].

Proteases, on the other hand, are extensively used in peptide synthesis and modification. While typically associated with protein degradation, engineered proteases can perform selective hydrolysis of synthetic peptides or catalyze transpeptidation in peptide drug development [88]. These enzymes operate with exquisite sequence and bond specificity, making them ideal for modification of biologically active peptides under mild conditions.

Biocatalytic hydrolysis is attractive for its low energy requirements, operational simplicity, and ability to avoid the use of corrosive acids or bases typically employed in chemical hydrolysis. Furthermore, hydrolases are generally non-toxic, biodegradable, and readily available from microbial sources.

In detergent manufacturing, food processing, and pharmaceutical industries, hydrolases have largely replaced conventional catalysts. The enzymatic production of aspartame, synthesis of L-carnitine, and resolution of non-steroidal anti-inflammatory drugs (NSAIDs) are all examples where hydrolases have demonstrated superior yield and selectivity [1,89].

Generally, biocatalytic reduction and hydrolysis reactions offer powerful, green, and highly selective tools for modern chemical synthesis. Through continuous advances in enzyme discovery, engineering, and cofactor management, these catalytic processes now rival or surpass traditional chemical methods in both efficiency and sustainability. As industries continue to adopt biocatalysis for large-scale synthesis, particularly in the context of green manufacturing mandates, reductive and hydrolytic enzymes will remain indispensable tools.

2.7. Microbial cell factories for biocatalysis

Microbial cell factories refer to genetically optimized microorganisms capable of producing target metabolites, enzymes, or value-added chemicals via biocatalytic pathways. These biological systems have become a foundational platform in modern biotechnology, enabling the sustainable synthesis of pharmaceuticals, agrochemicals, biofuels, and specialty chemicals through metabolic engineering and synthetic biology tools [1,2,4,47].

Unlike isolated enzyme systems, microbial cell factories provide whole cell biocatalysis where enzymatic transformations occur within a living or non-growing but metabolically active microbial host. These systems offer advantages such as cofactor self-sufficiency, robustness under operational conditions, tolerance to toxic intermediates, and the ability to catalyze complex multistep reactions [21,26,47].

The concept of microbial cell factories involves redirecting and optimizing the native metabolic network of a microorganism to produce desired products efficiently and selectively. This often requires heterologous expression of biosynthetic genes, deletion

of competing pathways, optimization of precursor supply, and control of redox balance, energy flux, and metabolite export [47,64]. *Escherichia coli* and *Saccharomyces cerevisiae* are the most commonly used chassis organisms due to their well-characterized genetics, ease of transformation, and scalable cultivation. However, non-conventional hosts such as *Bacillus subtilis*, *Corynebacterium glutamicum*, and *Pseudomonas putida* are increasingly favored for their stress resistance, native metabolic traits, and secretion capabilities [47,48,64].

One of the core advantages of using whole cells as biocatalysts is their ability to regenerate cofactors in situ. Redox reactions catalyzed by dehydrogenases, oxygenases, or reductases require cofactors such as NADH, NADPH, or FAD, which can be continuously regenerated within the microbial metabolism [21,60]. This eliminates the need for costly exogenous cofactor supplementation and simplifies reactor operation.

Moreover, whole cells protect sensitive enzymes from degradation by encapsulating them in a natural environment, while maintaining high local concentrations of cofactors and stabilizing multienzyme complexes [50]. This cellular context also enables multistep reactions via intracellular cascades, where substrate channeling can improve conversion efficiency and reduce intermediate degradation.

For example, engineered strains of *E. coli* expressing both transaminase and ketoreductase enzymes have been used to convert ketoesters to amino alcohols in a single fermentation step, with high conversion and stereoselectivity [47,90].

2.7.1. Applications of microbial cell factories

Microbial cell factories have been successfully applied in a wide range of industrial and pharmaceutical contexts. In the synthesis of chiral amines, engineered strains of *E. coli* and *Pseudomonas putida* expressing ω-transaminases have demonstrated superior yields and stereoselectivity compared to isolated enzymes, owing to cofactor recycling and better enzyme stability [13,47].

In the field of statin production, microbial strains producing the polyketide compactin (a precursor to simvastatin) have been optimized for enhanced productivity through modular pathway engineering and precursor supply enhancement [48]. Similarly, recombinant *Corynebacterium glutamicum* strains have been developed to overproduce amino acids such as L-lysine, L-tryptophan, and L-valine, which serve as key precursors for pharmaceuticals and supplements [64,91].

Cyanobacterial cell factories have also shown increasing promises in light-driven biotransformations. For instance, *Synechococcus elongatus* and *Synechocystis sp.* have been engineered to produce fatty acids, isoprenoids, and even stereochemically pure alcohols by harnessing CO_2 and light through photosynthetic electron transport [45,46]. These systems align with sustainable development goals by providing carbon-neutral alternatives for chemical production.

Furthermore, microbial platforms are now being employed to produce complex natural products such as artemisinin, taxol precursors, and erythromycin through complete reconstruction of plant or bacterial biosynthetic pathways [91,92].

2.7.2. Challenges in microbial cell factory engineering

Despite their several advantages, microbial cell factories also face several limitations that require careful engineering:

- **Toxicity of products or intermediates**: Some bioproducts or pathway intermediates are toxic to the host, limiting titers. Engineering of efflux pumps, transporter proteins, or compartmentalization systems (e.g., peroxisomes or microcompartments) can help mitigate these effects [26,47].
- **Metabolic burden and genetic instability**: High-level expression of multiple heterologous enzymes can impose a significant metabolic burden, leading to growth arrest or loss of plasmids. Strategies to mitigate this include genomic integration of key genes, use of stable auxotrophic markers, and dynamic expression systems that balance growth and production phases [47,92].

- **By-product formation and pathway competition**: Native enzymes may compete with the engineered pathway, reducing carbon flux to the desired product. Targeted gene knockouts or synthetic rewiring of central metabolism has be used to minimize these diversions [90,91].
- **Oxygen and cofactor limitations**: In redox-intensive pathways, cofactor imbalance and oxygen availability become limiting. Metabolic cofactor balancing and the use of synthetic redox shuttles could alleviate these challenges [21,60].
- **Scale-up and bioprocess design**: Industrial application of microbial factories requires scalable bioreactors with precise control of pH, oxygen transfer, substrate feed, and biomass density. Additionally, downstream processing of intracellular products requires efficient cell disruption and extraction strategies [65,67].

2.8. Metabolic diversity and biotechnological potential of cyanobacterial metabolites

Cyanobacteria have been explored not only as photobiocatalysts but they are also meaningful for other fields of biotechnology. The exceptional metabolic plasticity of cyanobacteria enables the biosynthesis of a wide array of primary and secondary metabolites with applications spanning healthcare, agriculture, and environmental remediation. Cyanobacteria are prolific producers of bioactive compounds, including cyanotoxins, alkaloids, carotenoids, and polysaccharides [93]. Welker and von Döhren [94] reviewed the metabolic diversity and biosynthetic pathways of cyanobacterial peptides such as microcystins and anatoxins, which exhibit cytotoxic and neurotoxic activities, respectively, and are under investigation for pharmacological applications.

These metabolites (Table 4) are products of core processes such as photosynthesis and carotenogenesis, and their production can be modulated by environmental factors. Primary metabolites are directly involved in cellular functions such as growth, division, and reproduction, while secondary metabolites are generally not essential for survival but confer ecological advantages, particularly under stress conditions. Primary metabolites produced by cyanobacteria include essential lipids, proteins, and antioxidant molecules. These compounds are pivotal in supporting fundamental

physiological functions and can be harnessed industrially to produce food additives, bioplastics, natural dyes, and biofertilizers [95–100]. Secondary metabolites, in contrast, are often produced in response to environmental stimuli and are typically species-specific. These include a wide array of bioactive compounds such as alkaloids, phenolic compounds, steroids, essential oils, antibiotics, and cyanotoxins [46,101–108].

Cyanobacteria's relatively simple genetic architecture facilitates genetic manipulation and biosynthetic optimization, enabling the tailored production of valuable metabolites. Such manipulations are often directed by the cellular response to environmental stressors like nutrient limitation and altered light regimes, which can significantly modulate photosynthetic and metabolic pathways [109,110]. For example, a study by Chen *et al*. [111] demonstrated that growth under nutrient-deficient and high-light conditions induced substantial production of biopolymers, lipids, essential oils, and starches, in contrast to growth in nutrient-rich media. This two-phase cultivation strategy clearly delineates the stress-induced enhancement of secondary metabolism in cyanobacteria [111,112]. Further evidence by Singh *et al*. [113] described how the Methylerythritol 4-phosphate (MEP) pathway is exploited in cyanobacteria for the synthesis of chlorophylls, fatty acids, and hormonal metabolites, many of which possess potent antimicrobial, anticancer, and antibiotic activities that support their relevance in pharmaceutical applications [113,114].

Table 4. Cyanobacterial metabolites and their applications

Metabolite class	Representative compounds	Functions in cyanobacteria	Biotechnological/pharmaceutical applications	Reference
Phenolic Acids	Gallic acid, Vanillic acid, Chlorogenic acid, Caffeic acid, Ferulic acid, Syringic acid, Gentisic acid	Antioxidant defense against ROS; UV and metal stress tolerance	Anti-aging (gallic, ferulic), skin care (ferulic), cardiac health (syringic, gentisic), antimicrobial	[115–118]
Vitamins	B-complex (B12), C, A, D, E, K	Growth, differentiation, cofactor in enzymatic	Dietary supplements; Spirulina as a rich source	[119–121]

		reactions; stress-induced synthesis	of B12, β-carotene, and E; vitamin D via UV stress	
Peptides	Microviridins, Cyanobactins, NRPs, PKs	Secondary metabolism; defense and competition	Antitumor, antimicrobial, antiviral drug leads; structural diversity for drug design	[94,122,123]
Terpenoids	β-carotene, Zeaxanthin, Myxoxanthophyll, Canthaxanthin, Geosmin, 2-MeBHPs	Photoprotection, oxidative stress response, signaling	Anti-aging (carotenoids), antimicrobial (sesterterpenes), environmental biomarkers (2-MeBHPs, geosmin)	[124–126]

2.9. Rare earth elements (REE) and their bioaccumulation mechanisms in cyanobacteria

REEs are essential components in a wide array of high-tech applications, including electric vehicles, wind turbines, smartphones, and medical imaging equipment, yet their extraction from ores and waste streams is environmentally damaging and geopolitically sensitive. Conventional mining and hydrometallurgical techniques employed in REE production are associated with extensive ecological degradation. These processes often involve open-pit mining, acid leaching, and solvent extraction, resulting in considerable greenhouse gas emissions, toxic wastewater discharge, and the generation of radioactive by-products, especially in deposits co-located with thorium or uranium. A comprehensive review by Haque *et al*. [127] published in *Resources* outlines these impacts, noting that current REE extraction techniques are energy-intensive and environmentally burdensome [127]. Further life cycle assessment analyses, such as those conducted by Schulze [128], reinforce these findings by quantifying the carbon and toxicity footprints associated with conventional REE supply chains. Additionally, the U.S. Geological Survey (USGS) has emphasized that REE mining activities pose considerable risks to aquatic systems and soil stability due to the leaching of heavy metals and acidic compounds during ore processing [129].

In response to these environmental concerns, biotechnology offers an emerging, ecologically responsible alternative for REE recovery, particularly through the use of cyanobacteria. As photosynthetic prokaryotes, cyanobacteria possess cell surface structures enriched with functional groups such as carboxyl, hydroxyl, phosphate, and amino moieties, which exhibit strong affinities for metal ions. Recent studies have demonstrated that these organisms are capable of binding and concentrating REEs from dilute aqueous environments. For instance, a 2023 investigation by Paper *et al*. in *Frontiers in Bioengineering and Biotechnology* reported that engineered cyanobacterial strains could adsorb lanthanides from solution with high specificity and efficiency, highlighting the role of extracellular polymeric substances in metal sequestration [130]. Complementary findings by Dell'Aversano *et al*. [131], published in the *Journal of Chromatography A*, demonstrated the analytical characterization of cyanobacterial metabolites involved in metal binding, employing advanced NMR and LC-MS techniques to identify binding interactions and metal-induced changes in metabolite profiles [131]. Furthermore, emerging experimental models show that even low-cost wild-type cyanobacterial consortia can effectively concentrate REEs from mine tailings or e-waste leachates, making this approach particularly attractive for circular economy applications [130,132].

Unlike conventional techniques, cyanobacterial biosorption operates under ambient conditions, requires minimal chemical input, and produces negligible hazardous waste. As the global demand for rare earths continues to rise, the integration of cyanobacterial biotechnology into REE recovery systems could offer a scalable, low-carbon alternative to current practices, contributing to more sustainable and secure critical material supply chains.

Cyanobacteria have garnered significant attention for their ability to biosorb rare earth elements (REEs), a process facilitated by various cellular mechanisms. The primary mode of REE uptake involves surface adsorption, where functional groups on the cyanobacterial cell wall, such as carboxyl, phosphate, and hydroxyl groups, bind metal ions. Research by Gardea-Torresdey *et al*. [133] highlighted the presence of functional

groups such as carboxyl, aldehyde, sulfhydryl, and phosphoryl in the cell walls, which are responsible for the high ion exchange capacity observed in cyanobacteria. These groups provide the cell wall with an overall negative charge, facilitating the attraction and binding of positively charged metal ions. These interactions are predominantly electrostatic or involve ligand exchange mechanisms. For instance, a study by Paper *et al*. [134] highlighted the role of extracellular polymeric substances (EPS) produced by cyanobacteria in the biosorption of REEs like cerium (Ce), neodymium (Nd), terbium (Tb), and lanthanum (La), emphasizing the significance of these functional groups in metal binding processes [134].

Beyond surface adsorption, certain cyanobacterial strains, notably those from the genera *Nostoc* and *Anabaena*, have demonstrated the capability to internalize and sequester REEs intracellularly. This bioaccumulation often results in the formation of nanoscale aggregates or intracellular crystallization of lanthanides. Such intracellular processes not only aid in detoxification but also present opportunities for the recovery and refinement of these metals. The presence of specialized cells, like heterocysts in *Anabaena*, which are known for nitrogen fixation, might also play a role in metal sequestration, although further research is needed to elucidate this connection [130]. This insights into the biosorption capabilities of cyanobacteria provided by Fischer *et al*. [135] examined the enrichment of europium, samarium, and neodymium by *Anabaena* species, revealed an almost complete (>99%) biosorption of REE within the first hour of exposure, indicating a highly efficient uptake process. The study also utilized laser-induced breakdown spectroscopy (LIBS) and transmission electron microscopy (TEM) to confirm the presence of electron-dense particles, presumably europium, within the vegetative cells, suggesting active intracellular accumulation of REEs [135].

Following biotransformation, cyanobacterial biomass frequently demonstrates an enhanced capacity for metal ion binding. This improvement is often attributed to cell wall remodeling and increased porosity, both of which facilitate the exposure of additional functional groups capable of interacting with metal ions. Notably,

biotransformation-induced stress, such as that triggered by substrate exposure, can stimulate the overproduction of extracellular polymeric substances (EPS). These EPS are enriched with negatively charged functional moieties, including carboxyl, hydroxyl, and phosphate groups, that not only confer cellular protection but also serve as effective metal-binding sites. As highlighted by Paper *et al*. [134], the structural and chemical complexity of EPS plays a critical role in the sequestration of rare earth elements, with their architecture significantly enhancing biosorption efficiency. Inductively Coupled Plasma Mass Spectrometry (ICP-MS) was employed for the quantification of REEs due to its exceptional sensitivity, broad dynamic range, and multi-elemental detection capabilities [136]. This technique is particularly well-suited for trace-level analysis of REEs in complex biological and environmental matrices [137,138].

2.10. Synthetic biology tools, research gaps and prospects

The integration of synthetic biology with microbial biocatalysis has significantly advanced the design of cell factories. Modular DNA assembly methods, such as Golden Gate, Gibson Assembly, and CRISPR-assisted techniques, now allow rapid prototyping of multigene biosynthetic pathways [48,92].

Additionally, systems such as biosensors, feedback loops, and logic gates have been employed to dynamically regulate metabolic flux, ensuring optimal productivity while minimizing cellular stress [91]. For example, metabolite-responsive riboswitches can activate or repress gene expression based on intracellular levels of a key intermediate, maintaining flux balance in long biosynthetic routes.

Microbial cell factories are powerful biocatalytic systems that integrate natural enzymatic selectivity with the robustness and adaptability of engineered metabolism. They represent a cornerstone of green bioprocessing, particularly for complex, multistep chemical synthesis that is impractical or inefficient through chemical catalysis alone. As synthetic biology tools evolve and genome-scale engineering

becomes routine, the versatility, productivity, and scalability of microbial cell factories will continue to improve.

Despite considerable progress, key knowledge gaps include: The molecular mechanisms underlying substrate specificity and enantioselectivity in biocatalysts, including cyanobacteria; genetic tools and metabolic engineering approaches tailored to enhance biocatalytic and biosorptive capacities; long- term stability and reuse potential of cyanobacterial biomass in cyclic processes; integration of cyanobacterial systems with downstream chemical recovery and purification technologies.

The present research affirms cyanobacteria's promising dual role in photobiocatalysis and rare earth element bioaccumulation. Their photosynthetic metabolism, versatile enzymatic toolkit, and metal- binding capabilities uniquely position them for sustainable applications in green chemistry and resource recovery.

CHAPTER THREE

Materials and Methods

3.1. Reagents

Table 5 provides a comprehensive summary of the chemical reagents used in this research.

Table 5. Chemical reagents

Reagent name	Purpose	Source/manufacturer
Photobiocatalysis substrates		
7-Octenoic acid	Substrate	Sigma-Aldrich (USA)
6-Heptenoic acid	Substrate	Sigma-Aldrich (USA)
10-Undecenoic acid	Substrate	Sigma-Aldrich (USA)
4-Pentenoic acid	Substrate	Sigma-Aldrich (USA)
1-Phenylethyl acetate	Substrate	Sigma-Aldrich (USA)
Dimethyl vinylphosphonate	Substrate	Sigma-Aldrich (USA)
Diethyl vinylphosphonate	Substrate	Sigma-Aldrich (USA)
Epoxymethyl dimethyl phosphonate	Substrate	Specific Polymers (France)
Media macronutrients and buffers		
Sodium bicarbonate ($NaHCO_3$)	Carbon source	Chempur (Poland)
Sodium carbonate (Na_2CO_3)	Buffer	Chempur (Poland)
Dipotassium hydrogen phosphate (K_2HPO_4)	Phosphate source	Sigma-Aldrich (USA)
Sodium nitrate ($NaNO_3$)	Nitrogen source	Avantor (Poland)
Potassium sulfate (K_2SO_4)	Sulfate source	Sigma-Aldrich (USA)
Sodium chloride (NaCl)	Osmotic balance	Sigma-Aldrich (USA)
Magnesium sulfate heptahydrate ($MgSO_4 \cdot 7H_2O$)	Magnesium source	Sigma-Aldrich (USA)

Calcium chloride dihydrate ($CaCl_2 \cdot 2H_2O$)	Calcium source	Sigma-Aldrich (USA)
Iron-ammonium citrate	Iron source	Sigma-Aldrich (USA)
Chelators & pH stabilizers		
Disodium EDTA dihydrate ($Na_2EDTA \cdot 2H_2O$)	Chelator	Sigma-Aldrich (USA)
Magnesium sodium EDTA monohydrate	Chelator	Sigma-Aldrich (USA)
Citric acid monohydrate	pH buffer/stop reagent	Sigma-Aldrich (USA)
Micronutrients (trace elements)		
Zinc sulfate tetrahydrate ($ZnSO_4 \cdot 4H_2O$)	Micronutrient	Sigma-Aldrich (USA)
Manganese sulfate heptahydrate ($MnSO_4 \cdot 7H_2O$)	Micronutrient	Sigma-Aldrich (USA)
Boric acid (H_3BO_3)	Micronutrient	Sigma-Aldrich (USA)
Cobalt nitrate hexahydrate ($Co(NO_3)_2 \cdot 6H_2O$)	Micronutrient	Sigma-Aldrich (USA)
Sodium molybdate dihydrate ($Na_2MoO_4 \cdot 2H_2O$)	Micronutrient	Sigma-Aldrich (USA)
Copper sulfate pentahydrate ($CuSO_4 \cdot 5H_2O$)	Micronutrient	Sigma-Aldrich (USA)
Ferrous sulfate heptahydrate ($FeSO_4 \cdot 7H_2O$)	Iron source	Sigma-Aldrich (USA)
Vitamin B_{12} (cyanocobalamin)	Growth factor	Sigma-Aldrich (USA)
Analytical & instrumental reagents		
Deuterated chloroform ($CDCl_3$)	NMR solvent	Sigma-Aldrich (USA)
Triphenyl phosphate (TPP)	NMR internal standard	Sigma-Aldrich (USA)
Anhydrous magnesium sulfate ($MgSO_4$)	Drying agent	Sigma-Aldrich (USA)
Sodium methoxide in methanol	Base catalyst	Sigma-Aldrich (USA)
Dowex® 50W-X8 resin	Ion-exchange catalyst	Sigma-Aldrich (USA)
Acetonitrile	HPLC solvent	Sigma-Aldrich (USA)
Ultrapure water	Universal solvent	In-house (Milli-Q)
Antimicrobial testing reagents		

Dimethyl sulfoxide (DMSO)	Solvent	Sigma-Aldrich (USA)
Cefoperazone	Antibiotic control	Sigma-Aldrich (USA)
Mueller-Hinton agar	Bacterial growth medium	Sigma-Aldrich (USA)
Nutrient broth	Bacterial culture	Sigma-Aldrich (USA)
Sterile paper discs	Antimicrobial diffusion assays	Sigma-Aldrich (USA)

The organic substrates (Figure 4) used for photobiocatalytic transformations in this study include 7-octenoic acid, 6-heptenoic acid, 10-undecenoic acid, 4-pentenoic acid, 1-phenylethyl acetate, dimethyl vinylphosphonate, diethyl vinylphosphonate, and epoxymethyl dimethyl phosphonate. These compounds were procured from Sigma-Aldrich (St. Louis, MO, USA) and Specific Polymers (Castries, France) and were utilized without further purification. Rare earth element salts, namely gadolinium chloride and europium chloride, were obtained from Sigma-Aldrich and applied in both bioaccumulation and ecotoxicological assays to evaluate their uptake and physiological impacts on selected cyanobacterial strains.

Components used in the preparation of cyanobacterial growth media, including Spirulina medium, BG-11, and BG-11_0, were purchased from Sigma-Aldrich, Chempur (Piekary Śląskie, Poland), and Avantor Performance Materials (Gliwice, Poland). These include macronutrients such as sodium bicarbonate, sodium carbonate, dipotassium hydrogen phosphate, sodium nitrate, potassium sulfate, sodium chloride, magnesium sulfate heptahydrate, calcium chloride dihydrate, and iron-ammonium citrate. Additional reagents involved in chelation and pH stabilization, including disodium EDTA dihydrate, magnesium sodium EDTA monohydrate, and citric acid monohydrate, were incorporated as part of standard media formulations. Vitamin B_{12} (cyanocobalamin) was prepared as a 5 mg/L stock solution in sterile distilled water, filter-sterilized, and stored at –20 °C in microcentrifuge tubes wrapped in aluminum foil to prevent photodegradation.

Trace element solutions were prepared using zinc sulfate tetrahydrate, manganese sulfate heptahydrate, boric acid, cobalt nitrate hexahydrate, sodium molybdate dihydrate, copper sulfate pentahydrate, and ferrous sulfate heptahydrate. These micronutrients were incorporated in media according to established protocols for cyanobacterial cultivation and adjusted where necessary to support substrate stability during photobiocatalysis.

Analytical and instrumental reagents used throughout the study were obtained from Sigma-Aldrich except where otherwise specified. These include high-purity solvents such as acetonitrile for HPLC, ultrapure water, and deuterated chloroform ($CDCl_3$) for NMR spectroscopy. Triphenyl phosphate was employed as an internal standard in quantitative phosphorus-31 NMR analysis. Anhydrous magnesium sulfate was used for drying organic extracts, and Dowex® 50W-X8 ion-exchange resin (H^+ form, 200–400 mesh) was used during the chemical synthesis of dimethyl (1*E*)-3-hydroxyprop-1-enylphosphonate. Sodium methoxide in methanol was used as a base catalyst for this chemical synthesis.

The Malachite Green Assay, used for inorganic phosphate quantification, involved reagents also obtained from Sigma-Aldrich unless otherwise stated. These include malachite green dye prepared at a concentration of 0.045% (w/v) in deionized water, ammonium molybdate tetrahydrate dissolved at 4.2% (w/v) in 4 M hydrochloric acid, and a stop solution consisting of 34% (w/v) citric acid monohydrate. Hydrochloric acid was used to prepare a 4 M stock solution, and phosphate standard solutions were prepared using potassium hydrogen phosphate to establish a standard calibration curve.

Reagents employed in the antimicrobial susceptibility testing of DMHPP were similarly sourced from Sigma-Aldrich unless otherwise stated. Dimethyl sulfoxide (DMSO) was used as the solvent for preparing stock and working solutions of DMHPP. Cefoperazone was used as the positive control antibiotic, while sterile paper discs and nutrient broth were used for bacterial inoculation and testing. Mueller-

Hinton agar was prepared according to manufacturer specifications for both disk diffusion and agar well diffusion assays.

All reagents used in this study were of analytical grade or higher, and all solution preparations and handling steps were conducted under aseptic or sterile conditions where required. The consistent use of high-purity reagents ensured the reliability, reproducibility, and accuracy of all experimental procedures, including photobiocatalysis, product purification, analytical quantification, phosphate detection, antimicrobial screening, and rare earth element bioaccumulation.

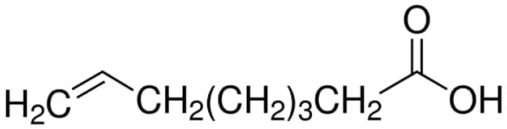

(a) 7-Octenoic acid

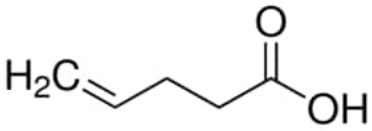

(b) 4-Pentenoic acid

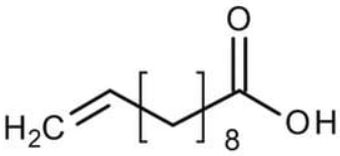

(c) 10-Undecenoic acid

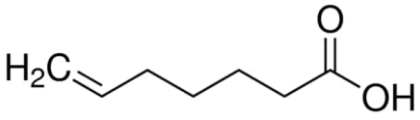

(d) 6-Heptenoic acid

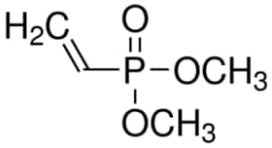

(e) Dimethyl vinylphosphonate

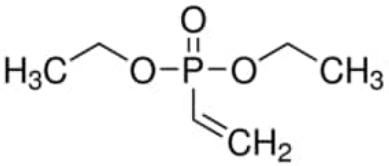

(f) Diethyl vinylphosphonate

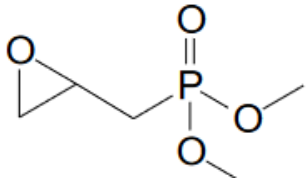

(g) Epoxymethyl dimethyl phosphonate

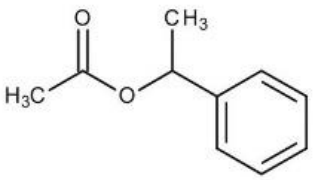

(h) 1-phenylethyl acetate

Figure 4. Selected substrates for photobiocatalysis and bioaccumulation with cyanobacterial strains

3.2. Microorganisms

The primary photobiocatalysts employed in this study (Table 6) were cyanobacterial strains obtained from the Culture Collection of Autotrophic Organisms (CCALA) at the Institute of Botany, Czech Academy of Sciences and Pasteur Culture Collection (PCC), France respectively. These include *Synechococcus bigranulatus* CCALA 187, *Nostoc cf-muscorum* CCALA 129, *Limnospira indica* PCC 8005, *Limnospira maxima* CCALA 27, *Leptolyngbya foveolarum* CCALA 76, and *Kamptonema animale* CCALA 138. Each strain was cultivated in its respective growth medium: BG-11 or BG-11_0 for *Synechococcus* sp., *Nostoc* sp., *Leptolyngbya* sp., and *Kamptonema* sp., and Spirulina Medium for the *Limnospira* sp. The selection of these strains was based on their documented photosynthetic efficiency, metabolic versatility, and previous applications in biocatalysis and bioaccumulation.

In addition to these cyanobacteria, two heterotrophic bacterial species, *Escherichia coli* ATCC8937 (*E. coli*) and *Staphylococcus aureus* ATCC 6538 (*S. aureus*), were included in the study (Table 6) for antimicrobial susceptibility assays. These organisms served as representative Gram-negative and Gram-positive bacteria, respectively, and were selected based on their clinical relevance and frequent application as standard test strains in antimicrobial screening. The bacterial cells were obtained from the stock culture collection of the Faculty of Chemistry, Department of Biochemistry, Molecular Biology, and Biotechnology, Wrocław University of Science and Technology. The bacterial strains were cultivated in sterile nutrient broth under standard aerobic conditions at 37°C with continuous shaking. Prior to antimicrobial assays, cultures were adjusted to a 0.5 McFarland standard, corresponding to approximately 1.5×10^8 CFU/mL, to ensure consistency across replicates.

Table 6. Microbial strains

Microorganism	Strain code	Collection country	Medium	Function
Cyanobacteria (phototrophic)				
Synechococcus bigranulatus	CCALA 187	Czech Republic	BG-11	Biocatalysis/ bioaccumulation
Nostoc cf-Muscorum (cf = *confer*, i.e., similar to *Nostoc muscorum* morphologically)	CCALA 129	Czech Republic	$BG\text{-}11_0$	Biocatalysis
Limnospira indica	PCC 8005	France	SM	Biocatalysis/ bioaccumulation
Limnospira maxima	CCALA 27	Czech Republic	SM	Biocatalysis/ bioaccumulation
Leptolyngbya foveolarum	CCALA 76	Czech Republic	BG-11	Biocatalysis/ bioaccumulation
Kamptonema animale	CCALA 138	Czech Republic	BG-11	Biocatalysis
Nodularia moravica	CCALA 114	Czech Republic	BG-11	Biocatalysis
Heterotrophic bacteria				
Escherichia coli	ATCC8937	WUST	N. b.	Antimicrobial susceptibility testing
Staphylococcus aureus	ATCC 6538	WUST	N. b.	Antimicrobial susceptibility testing

Note: CCALA = Culture Collection of Autotrophic Organisms; PCC = Pasteur Culture Collection; BG = Blue-Green medium; SM = Spirulina medium; N. b. = Nutrient broth; WUST = Wrocław University of Science and Technology, Poland.

Collectively, these phototrophic and heterotrophic microorganisms formed the biological foundation for evaluating both the biocatalytic conversion of

organophosphorus substrates and the subsequent bioactivity of the resulting products, including antimicrobial effects of biotransformation products such as dimethyl (1*E*)-3-hydroxyprop-1-enylphosphonate.

3.3. Analyses

The analytical framework adopted in this study integrates a combination of advanced instrumental and statistical methods to assess photobiocatalytic efficiency, substrate stability, and bioaccumulation outcomes. Quantitative yield and conversion data were derived from validated approaches involving calibration curves, internal standards, and peak integration, standard practices in biocatalysis. For statistical interpretation, replicates and standard deviation metrics ensure the reproducibility and reliability of experimental outcomes.

3.3.1. Instrumental analysis

All instrumental analyses were carried out using calibrated and validated analytical platforms.

3.3.1.1. Nuclear Magnetic Resonance (NMR) Spectroscopy

NMR spectra were acquired using two systems: a Bruker Avance™ 600 MHz NMR spectrometer (Bruker BioSpin GmbH, Billerica, MA, USA), operating at 600.58 MHz for proton (^{1}H) and 243.12 MHz for phosphorus (^{31}P), and a JEOL ECZ 400 S NMR spectrometer (JEOL Ltd., Tokyo, Japan), operating at 161.92 MHz for ^{31}P. Chemical shifts (δ) are reported in parts per million (ppm) relative to tetramethylsilane (TMS), and coupling constants (*J*) are expressed in hertz (Hz). Signal integration of ^{31}P resonances was used to calculate substrate conversion and product yields.

3.3.1.2. High-Performance Liquid Chromatography (HPLC)

Preparative chromatography system for unsaturated fatty acid bioconversion employed ACCQPrep HP125 (Teledyne ISCO, Lincoln, NE, USA), equipped with a built-in UV–Vis detector. Separations were carried out on a Supelcosil™ LC – 18 column (4.6 × 150 mm, 5 μm). The mobile phase consisted of HPLC-grade water

(solvent A) and acetonitrile (solvent B) delivered isocratically at a 50:50 (v/v) ratio with a flow rate of 1.0 mL min^{-1}. Samples were prepared by dissolving 10 mg of each analyte sample in a total of 10 mL of HPLC solvent (5 mL deionized H_2O + 5 mL acetonitrile). A 100 μL aliquot of each 1.0 mg mL^{-1} solution was injected for analysis. UV–Vis detector was set to measure absorbances at 210 and 220 nm respectively. Chromatographic peaks were recorded and identified based on retention time.

3.3.1.3. Gas Chromatography (GC)

GC analyses for the enantiomeric resolution and quantification of 1-PEAc and its chiral bioconversion products were performed on a Shimadzu GC-2010 Plus system (Shimadzu Corporation, Japan) equipped with a flame ionization detector (FID) powered by compressed air and hydrogen. Measurements were made using a Chirasil-DEX CB column ((25 m × 0.25 mm, 0.25 μm); (Agilent, Santa Clara, USA)) and nitrogen as the carrier gas. In the standard program, lasting 21 min, the initial column temperature 110°C was maintained for 15 min and then increased to 200°C at a rate of 15.0°C min^{-1}. The FID temperature was 200°C, and the nitrogen, air, and hydrogen flows were set at 30 mL min^{-1}, 400 mL min^{-1}, and 40 mL min^{-1}, respectively. Analyses were performed in split (20:1) mode at an SPL1 temperature of 200°C and a flow rate of 1.2 mL min^{-1}; the injection volume was 1 μL. Standard retention times were 10.49 and 12.19 min for 1-PEAc, and 15.97 and 16.73 min for 1-phenylethanol respectively.

3.3.1.4. Mass Spectrometry (MS)

High-resolution mass spectrometry (HRMS) was conducted using a Waters LCT Premier™ XE time-of-flight mass spectrometer (Waters Corporation, Milford, MA, USA), equipped with an electrospray ionization (ESI) source operating in positive ion mode. Molecular weights and elemental compositions of products were confirmed using exact mass measurements.

3.3.1.5. Product (DMHPP) purification

Crude DMHPP was purified via preparative high-performance liquid chromatography (HPLC) using a Teledyne ISCO ACCQPrep HP125 system with a

RediSep® Prep C18 reversed-phase column (250 mm × 10 mm, 5 μm). Elution was carried out using a programmed gradient of water and acetonitrile: 10% acetonitrile isocratic for 10 minutes, a linear increase to 30% over 10 minutes, and isocratic elution at 30% for an additional 10 minutes. The flow rate was 5 mL/min. The primary product of EMDP bioconversion eluted at a retention time of 23 minutes. Additional purification of DMHPP was performed using a CombiFlash® Rf 150 system and a PuriFlash® C18-HP column [139,140].

3.3.1.6. UV-Visible Spectrophotometry

Spectrophotometric analyses were performed using a UV–Vis spectrophotometer (Lambda Bio, PerkinElmer Inc., Waltham, MA, USA). Inorganic phosphate concentrations were quantified using the malachite green assay, with absorbance measured at 620 nm. Cyanobacterial growth was monitored at 720 nm, and chlorophyll content was estimated via absorbance at 682 nm.

3.3.1.7. Inductively Coupled Plasma Mass Spectrometry (ICP-MS)

Elemental analysis of rare earth element (REE) accumulation was performed on an Elan DRC-e (Perkin Elmer, Concord, ON, Canada) equipped with a concentric PTFE nebulizer and cyclonic spray chamber. Samples were subjected to acid digestion and diluted appropriately. Calibration was achieved using certified multielement standards, and detection was carried out in standard mode.

3.3.1.8. Optical Microscopy

Cyanobacterial cell morphology and culture purity were examined using an Axio Lab.A1 transmitted light microscope (Carl Zeiss AG, Oberkochen, Germany) equipped with a high-resolution camera. Microscopic evaluation was carried out at magnifications up to 600×, and images were digitally recorded for documentation.

3.3.2. Statistical analysis

All experiments were conducted in triplicate, unless otherwise stated, to ensure reproducibility and statistical reliability. Descriptive statistics were applied to both

quantitative and qualitative data obtained from spectrophotometric, chromatographic, gravimetric, and spectroscopic analyses. Data were primarily analysed using spreadsheet software, with results expressed as mean values. Standard deviations (± SD) were calculated to quantify variability across replicates. A variation below 15% between replicates was considered acceptable, consistent with standard practices in biocatalytic and bioaccumulation studies [141,142].

3.3.2.1. Quantification of biotransformation efficiency via GC

For biotransformation reactions, the conversion degree (CD) was determined using peak area integration from chromatograms. The conversion percentage was calculated as:

$$\text{Conversion degree (\%)} = \left(\frac{A_p}{A_s + A_p}\right) \text{x } 100$$

where, A_s is the initial peak area of the substrate, and A_p is the peak area of the product. This formula was used to assess the substrate conversion across various time intervals during photobiocatalysis [143–145].

3.3.2.2. Evaluation of enantioselectivity via chiral gas chromatography

The enantiomeric excess (e.e.) of chiral products, particularly in the conversion of 1-phenylethyl acetate, was determined using chiral gas chromatography. The enantiomeric excess was calculated using the formula:

$$\text{e.e. (\%)} = \left|\frac{R-S}{R+S}\right| \text{ x } 100$$

where R and S are the integrated peak areas of the (*R*)- and (*S*)-enantiomers, respectively. This metric was used to evaluate the enantioselectivity of cyanobacterial strains, particularly *S. bigranulatus* CCALA 187 and *L. foveolarum* CCALA 76 [44,146].

3.3.2.3. Conversion degree assessment using ^{31}P NMR spectroscopy

In cases where biotransformation progress was monitored using ^{31}P NMR spectroscopy, the conversion degree was calculated by integrating the resonance

signals corresponding to the phosphorus nuclei in the substrate and product, using the formula:

$$\text{Conversion degree (\%)} = \left(\frac{Ip}{Is+Ip}\right) \text{x } 100$$

where Is and Ip are the integrated intensities of the substrate and product phosphorus signals, respectively. This approach was applied in the transformation of phosphonate-containing compounds such as vinyl and epoxy phosphonates respectively, allowing semi-quantitative estimation of conversion [147–149].

3.3.2.4. Calibration-based quantification of inorganic phosphate using malachite green assay

Standard calibration curves were generated by plotting absorbance at 620 nm against known phosphate concentrations. Linear regression was used to derive the best-fit line, and sample concentrations were interpolated from this curve using the equation:

$$[\text{Phosphate}] = \frac{A_{620} - b}{m}$$

where A_{620} is the measured absorbance, m is the slope, and b is the intercept of the regression line. The method was used to quantify free phosphate released during the photobiocatalytic transformation of organophosphonates [150–152].

3.3.2.5. Quantitative yield determination of DMHPP via internal standardized ^{31}P NMR

Quantitative yield of the product, dimethyl (1*E*)-3-hydroxyprop-1-enylphosphonate was achieved using ^{31}P NMR spectroscopy with triphenyl phosphate (TPP) as an internal standard [153–155]. The molar yield of DMHPP was calculated relative to the known concentration of TPP using integrated NMR peak areas. The formula used was:

$$n_p = \left(\frac{I_p}{I_s}\right) \text{x } n_s$$

Where n_P and n_s represent the amount (mmol) of product (DMHPP) and the amount (mmol) of internal standard (TPP) respectively, while I_P and I_s represent their

respective integrated intensities. Yields were subsequently expressed as percentages relative to the amount as:

$$\text{Yield (\%)} = \left(\frac{\text{Amount of product obtained (mol)}}{\text{Theoretical amount of product (mol)}}\right) \text{x } 100$$

This approach provided reproducible quantitative data for product formation, with mean values and standard deviations calculated from the triplicate NMR measurements.

3.4. Cyanobacterial media preparation

Cyanobacterial growth media were prepared according to standard laboratory protocols [156], with particular attention to nutrient composition and sterility (Table 7 and Table 8).

3.4.1. Spirulina medium

The Spirulina medium was constituted by preparing three essential components: Solution 1, Solution 2, and a trace element solution (Table 7 and Table 9). The trace element solution was formulated in accordance with the specified concentrations and stored under refrigeration to maintain chemical stability. Additionally, the Vitamin B_{12} stock solution was prepared by dissolving 5 mg of cyanocobalamin in 1 L of sterile distilled water. This solution was subsequently filter-sterilized, aliquoted into 1.5 mL microcentrifuge tubes, wrapped in aluminium foil to prevent photodegradation, and stored frozen until use.

To prepare Solution 1, 500 mL of distilled water was transferred into a beaker containing a magnetic stir bar, and the mixture was gently heated to a temperature range of 50 to 60 °C. The components designated under “Spirulina Medium (Solution 1)” in Table 7 were added sequentially to the warmed water. Each solute was allowed to dissolve completely before the subsequent component was introduced, to prevent precipitation and ensure a homogenous solution.

A similar approach was employed in the preparation of Solution 2. An additional 500 mL of distilled water was dispensed into a separate beaker, equipped with a stir bar, and heated to 50–60 °C. The ingredients listed under "Spirulina Medium (Solution 2)" in Table 7 were added individually, ensuring complete dissolution before adding the next. It was critical at this stage to omit the addition of Vitamin B_{12}, which is heat-labile and was instead incorporated after sterilization.

Solution 1 was prepared in a container with double the required volume capacity to allow for easy combination with Solution 2. Both solutions were sterilized using appropriate sterilization techniques. Upon cooling, the previously prepared and frozen Vitamin B_{12} solution was aseptically introduced into Solution 2 and mixed gently but thoroughly. Subsequently, Solution 1 and Solution 2 were combined under sterile conditions to yield 1 L of complete Spirulina growth medium (Table 7).

Table 7. Spirulina medium composition and it's modification

Ingredient	**Solution 1 (per 0.5 L dH_2O)**	**Solution 2 (per 0.5 L dH_2O)**	**Modified medium (per 1 L dH_2O)**
$NaHCO_3$	13.61 g	—	1.0 g
Na_2CO_3	4.03 g	—	0.2 g
K_2HPO_4	0.50 g	—	1.0 g
$Na_2EDTA{\cdot}2H_2O$	—	0.08 g	0.08 g
$NaNO_3$	—	2.5 g	2.5 g
K_2SO_4	—	1.0 g	Removed
NaCl	—	1.0 g	Removed
$MgSO_4{\cdot}7H_2O$	—	0.2 g	0.2 g
$CaCl_2{\cdot}2H_2O$	—	0.04 g	0.04 g
$FeSO_4{\cdot}7H_2O$	—	0.01 g	—
Iron-ammonium citrate	—	—	1 mL (from BG-11 stock)

Trace element solution (SM)	—	1 mL	—
Trace element solution (BG-11)	—	—	1 mL
Vitamin B_{12}	—	1 mL	1 mL

Note: "–" denotes a non-applicable ingredient.

3.4.2. BG-11/BG-11$_0$ medium

The preparation of BG-11$_0$ medium was identical to that of BG-11, except for the exclusion of sodium nitrate ($NaNO_3$) as a nitrogen source. This modification was used to support the growth of nitrogen-fixing cyanobacteria such as *Nostoc* sp., which do not require an external nitrogen source due to their ability to fix atmospheric nitrogen [157].

Table 8. BG-11/BG-11$_0$ medium composition and it's modification

Ingredient	**BG-11 Stock Solution (g/10 mL H_2O)**	**BG-11 Medium (per 1 L)**	**Modified BG-11 Medium (per 1 L)**
K_2HPO_4	0.4	1 mL	1 mL
$Na_2EDTA{\cdot}2H_2O$	0.1	1 mL	1 mL
$NaNO_3$	—	1.5 g	1.5 g
$MgSO_4{\cdot}7H_2O$	0.75	1 mL	1 mL
$CaCl_2{\cdot}2H_2O$	0.36	1 mL	1 mL
Iron-ammonium citrate	0.06	1 mL	1 mL
Citric acid monohydrate	0.06	1 mL	1 mL
$MgNa_2EDTA{\cdot}H_2O$	0.1	1 mL	1 mL
Trace element solution	—	1 mL	1 mL
Vitamin B_{12} solution	—	—	1 mL

Note: "–" denotes a non-applicable ingredient.

Stock solutions of the BG-11/BG-11$_0$ components were prepared by dissolving the relevant quantities of each component (Table 8), in 10 mL of distilled water. These

stock solutions were stored under refrigeration to preserve their integrity until required.

For the preparation of 1 L of BG-11 or BG-11$_0$ medium, 960 mL of distilled water was preheated to 50–60 °C in a sterile beaker containing a magnetic stir bar. Initially, 1 mL of $MgNa_2EDTA{\cdot}H_2O$ stock solution was added to the preheated water and allowed to dissolve completely. Immediately prior to use, 1.5 g of $NaNO_3$ was weighed and added to the medium, ensuring full dissolution; this step was omitted in the preparation of BG-11$_0$ medium. Subsequently, 1 mL each of citric acid, $MgSO_4{\cdot}7H_2O$, and $CaCl_2{\cdot}2H_2O$ stock solutions were added sequentially, with gentle stirring and a wait period of approximately 10 minutes to ensure thorough integration.

Meanwhile, four additional tubes were prepared, each containing 1 mL of the following stock solutions: Na_2CO_3, $K_2HPO_4{\cdot}3H_2O$, iron-ammonium citrate, and the trace elements solution (Table 9). Each of these tubes was made up to a total volume of 10 mL using distilled water. The contents of all bottles and tubes were sterilized appropriately. Once sterilized and cooled, the contents of the four tubes were aseptically transferred into the main preparation bottle. The mixture was gently stirred to ensure homogeneity, and the final volume was adjusted to 1 L, thus completing the preparation of sterile BG-11 or BG-11$_0$ medium suitable for cyanobacterial culture (Table 8).

Table 9. Trace element composition in spirulina and BG-11 media

Ingredient	Spirulina Medium (g/L dH_2O)	BG-11 Medium (g/L dH_2O)
$ZnSO_4{\cdot}4H_2O$	1.0	0.220
$MnSO_4{\cdot}7H_2O$	2.0	1.810
H_3BO_3	10.0	2.860
$Co(NO_3)_2{\cdot}6H_2O$	1.0	0.0494
$Na_2MoO_4{\cdot}2H_2O$	1.0	0.391
$CuSO_4{\cdot}5H_2O$	0.005	0.079
$Na_2EDTA{\cdot}2H_2O$	0.8	—

$FeSO_4 \cdot 7H_2O$	0.7	—

Note: "–" denotes a non-applicable ingredient.

3.5. Media modification for *Limnospira* sp.: balancing growth promotion with epoxymethyl dimethylphosphonate stability

The modifications introduced in Table 7 and Table 8 reflect a deliberate optimization of the cyanobacterial growth media with the primary aim of minimizing the degradation of the substrate epoxymethyl dimethylphosphonate during a 7-day incubation period, while simultaneously enhancing the growth performance of *Limnospira* species. The changes represent a strategic balance between maintaining the physiological requirements of cyanobacterial cultures and mitigating adverse chemical interactions that could compromise experimental integrity. In the modified Spirulina medium, the concentration of sodium bicarbonate ($NaHCO_3$) was significantly reduced from 13.61 g/500 mL (equivalent to ~27.22 g/L) to 1.0 g/L. This reduction was necessary to limit the excessive alkalinity typically induced by high bicarbonate concentrations, which can destabilize organophosphonate compounds like EMDP through non-enzymatic hydrolysis or base-catalyzed degradation mechanisms [160]. Likewise, sodium carbonate (Na_2CO_3) was reduced to 0.2 g/L to support minimal buffering while avoiding synergistic effects that might exacerbate pH elevation.

Furthermore, the phosphate content, provided as K_2HPO_4, was slightly increased to 1.0 g/L in the modified Spirulina medium. Phosphate acts as both a macro-nutrient and a buffering agent; however, it can also catalyze organophosphorus breakdown when present at high concentrations or in the presence of metal ions. The increase here reflects a compromise to support cyanobacterial growth, particularly under nutrient-limited conditions, without reaching levels that would pose a significant risk to substrate integrity.

Iron availability was carefully modulated, as iron salts - especially in the presence of EDTA - can catalyze Fenton-type reactions that generate reactive oxygen species, potentially leading to oxidative degradation of sensitive substrates [161]. Therefore,

the iron-ammonium citrate concentration was narrowed to 0.06 g/L to ensure sufficient micronutrient availability while minimizing redox reactivity. Similarly, magnesium sulfate ($MgSO_4 \cdot 7H_2O$) and calcium chloride ($CaCl_2 \cdot 2H_2O$) concentrations were moderately adjusted to match physiological requirements without promoting excess ion exchange that might destabilize substrate molecules.

Sodium chloride (NaCl) and potassium sulfate (K_2SO_4) were deliberately excluded from the modified Spirulina medium to reduce ionic strength and minimize potential substrate destabilization. These salts, although commonly included for osmotic balance and sulfur supply, were deemed unnecessary in this context, as their absence does not hinder cyanobacterial growth under controlled laboratory conditions [162]. Their exclusion reduces the ionic complexity of the medium, which could otherwise facilitate unintended chemical interactions with EMDP.

The inclusion of Vitamin B_{12} (cyanocobalamin) at a concentration of 1 mL/L in both modified media formulations reflects its documented role in supporting the growth of *Limnospira* sp., which, although capable of photoautotrophic growth, may benefit from exogenous B_{12} under nutrient-stressed or experimental conditions [163,164]. Additionally, B_{12} has been shown to enhance cellular enzymatic stability, indirectly contributing to reduced substrate degradation.

In the modified BG-11 medium, the core macronutrients remained largely unchanged. However, Vitamin B_{12} was added to the formulation of modified BG-11 to support enhanced growth kinetics of *Limnospira* sp., which were co-cultivated in the system. More importantly, B_{12}'s role in preventing EMDP degradation was highlighted, possibly through its coenzyme functions in cellular redox regulation and metabolic stabilization [165]. The trace elements solution remained consistent with standard BG-11 to retain microelement sufficiency, while the adjusted iron and phosphate contents paralleled those in the Spirulina modifications to ensure compatibility across both media types.

The modified media formulations represent a targeted re-design of classical cyanobacterial growth media to support both biomass productivity and the stability of chemically sensitive substrates. These changes exemplify an integration of microbiological growth requirements with organic substrate stability considerations, making them a potential consideration for photobiocatalytic assays involving EMDP and related organophosphorus compounds.

3.6. Substrate stability analysis

The stability of the substrates in culture media was assessed to ensure their suitability for biotransformation. Each substrate (1 mM) was incubated in BG-11, BG-11_0, and Spirulina media for 7 days and analyzed using HPLC and NMR to detect any degradation or transformation.

3.7. Culturing of cyanobacterial strains

Cyanobacterial strains were aseptically inoculated into 250 mL Erlenmeyer flasks containing 100 mL of the appropriate growth medium. However, modified SM and BG-11 were used in addition to the unmodified media for the culturing of *Limnospira* sp. Cultures were maintained in a controlled photobioreactor system parameters such as, continuous illumination at an intensity of 15 – 22 μmol photons m^{-2} s^{-1}, provided by a Power Glo fluorescent bulb (30W, Hagen, QC, Canada); the incubation temperature was maintained at 29 ± 1°C under sterile conditions, with cultivation periods ranging from 14 to 21 days, depending on the strain-specific growth requirements. Cyanobacterial growth was monitored spectrophotometrically by measuring optical density at 720 nm (OD_{720}).

3.8. Biotransformation process

The biotransformation process focused on assessing the capacity of cyanobacterial cultures to convert selected substrates under defined experimental conditions. This step involved preparing actively growing biomass, introducing the substrates at specified concentrations, and maintaining the reactions under controlled light and temperature regimes. The process was monitored to ensure reproducibility and to

generate reliable data for subsequent analysis of product formation and in bioaccumulation phase.

The photobiocatalytic reaction was initiated by introducing an appropriate aliquot of the substrate into 100 mL of cyanobacterial biomass suspension, followed by gentle agitation to ensure homogenous distribution and achieve a final substrate concentration of 1 mM (as detailed in Table 10). Cultures were incubated for 1 to 7 days under defined light and temperature conditions to assess substrate conversion efficiency. All experiments were performed in triplicate to ensure reproducibility. Upon completion of the biotransformation, the cultures were centrifuged at 4000 rpm for 20 minutes to separate the biomass, and the resulting supernatant was carefully decanted. The supernatant was extracted twice with 50 mL of ethyl acetate. The combined organic phases were dried over anhydrous magnesium sulfate ($MgSO_4$) for 24 hours, filtered, and then concentrated under reduced pressure using a rotary evaporator (IKA® RV 10 digital, with HB 10 digital heating bath, IKA-Werke GmbH & Co. KG, Staufen, Germany) set at 60 °C.

Table 10. Substrate-specific bioconversion by cyanobacterial strains

Substrate	**Amount (mg/100 mL biocatalyst) – 1 mM**	**Biocatalyst (14 to 21 days culture)**	**Scalability (mg/ 100 mL biocatalyst) – 4 mM**
7-Octenoic acid	15.3	*Synechococcus* sp., *Nostoc* sp., *Kamptonema* sp., *Limnospira* sp.	-
6-Heptenoic acid	13.5	*Synechococcus* sp., *Nostoc* sp., *Kamptonema* sp., *Limnospira* sp.	-
10-Undecenoic acid	20.0	*Synechococcus* sp., *Nostoc* sp., *Kamptonema* sp., *Limnospira* sp.	-

4-Pentenoic acid	10.0	*Synechococcus* sp., *Nostoc* sp., *Kamptonema* sp., *Limnospira* sp.	-
Dimethyl vinylphosphonate	16.0	*Synechococcus* sp., *Nostoc* sp., *Kamptonema* sp., *Limnospira* sp.	-
Diethyl vinylphosphonate	16.0	*Synechococcus* sp., *Nostoc* sp., *Kamptonema* sp., *Limnospira* sp.	-
1-phenylethyl acetate	16.2	*Synechococcus* sp., *Leptolyngbya* sp.	-
Epoxymethyl dimethyl phosphonate	16.6	*Synechococcus* sp., *Limnospira* sp. *Nostoc sp.* *Nodularia moravica*	**66.4** [Applied only for *Synechococcus* sp.]

Note: "–" denotes that scalability is not applicable.

3.8.1. Product purification and analysis

Following the biotransformation process, the resulting oily residue, supposed to contain the target product, was subjected to purification using a High-Pressure Preparative Liquid Chromatography system (Teledyne ISCO ACCQPrep HP125, Lincoln, NE, USA) equipped with a reversed-phase RediSep Prep C18 column (5 μm, 250 mm; Teledyne ISCO, Lincoln, NE, USA). The purification protocol employed a gradient elution as follows: an initial isocratic phase with 10% acetonitrile in water for 10 minutes; a transition to 15% acetonitrile for 5 minutes; a linear gradient from 15% to 30% acetonitrile over the next 5 minutes; followed by a final isocratic phase with 30% acetonitrile for 10 minutes. The flow rate was maintained at 5 mL/min, with the target compound eluting at approximately 23 minutes (Rf_1 = 23 min). The purified products were subsequently characterized and confirmed using analytical techniques

including Gas Chromatography (GC), Mass Spectrometry (MS), Infrared Spectroscopy (IR), and Nuclear Magnetic Resonance Spectroscopy (NMR).

3.8.2. *In-vitro* chemical synthesis of dimethyl (1*E*)-3-hydroxyprop-1-enylphosphonate

To complement the biocatalytic route, the target compound, dimethyl (1*E*)-3-hydroxyprop-1-enylphosphonate, was also synthesized via a chemical method [166]. In this procedure, sodium methoxide in methanol (0.1 equivalents) was added dropwise to a stirred solution of epoxymethyl dimethyl phosphonate (3.01 mmol, 500 mg) at 0 °C. Following complete addition, the reaction mixture was maintained under stirring at ambient temperature for 1 hour. Subsequently, 2.00 g of Dowex® 50W-X8 (H^+) ion-exchange resin (200–400 mesh; Sigma-Aldrich, St. Louis, MO, USA), pre-conditioned with methanol, was introduced to quench the reaction. The mixture was stirred for an additional 15 minutes, after which the resin was removed by filtration and rinsed with methanol. The combined filtrates were concentrated under reduced pressure to afford the crude product (490 mg). Purification of the crude compound was carried out using similar method described in section 3.8.1 - a CombiFlash® Rf 150 flash chromatography system (Teledyne ISCO, Lincoln, NE, USA) equipped with a PuriFlash® C18-HP reversed-phase column (15 μm, 25 g; Teledyne ISCO). An isocratic elution with ultrapure water at a flow rate of 10 mL/min was employed, yielding the target compound at a retention time (Rf) of 2.5 minutes.

Structural elucidation of the purified product was performed by Nuclear Magnetic Resonance (NMR) spectroscopy. Assignments of chemical shifts in the ^{1}H and ^{13}C NMR spectra were confirmed using two-dimensional correlation techniques including $^{1\text{-}1}H$ COSY, ^{1}H-^{13}C HMQC, and ^{1}H-^{13}C HMBC spectra. The spectral data were found to be in agreement with literature values [167]. This synthetic protocol yielded DMHPP with an isolated yield of 81.4% and a purity of 85%.

3.8.3. Malachite Green phosphate assay

The Malachite Green assay is a well-established colorimetric method for detecting inorganic phosphate (Pi) in aqueous solutions. In the present study, the assay was utilized to confirm the release of trace amounts of phosphate during photobiocatalysis involving dimethyl vinylphosphonate and cyanobacterial species, specifically *Nostoc cf-muscorum* CCALA 129, *Synechococcus bigranulatus* CCALA 187, *Limnospira indica* PCC 8005, and *Limnospira maxima* CCALA 27. The analytical method is based on the formation of a green-colored complex resulting from the interaction of phosphate ions with malachite green dye ($C_{23}H_{25}ClN_2$) and ammonium molybdate under acidic conditions. This complex exhibits maximum absorbance in the range of 620 to 650 nm, allowing its quantification via spectrophotometry. The assay is widely used in biochemical and environmental research for accurate phosphate determination [168–170].

To prepare the assay reagents, the Malachite Green solution was formulated at a concentration of 0.045% (w/v) in deionized water. The ammonium molybdate solution was prepared by dissolving 4.2% (w/v) ammonium molybdate tetrahydrate ($(NH_4)_6Mo_7O_{24}{\cdot}4H_2O$) in 4 M hydrochloric acid (HCl). The stop solution consisted of 61.88 g of citric acid monohydrate ($C_6H_8O_7{\cdot}H_2O$) dissolved in 100 mL of deionized water, resulting in a 34% (w/v) citric acid solution. A 4 M HCl stock solution was prepared by carefully adding 170 mL of concentrated HCl (35-38 %, 36.46 g/mol) to deionized water and diluted to a final volume of 500 mL. The phosphate standard stock solution was prepared by dissolving 0.0871 g of potassium hydrogen phosphate (K_2HPO_4) in 50 mL of deionized water, yielding a 10 mM standard [168].

A series of standard solutions was prepared from the 10 mM phosphate stock to establish a calibration curve. The concentrations used included 0.1 mM, 0.5 mM, 1.0 mM, 2.0 mM, and 5.0 mM, with deionized water serving as the blank. Each standard was prepared through volumetric dilution using precise aliquots of the stock solution added to deionized water in a total volume of 10 mL.

The Malachite Reagent used in the assay was freshly prepared by mixing 30 mL of the Malachite Green solution with 70 mL of the ammonium molybdate solution. For each assay, 1 mL of either the phosphate standard or the test sample was transferred to labeled test tubes. Subsequently, 1 mL of the Malachite Reagent was added to each tube, and the contents were gently mixed. The reactions were allowed to proceed for approximately 20 minutes at ambient temperature. Then, the reactions were terminated by the addition of 200 μL of the 34% citric acid solution, followed by thorough mixing. The absorbance of each mixture was recorded at 620 nm using a UV-Vis spectrophotometer [171].

Quantitative analysis of phosphate concentration in the samples was performed by plotting the absorbance values of the phosphate standards against their respective concentrations to generate a calibration curve. A linear regression model was applied to derive the best-fit line, from which the phosphate concentration of unknown samples was determined.

The assay was applied to assess phosphate content in selected media and biological samples. These included BG-11, BG-11$_0$, and Spirulina Medium (SM), along with 21-day cultures of *Synechococcus bigranulatus* CCALA 187, *Limnospira indica* PCC 8005, *Limnospira maxima* CCALA 27, and *Nostoc cf-muscorum* CCALA 129 both prior to and following substrate addition. In addition, bioconversion experiments involving DMVP were analyzed, including three-day reactions with *Synechococcus bigranulatus* CCALA 187, *Limnospira indica* PCC 8005, and *Limnospira maxima* CCALA 27, and a seven-day reaction with *Nostoc cf-muscorum* CCALA 129.

3.8.4. Antimicrobial susceptibility testing using disk and agar well diffusion methods

The antibacterial activity of dimethyl (1*E*)-3-hydroxyprop-1-enylphosphonate was evaluated using disk diffusion and agar well diffusion methods against *Escherichia coli* (Gram-negative) and *Staphylococcus aureus* (Gram-positive) on Mueller-Hinton agar. DMHPP solutions at varying concentrations were applied to sterile filter discs and

agar wells, with cefoperazone as a positive control and dimethyl sulfoxide (DMSO) as negative controls. After incubation at 37°C for 16–24 hours, inhibition zones were measured to assess antibacterial efficacy.

The DMHPP stock solution was prepared by dissolving 15.8 mg of DMHPP in 1 mL of DMSO to obtain a concentration of 15.8 mg/mL. Serial dilutions were performed to achieve additional concentrations of 7.9 mg/mL, 3.95 mg/mL, and 1.98 mg/mL. The preparation followed standard antimicrobial susceptibility testing procedures as outlined in the Kirby-Bauer disk diffusion susceptibility test protocol [172,173].

Bacterial cultures were inoculated in sterile nutrient broth using aseptic techniques and incubated at 37°C for 12 to 16 hours in a shaking incubator set at 150 to 200 rpm. The bacterial suspension was adjusted to a 0.5 McFarland turbidity standard, corresponding to an optical density at 600 nm of 0.1, which equates to approximately 1.5×10^8 CFU/mL [174].

Mueller-Hinton agar was prepared according to the manufacturer's instructions. A 1 mL aliquot of the bacterial suspension was evenly spread over the agar surface to ensure uniform distribution. Excess culture was removed using a sterile pipette, ensuring consistency in microbial growth assessment [172].

For the disk diffusion method, sterile paper discs were impregnated with 20 μL of each DMHPP concentration and allowed to absorb under a laminar flow hood. The negative control consisted of solvent only, while the positive control used cefoperazone. The discs were placed on the bacterial lawn using sterile forceps, ensuring appropriate spacing to prevent overlapping zones of inhibition. Each experiment was performed in triplicate to ensure reproducibility, in accordance with established antimicrobial susceptibility testing protocols [172,173].

For the agar well diffusion method, a sterile tip borer was used to create 6 mm diameter wells in the agar. The wells were spaced at least 2 to 3 cm apart. Volumes of 70 μL of each DMHPP concentration were added into separate wells. The positive control involved placing an antibiotic disc (cefoperazone, 30 μg) directly onto the bacterial

lawn. The negative control consisted of 70 μL of solvent. Each assay was conducted in triplicate.

Agar plates were incubated at 37°C for 16 to 24 hours. Zones of inhibition were measured using a ruler to assess antibacterial activity. Comparative analyses were conducted based on inhibition zone diameters to evaluate the efficacy of DMHPP against bacterial strains [172].

3.8.5. Scaling-up process

The process optimization phase involved a systematic scale-up strategy aimed at enhancing the photobiocatalytic performance of the system using *Synechococcus* species and the target substrate, epoxymethyl dimethylphosphonate. This optimization effort involved a stepwise increase in EMDP concentration from 1 mM to 4 mM, while strictly maintaining constant parameters such as the culture volume, light intensity, temperature, aeration, and nutrient compositions. The rationale behind this design was to examine the impact of substrate loading on catalytic performance without introducing confounding variables, thereby enabling a precise evaluation of system tolerance and reaction kinetics at elevated substrate levels.

Among the cyanobacterial strains assessed, *Synechococcus bigranulatus* CCALA 187 demonstrated exceptional catalytic robustness, exhibiting sustained metabolic activity, growth viability, and efficient substrate conversion even at high tested concentration. Its superior photobiocatalytic profile, marked by high substrate turnover and minimal physiological stress (such as decreased growth rate or pigment loss), distinguished it as the most promising chassis for biotechnological exploitation. Consequently, *S. bigranulatus* was selected as the reference strain for downstream process optimization and scale-up studies, establishing a foundational model for the development of scalable photobiocatalytic platforms targeting organophosphonate compounds.

3.8.6. Product yield

The product yield of dimethyl (1*E*)-3-hydroxyprop-1-enylphosphonate, synthesized via the biocatalytic transformation of epoxymethyl dimethyl phosphonate, was

determined using quantitative ^{31}P NMR spectroscopy. This analytical technique enables direct, non-destructive quantification of phosphorus-containing compounds in a homogeneous solution, offering both structural and concentration information with high specificity [153].

To determine the yield, Triphenyl Phosphate (TPP) was employed as an internal standard. A known mass of the standard (10 mg), corresponding to a molar concentration of 32.2 mM, was co-dissolved with the reaction mixture in 1 mL of deuterated chloroform ($CDCl_3$). The sample thus contained both the biotransformation product (DMHPP) and the standard (TPP) within the same NMR tube. The use of an internal standard allows for quantitative comparison of integrated peak areas in the ^{31}P NMR spectrum, correlating signal intensity with molar concentration under identical experimental conditions [175].

Product yield was evaluated for two substrate concentrations: an initial concentration of 1 mM EMDP in early bench-scale experiments and a scaled-up concentration of 4 mM EMDP in subsequent photobiocatalytic runs. For the 1 mM setup, samples were taken after approximately 3 days, at which point complete bioconversion was observed. For the 4 mM runs, complete biotransformation was achieved between days 5 to 9, with samples taken at day 5, day 7, and day 9 to confirm reproducibility and monitor potential degradation.

3.9. Bioaccumulation process

This phase focused on how the cyanobacterial strains interact with and retain REEs under controlled conditions. Cultures were exposed to measured amounts of gadolinium and europium, after which the biomass was collected and analyzed to determine the extent of accumulation. This allowed a clear comparison of uptake capacity between strains and an evaluation of whether prior biotransformation influenced their sequestration potential.

3.9.1. Ecotoxicological screening

Both pre-bioconversion and post-bioconversion cyanobacterial biomasses, obtained as cell pellets after centrifugation during the photobiocatalysis phase, were assessed for their tolerance to, and bioaccumulation capacity of REEs, specifically Gd and Eu. Stock solutions of each REE were prepared in sterile BG-11 medium and SM at 8 mM by dissolving 0.084 g of $GdCl_3$ or 0.083 g of $EuCl_3$ in 40 mL. Working concentrations for preliminary ecotoxicity screening were prepared as nominal exposure levels of 20, 40, and 80 μM. Growth inhibition tests (72 h) were conducted according to OECD Test Guideline 201 (Freshwater Alga and Cyanobacteria, Growth Inhibition Test) in sterile 96-well polystyrene microtiter plates to determine sublethal concentrations for each cyanobacterial strain. Cyanobacterial inocula were standardized to 400,000 cells/mL based on absorbance measurements and diluted 1:1 with treatment solutions to yield final test concentrations of 200,000 cells/mL. Each well received 125 μL of REE treatment and 125 μL of the algal suspension, resulting in 250 μL total volume. Columns designated for controls include biomass without REE exposure (post- and pre-bioconversion) and blanks containing only SM and BG-11 medium respectively. Plates were incubated under the same temperature (29 ± 1 °C) and illumination regime (*Limnospira* sp. and *Leptolyngbya* sp. were exposed to 60–69 μmol photons·m^{-2}·s^{-1}, while *Synechococcus* sp. was exposed to 80–98 μmol photons·m^{-2}·s^{-1}). Each treatment was conducted in quintuplicate.

During ecotoxicity assessments, optical densities (OD_{750} and OD_{682}) were measured at 0, 24, 48, and 72 h to monitor growth inhibition, pigment integrity, and overall cell viability. Based on these preliminary assays and prior knowledge of strain-specific sensitivities, definitive bioaccumulation exposures were carried out using empirically optimized REE concentrations: *Limnospira* spp. were exposed to 0.02 mM Eu and Gd, *L. foveolarum* to 0.04 mM, and *S. bigranulatus* to 0.08 mM.

After ecotoxicological screening, bioaccumulation was conducted on both pre-bioconversion and post-bioconversion biomasses in sterile 100 mL glass test tubes, placed within a controlled photobioreactor aquarium chamber. Incubations were

performed in triplicate for each treatment, maintained under constant photoautotrophic conditions at 29 ± 1 °C, with continuous illumination at 20 µmol photons·m^{-2}·s^{-1}. During the 72-h exposure period, OD_{750} measurements were periodically recorded to monitor biomass development. Morphological observations of the cells were performed microscopically using an Olympus BX51 (Olympus, Tokyo, Japan) to detect cellular bleaching, granulation, lysis, or contamination during the bioaccumulation processes.

3.9.2. Dry mass determination

Dry mass determination and quantification of biomass productivity were conducted independently of the elemental analysis. Specifically, 10 mL aliquots of each culture were withdrawn at t = 0 and 72 h, and cells were collected by centrifugation at 4800 rpm for 10 min. Pellets were transferred to sterile Eppendorf tubes and dried in an oven at 105 °C for 24 h. Dry biomass was determined gravimetrically.

3.9.3. Rare earth element quantification by ICP-MS

After the 72 h bioaccumulation phase, cyanobacterial biomass was harvested for REEs quantification using protocols adapted from Čížková *et al*. [176] and Vítová *et al*. [177]. Cultures were centrifuged at 4800 rpm for 10 minutes, and the resulting cell pellets were subjected to three consecutive washes with their respective media. These washing steps were essential for removing any residual REEs remaining in the supernatant or loosely adsorbed to extracellular polymeric substances (EPS), ensuring that subsequent elemental analysis would reflect only internalized REEs and not loosely bound surface-associated ions. After the final wash, biomass was immediately frozen at –80 °C and subsequently freeze-dried. This procedure preserved cellular structure and minimizing any redistribution or loss of accumulated metals during processing.

ICP-MS measurements were performed using an Elan DRC-e (Perkin Elmer, Concord, ON, Canada) equipped with a concentric PTFE nebulizer and cyclonic spray chamber. This approach, combining thorough washing, freeze-drying, complete acid digestion,

internal standard correction. Validated ICP-MS quantification, ensures that the reported Gd and Eu content reflects true bioaccumulation rather than superficial adsorption or procedural artifact [176,177]. REE accumulation was expressed as micrograms of element per gram of dry biomass (μg/g DW), calculated using the known sample mass and dilution factors.

CHAPTER FOUR

Results and Discussion

4.1. Substrate stability and medium composition effects

Understanding the chemical stability of substrates in biological media is critical for the success of biotransformation studies. The stability of selected substrates in cyanobacterial media demonstrated the interaction between medium composition, substrate integrity, and experimental reliability.

One of the key formulations used was BG-11_0, which is compositionally identical to BG-11, except for the omission of sodium nitrate ($NaNO_3$), the primary nitrogen source. This modification is intended to support the growth of diazotrophic cyanobacteria, such as *Nostoc* sp., which can fix atmospheric nitrogen (N_2) and do not require external combined nitrogen sources [157]. The physiological impact of sodium nitrate supplementation on *Nostoc* has been well documented. Studies by Johnson *et al*. [158] and Nayak *et al*. [159] revealed that the presence of $NaNO_3$ in the growth medium can enhance the synthesis of phycobiliproteins, key accessory pigments involved in light harvesting, by up to fivefold compared to nitrogen-deprived conditions. The highest phycobiliprotein yield was observed at a $NaNO_3$ concentration of 17.65 mM, corresponding to approximately 0.10 g of pigment per gram of dry cell biomass. However, further increases in nitrate concentration beyond this threshold led to a decline in pigment production, which was attributed to substrate inhibition of nitrogen assimilation pathways or a regulatory feedback response in nitrogen metabolism [157–159].

4.1.1. Unsaturated fatty acids stability

Table 11 illustrates the stability of these fatty acids in different media (BG-11, BG-11_0, and Spirulina Medium (SM)) over seven days. The results suggest that 4-Pentenoic acid exhibited the highest stability, as indicated by its consistent retention time across all media. The other fatty acid substrates demonstrated varying degrees of instability,

as evidenced by shifts in retention times. This inconsistency suggests either degradation or interaction with medium components. The presence of multiple peaks in HPLC analysis further supports potential degradation or transformation.

Table 11. Unsaturated fatty acids stability test in growth media (7 days)

Fatty Acid Substrate	Growth Media	Avg. Weight (mg)	HPLC Retention Time (Min.)
7-Octenoic acid	-	4.1	6.92
	BG-11	4.1	5.68; 6.39
	$BG\text{-}11_0$	4.1	5.63; 6.21
	SM	4.1	-
6-Heptenoic acid	-	4.1	4.43; 5.62
	BG-11	4.1	5.65
	$BG\text{-}11_0$	4.1	5.62
	SM	4.1	-
10-Undecenoic acid	-	5.6	8.17; 10.11
	BG-11	5.6	10.08
	$BG\text{-}11_0$	5.6	10.08
	SM	5.6	-
4-Pentenoic acid	-	5.7	4.85
	BG-11	5.7	4.85
	$BG\text{-}11_0$	5.7	4.85
	SM	5.7	4.85
-	Media (BG-11, $BG\text{-}11_0$, SM)	5.0	2.50

Note: "–" indicates a non-applicable or untested condition in the context of substrate, growth medium, or HPLC retention time.

4.1.2. Phosphonates stability

The stability of the substrate, epoxymethyl dimethyl phosphonate, was also evaluated in various cyanobacterial growth media over a 7-day incubation period. The NMR results (^{31}P and ^{1}H) revealed that EMDP demonstrated high stability in BG-11 and $BG\text{-}11_0$ media, with no detectable degradation, indicating their suitability for sustained photobiocatalytic applications. In contrast, degradation of EMDP was observed in Spirulina Medium (SM) and its modified variant, as well as in the modified BG-11 medium over a 7-day incubation period (Figure 5). These results indicate that specific medium components, such as elevated bicarbonate, phosphate, or metal ion levels,

chemically interact with organophosphonates, compromising substrate stability as expounded by Mian *et al*. [178].

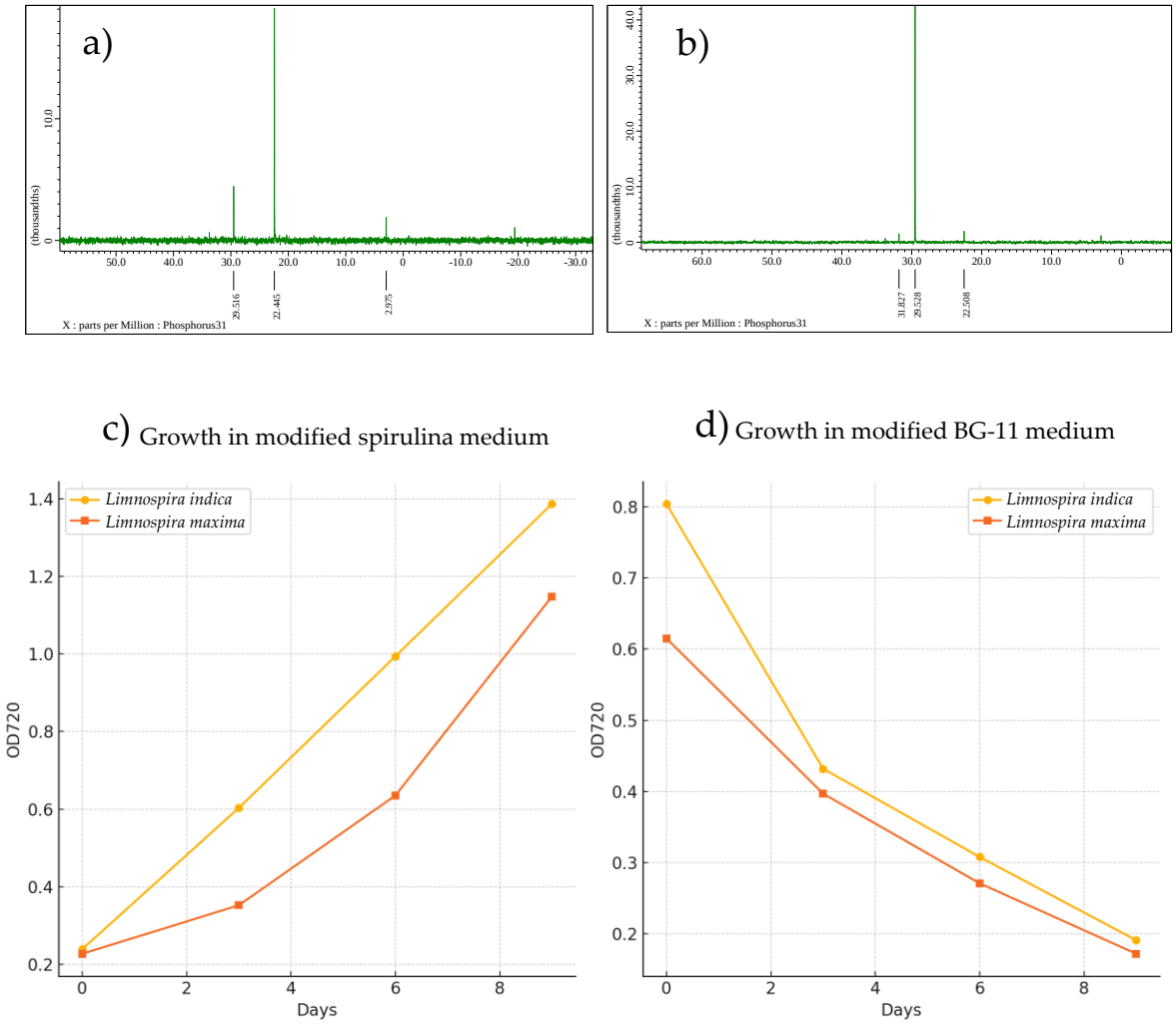

Figure 5. Comparative stability of EMDP and biomass growth of *Limnospira* sp. in modified media over 7 days: (a) ^{31}P NMR spectrum of EMDP in modified spirulina medium; (b) ^{31}P NMR spectrum of EMDP in modified BG-11 medium; (c) growth curve of *L. indica* and *L. maxima* in modified SM; (d) growth curve of both strains in modified BG-11.

Spectroscopic analysis using ^{31}P NMR revealed that EMDP maintained substantial chemical stability in modified BG- 11 medium over the 7- day incubation (Figure 5b), with minimal spectral changes observed. In contrast, modified spirulina medium induced pronounced instability in the substrate (Figure 5a), implicating chemical interaction of the substrate with the medium components.

Parallel to these findings, the growth dynamics of *Limnospira* species displayed a medium-dependent pattern. In modified spirulina medium, both *L. indica* and *L.*

maxima exhibited exponential growth (Figure 5c), with *L. indica* achieving higher biomass density. Conversely, modified BG-11 medium supported limited growth (Figure 5d), with both strains experiencing a progressive decline in OD_{720}, indicative of physiological stress or suboptimal nutrient composition despite its compatibility with substrate stability. These dual observations emphasize the inherent adjustment between medium formulations optimized for biomass growth against those favouring substrate stability. Future medium development should focus on achieving a balance between biocompatibility and chemical inertness, particularly when working with organophosphorus compounds such as EMDP.

The primary aim behind modifying SM and BG-11 was to optimize cyanobacterial biomass production while concurrently minimizing substrate instability. However, the observed instability of EMDP in the modified media indicates that further refinement is necessary on balancing the nutritional needs of the biomass with the chemical stability of sensitive substrates such as EMDP.

Importantly, the unmodified BG- 11 and BG-11_0 media, which are the principal media used for cyanobacterial cultivation and photobiocatalytic assays, provided a chemically inert environment for EMDP. This compatibility ensures that these media remain the platforms of choice for evaluating cyanobacterial biocatalysis involving epoxyphosphonate substrates.

4.2. Bioconversions with cyanobacteria

Based on the preliminary assessment of substrate–medium compatibility (Section 4.1), a series of structurally distinct model substrates were selected to investigate the catalytic potential of cyanobacterial strains under photoautotrophic conditions. These substrates encompassed several functional group classes (Figure 4), including unsaturated carboxylic acids, aromatic esters, and phosphonic esters, with the goal of exploring diverse enzymatic transformations.

The initial group investigated includes short- to medium-chain unsaturated fatty acids, namely, 7-octenoic, 6-heptenoic, 10-undecenoic, and 4-pentenoic acid. These

were evaluated as potential substrates for reductive or hydratase-mediated modification of carbon–carbon double bonds. However, biotransformation outcomes were inconsistent and non-reproducible across all tested strains, including *Synechococcus bigranulatus* CCALA 187, *Nostoc cf-muscorum* CCALA 129, *Limnospira indica* PCC 8005, *Limnospira maxima* CCALA 27, and *Kamptonema animale* CCALA 138.

Vinyl phosphonates (dimethyl and diethyl esters), selected for potential alkene reduction or carbon–phosphorus bond cleavage, remained chemically unaltered in all strains, likely due to the absence or repression of phosphonate metabolism pathways within the tested strains' genomes.

The enantioselective hydrolysis of the substrate, 1-phenylethyl acetate, a mechanistically distinct transformation involving C–O bond cleavage by endogenous esterases, was previously tested in a manually constructed growth chamber, where light variability affected reproducibility. To overcome this, the experiment was repeated under phytotron-controlled conditions, allowing precise regulation of environmental factors. *Leptolyngbya foveolarum* CCALA 76 showed higher enantioselectivity than *Synechococcus bigranulatus* CCALA 187, with minor acetophenone formation indicating alcohol dehydrogenase activity.

In contrast, epoxymethyl dimethyl phosphonate was efficiently converted to dimethyl (1*E*)-3-hydroxyprop-1-enylphosphonate in *Synechococcus bigranulatus* CCALA 187 and *Limnospira* sp., consistent with epoxide hydrolase-mediated ring opening followed by isomerization. *Nostoc cf-muscorum* CCALA 129 lacked this activity, likely due to strain-specific enzymatic limitations.

Overall, bioconversion was strongly dependent on both substrate structure and cyanobacterial strain, with *Synechococcus bigranulatus* CCALA 187 and *Limnospira* spp. demonstrating the highest catalytic versatility in this study.

4.2.1 Unsaturated fatty acid bioconversion

Unsaturated fatty acids, including 7-octenoic acid, 6-heptenoic acid, 10-undecenoic acid, and 4-pentenoic acid, were expected to undergo carbon–carbon double bond

reduction, potentially catalyzed by alkene reductases or via enoyl hydratase-type enzymes. Such biotransformations have been described in microbial systems by Callaghan *et al*. [179], where olefinic acids act as electrophilic substrates for enzymatic modification, proceeding either through hydride addition or nucleophilic attack, depending on the organism's physiological state and metabolic framework.

In anaerobic microorganisms such as *Desulfatibacillum alkenivorans*, unsaturated fatty acids serve as substrates for alkene reductases that catalyze the hydrogenation of carbon–carbon double bonds via hydride transfer mechanisms, typically using reducing equivalents derived from NADH or similar cofactors. This enzymatic reduction neutralizes the electrophilic character of the double bond and yields saturated products, representing a key step in anaerobic alkene catabolism. Callaghan *et al*. provided a genomic and enzymatic characterization of such reductive pathways, indicating the biochemical specificity of olefin-targeting enzymes in obligate anaerobes. In contrast, under phototrophic or oxygenic conditions such as those found in cyanobacteria, the reactivity of olefinic acids may be modulated through alternative mechanisms involving nucleophilic addition. As described by Guschina and Harwood [180], unsaturated fatty acids in algae and cyanobacteria are commonly subjected to metabolic transformations such as hydration, where water or hydroxide ions, acting as nucleophiles, are enzymatically added across the double bond to form β-hydroxy fatty acid intermediates [180]. These reactions are often catalyzed by enoyl hydratases and are integrated into broader lipid remodeling or stress-response pathways [180]. Thus, although the precise enzymatic toolkit may differ between anaerobic and phototrophic systems, the fundamental role of the olefinic bond as a reactive electrophilic site remains central to microbial fatty acid metabolism [180]. The applicability of these mechanistic frameworks to cyanobacterial systems supports the rationale for exploring unsaturated fatty acids as substrates for photobiocatalytic transformation.

Table 12. Biotransformation of unsaturated fatty acids

Substrate	Biocatalyst	Weight (mg)	HPLC Retention Time (min.)			
			Day 1	Day 3	Day 5	Day 7
7-Octenoic acid	*Nostoc cf-muscorum*	7.5	6.9	6.8	3.72; 6.97	3.74; 6.9
	Synechococcus bigranulatus	3.3	2.68; 4.38; 7.83	2.55; 4.33; 7.83	2.73; 4.35; 8.47	2.78; 4.32; 8.45
6-Heptenoic acid	*Nostoc cf-muscorum*	7.3	3.24; 5.11; 5.61; 6.81	3.38; 4.99; 5.73; 6.76	3.45; 4.82; 5.62; 7.02	3.69; 4.96; 5.60; 6.70; 11.83
	Synechococcus bigranulatus	2.1	3.51; 5.02	3.48; 5.05; 6.61	3.58; 5.07; 6.76; 12.35	3.48; 5.05; 6.59; 11.84; 17.39
10-Undecenoic acid	*Nostoc cf-muscorum*	11.4	3.29; 5.03; 8.3; 10.2	3.7; 5.16; 6.76; 8.31; 10.2	3.55; 5.52; 6.65; 9.64	3.48; 5.62; 10.27
	Synechococcus bigranulatus	2.3	3.52; 4.94; 6.88; 8.49; 10.35; 12.26	3.34; 5.04; 6.92	3.5; 5.06; 6.82	3.48; 5.11; 6.92
	Limnospira indica	58.5	4.85	4.85	4.85	4.85
4-Pentenoic acid	*Limnospira maxima*	63.5	4.85	4.85	4.85	4.85
	Synechococcus bigranulatus	51.5	4.85	4.85	4.85	4.85
	Kamptonema animale	71.6	4.85	4.85	4.85	4.85

Table 12 summarizes the seven-day biotransformation assays performed on unsaturated fatty acids, using *Nostoc cf-muscorum* CCALA 129, *Synechococcus bigranulatus* CCALA 187, *Limnospira indica* PCC 8005, *Limnospira maxima* CCALA 27, and *Kamptonema animale* CCALA 138. Partial conversion of 7-octenoic, 6-heptenoic, and 10-undecenoic acids was observed in *Nostoc* sp., though never to completion, and the variability in retention times suggested the formation of a range of metabolic byproducts rather than a single product. *Synechococcus bigranulatus* CCALA 187, *Limnospira indica* PCC 8005, and *Limnospira maxima* CCALA 27 showed marginally broader substrate scope but, like *Nostoc* sp., did not convert 4-pentenoic acid. *Kamptonema animale* CCALA 138 displayed no activity under identical conditions, indicating a metabolic absence or repression. Crucially, all conversions were 'non-

reproducible', with inconsistent retention times across replicates, reinforcing the conclusion that any observed transformations were marginal and unreliable.

These substrate-specific patterns align with existing literature documenting how cyanobacteria regulate fatty acid metabolism according to chain length, unsaturation, and enzyme specificity. For instance, cyanobacteria exhibit selective incorporation and modification of exogenous fatty acids using acyl-ACP synthetase (Aas), with preference for certain chain lengths and degrees of unsaturation, as discussed by Kahn *et al*. [181]. Moreover, the absence of canonical β-oxidation in cyanobacteria, as highlighted by Kahn *et al*. [181] explains why complex catalytic processing of unsaturated fatty acids is limited in these organisms. Differences between strains can also be attributed to their fatty acid desaturase profiles; Chi *et al*. [182] demonstrated that cyanobacteria such as *Synechocystis* and *Synechococcus* encode specific desaturase enzymes that govern the degree and position of unsaturation, affecting downstream metabolic flexibility. Previous investigation by Ruffing [183] showed that engineered pathways in *Synechococcus* sp. PCC 7002 have shown efficient synthesis and secretion of free fatty acids, revealing that cyanobacterial strains differ widely in their enzymatic capacity for fatty acid handling and export [183].

These results also demonstrate that cyanobacteria possess narrow substrate preferences for unsaturated fatty acids, dictated by species-specific enzymatic expression and metabolic architecture, and the limited and inconsistent biotransformations observed align with broader patterns reported in cyanobacterial lipid metabolism.

4.2.2. Vinyl phosphonates bioconversion

Vinyl phosphonates were selected as a logical extension of the bioconversion experiments with compounds of high added value. However, unlike fatty acids, vinyl phosphonates incorporate a phosphonic-based moiety instead of a carboxyl group, testing the hypothesis that cyanobacterial systems could orchestrate reductive activity to vinylated phosphonic esters. This ties into the broader aim of assessing the substrate tolerance and reaction breadth of phototrophic whole-cell biocatalysts under uniform

experimental conditions.

Vinyl phosphonates such as dimethyl vinylphosphonate and diethyl vinylphosphonate are organophosphorus compounds characterized by a vinyl group ($–CH=CH_2$) conjugated to a phosphonate moiety ($–PO_3R_2$), possess structural features that make them attractive candidates for microbial transformation: a carbon–carbon double bond conjugated with a phosphonate moiety and also ester bounds, which can be hydrolyzed. This configuration allows two distinct routes of potential biocatalytic intervention, alkene reduction (of the unsaturated C=C bond) and carbon–phosphorus (C–P) bond cleavage, both of which have precedent in specialized bacterial systems. The double bond could serve as an electrophilic site for enzymatic reduction via alkene reductases, while the phosphonate group represents a target for cleavage by phosphonate-specific hydrolases or lyases, enzymes that have evolved in bacteria to access phosphorus from otherwise recalcitrant organophosphorus compounds. However, successful biotransformation depends not only on chemical reactivity but on the presence of specific enzymatic systems and transporters within the host organism. The reduction of alkenes in microbial systems has been well described in anaerobic and facultatively anaerobic bacteria, where terminal and internal C=C bonds serve as electrophilic targets for enoate reductases and related flavin-dependent enzymes. Singh and Walker [184] provide a foundational review of microbial degradation of organophosphorus compounds, including vinyl phosphonates. They explain that such enzymes use NAD(P)H as hydride donors to reduce double bonds, contributing to detoxification and carbon utilization. However, these enzymes are typically expressed under oxygen-limited conditions and are rare or inactive in photoautotrophic microbes such as cyanobacteria. Moreover, the presence of the phosphonate group could alter the electronic distribution across the vinyl system, potentially reducing its reactivity or accessibility to microbial reductases. However, in principle, the alkene can undergo hydride attack or protonation-deprotonation mechanisms leading to reduction [184].

In terms of C–P bond cleavage, microbial biotransformation-degradation of vinyl phosphonates is typically mediated through one of two main pathways: the C–P lyase pathway and hydrolytic cleavage via phosphonatases [185]. Drzyzga and Lipok [185] provide a detailed account of how bacteria, especially those inhabiting phosphorus-limited environments, can activate these pathways to exploit phosphonates as a phosphorus source. The C–P lyase system, encoded by the phn operon, facilitates the radical-mediated cleavage of the carbon–phosphorus bond in a variety of phosphonates, including alkyl and aromatic derivatives. Although this system is primarily documented in soil bacteria and enteric species such as *Escherichia coli*, it demonstrates the feasibility of microbial phosphonate catabolism under aerobic and anaerobic conditions alike. Additionally, phosphonatases, such as phosphonoacetate hydrolase and phosphonoformate hydrolase, catalyze the direct hydrolytic cleavage of the C–P bond without the need for radical intermediates. These enzymes often require metal cofactors and operate through mechanisms involving nucleophilic attack at the phosphorus center [185].

The evolutionary origin, diversity, and distribution of phosphonate utilization genes have been elucidated by several studies. Ternan *et al*. [186] were among the first to describe the biochemical diversity of phosphonate degradation enzymes in soil and aquatic bacteria, identifying structural and functional heterogeneity in *phn* operons. Hove-Jensen *et al*. [187] expanded this understanding by demonstrating that the *phn* system operates independently of oxygen, is tightly regulated by the Pho regulon, and requires cofactor-intensive radical chemistry. This is particularly relevant to the current study, where the absence of DMVP and DEVP transformation in cyanobacteria could be explained by Pho regulon inactivation under phosphorus-replete photobioreactor conditions [187].

The distribution of phosphonate metabolism genes in cyanobacteria is notably non-uniform. Villarreal-Chiu *et al*. [188] showed that while marine bacteria often carry full *phn* operons, the corresponding genes are sporadically distributed in cyanobacterial genomes. This aligns with recent genomic evidence provided by Ponce-Toledo *et al*.

[189] and Sosa *et al*. [190], who identified *phn* gene clusters in freshwater and marine cyanobacteria (*Synechococcus*, *Prochlorococcus*), suggesting lateral gene transfer from heterotrophic bacteria. These studies also noted that gene presence does not guarantee expression or metabolic functionality.

In general, the lack of observable enzymatic conversion of DMVP and DEVP in the cyanobacterial strains used in this study is due to fundamental genomic and physiological limitations. These include the lack of active *phn* gene expression, missing transport proteins, inadequate redox coupling, or prioritization of energy toward phototrophic metabolism rather than bioconversion.

DMVP and DEVP were evaluated as substrates of biotransformations using a range of cyanobacterial biocatalysts, including strains of *Nostoc cf-muscorum* CCALA 129, *Synechococcus bigranulatus* CCALA 187, *Limnospira indica* PCC 8005, *Limnospira maxima* CCALA 27, and *Kamptonema animale* CCALA 138. These substrates were selected due to their structural relevance to organophosphorus compounds with diverse industrial and biochemical applications. For instance, poly(diethyl vinylphosphonate) and related vinyl phosphonates have been explored for biocompatible coatings in tissue engineering applications such as osteoconductive films [191,192]. Additionally, they share the phosphonate group characteristic of the widely used herbicide glyphosate (N-(phosphonomethyl)glycine), which functions as a phosphonate analog of phosphoenolpyruvate and is extensively used in agriculture [193]. Furthermore, vinyl phosphonates often serve as stable transition-state mimics in medicinal chemistry, acting as enzyme inhibitors targeting dehydrogenases and other phospho-dependent enzymes [194,195]. Such functional and structural parallels highlight the biochemical significance of investigating vinyl phosphonates such as DMVP and DEVP in cyanobacterial biotransformation assays.

Over a 30- day incubation period, no enzymatic conversion or degradation of either compound by the cyanobacterial strains was observed, as confirmed by ^{31}P NMR spectra. Despite this lack of bioconversion, trace liberation of inorganic phosphonate was detected during photobiocatalytic exposure to DMVP in the presence of *Nostoc cf-*

muscorum CCALA 129, *Synechococcus bigranulatus* CCALA 187, and *Limnospira* spp. (PCC 8005 and CCALA 27), and was confirmed by the Malachite Green assay (Figure 6). This colorimetric assay, recognized for its high sensitivity in phosphate detection [196–198], has been validated in a range of environmental and biochemical contexts with reduced amine interference [199]. This suggests a non- enzymatic, likely hydrolytic process.

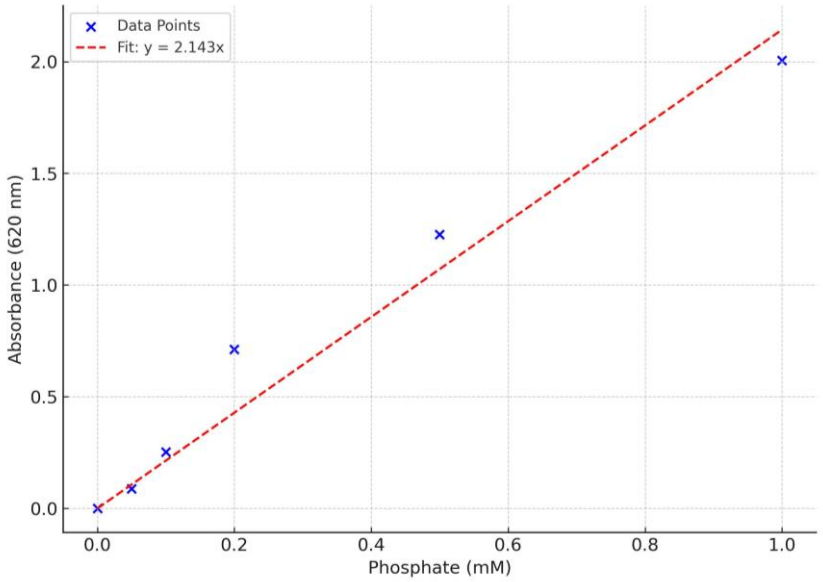

Figure 6. Malachite Green assay standard curve.

Figure 6 showed the standard curve using the Malachite Green Assay, establishing a correlation between phosphate concentration and absorbance at 620 nm. This standard curve was used to quantify the release of inorganic phosphonates (Table 13) during photobiocatalysis of vinyl phosphonates.

Table 13. Concentration (mM) of inorganic phosphonate in the test samples (A_{620})

Sample	0 h		72 h	
	A_{620}	Conc. (mM)	A_{620}	Conc. (mM)
Nostoc sp. + DMVP	0.082	0.007	0.049	0.023
Synechococcus sp. + DMVP	0.044	0.069	0.108	0.006
Limnospira indica + DMVP	0.141	0.023	0.037	0.066
Limnospira maxima + DMVP	0.520	0.212	0.195	0.050

Control:				
Nostoc sp. (21-days culture)	0.599	0.251	0.106	0.005
Synechococcus sp. (21-days culture)	0.572	0.237	0.056	0.020
Limnospira indica (21-days culture)	6.200	3.041	0.287	0.095
Limnospira maxima (21-days culture)	6.200	3.041	0.320	0.112
BG-11 Medium	0.572	0.237	–	–
BG-11$_0$ Medium	0.599	0.251	–	–
SM Medium	6.200	3.041	–	–

Note: "–" indicates that the test was not applicable under the given conditions.

The Malachite Green Assay results in Table 13 indicate that the detected inorganic phosphonate observed in the cultures of *Nostoc* sp., *Synechococcus* sp., and *Limnospira* sp. exposed to DMVP phosphate levels were relatively low. This showed that any phosphonate release was minimal and likely due to non-enzymatic hydrolysis rather than a direct biocatalytic process. The presence of background phosphate levels in control samples further supports this observation. The inability of cyanobacteria to transform DMVP and DEVP aligns with previous reports highlighting the limited enzymatic capability of cyanobacteria toward C-P bond cleavage in vinyl phosphonates by Singh and Walker [184].

4.2.3. Bioconversion of 1-phenylethyl acetate

Unlike previous substrates where reduction of double bonds was expected, the transformation of 1-phenylethyl acetate involves enantioselective hydrolysis of an ester bond, catalyzed by endogenous esterases. This reaction targets C–O bond cleavage, yielding chiral alcohol and acetophenone. It is mechanistically distinct and does not involve redox chemistry.

This experimental section was intended to extend the previously started experiments, conducted in manual control chamber and reported by Śliżewska *et al.* [140], by

adopting precisely regulated cultivation and bioconversion conditions in phytotron to ensure reproducibility and accurate comparison of cyanobacterial enantioselective activity. The setting of accurate and repeatable conditions was crucial for receiving the biomass for its further prospecting in bioaccumulation processes (as elaborated in section 4.3). Śliżewska *et al*. [140] demonstrated that enantioselective hydrolysis of 1-phenylethyl acetate to (*R*)-1-phenylethanol, with enantiomeric excesses exceeding 86% and selectivity (E) values up to 283, could be achieved using *Leptolyngbya foveolarum* CCALA 76, *Nostoc cf-muscorum* CCALA 129, and *Synechococcus bigranulatus* CCALA 187 cultivated for 21 days under a 16:8 light–dark photoperiod at 27 °C. Building on this approach and setup conditions, the current study employed both 21-day, 14-day, and 7-day cyanobacterial cultures, incubated in a phytotron-based photobioreactor system and a custom manual bioreactor, respectively. These tightly controlled conditions were selected specifically to enable reproducible, comparative evaluation of stereoselective hydrolytic activity among cyanobacterial strains and thereby establish a standardized model for photobiocatalytic transformation.

However, in this study, the transformation of 1-phenylethyl acetate was explored using *Synechococcus bigranulatus* CCALA 187 and *Leptolyngbya foveolarum* CCALA 76. The efficiency of biotransformation was assessed based on enantiomeric excess (e.e.) of 1-phenyl ethanol and 1-phenyl ethyl acetate, conversion degree, and product formation (Tables 14-16). This highlights the enantioselective potential of cyanobacteria, broadening their applicability beyond redox-based biocatalysis.

Although, the biotransformation reaction with the substrate, 1-phenylethyl acetate was previously conducted in a manually controlled growth chamber, which introduced variability in photoperiod, light intensity, and temperature. Therefore, the current experiments on this substrate employed a phytotron growth chamber offering high-fidelity control over illumination, temperature, and humidity, ensuring consistent metabolic conditions. The phytotron's programmable environment permits the manipulation of cyanobacterial cultivation and reaction parameters in a manner that enhances reproducibility, providing an ideal platform to study how light quality

and biomass age affect stereoselectivity in cyanobacterial systems. This methodological refinement was critical, given that enzyme expression and membrane transport processes in cyanobacteria are highly sensitive to photoregulation and nutrient state.

The role of environmental conditions in modulating microbial stereoselectivity is supported by the findings of Bartsch *et al*. [200], who explored the expression of recombinant stereoselective enzymes in *Chlamydomonas reinhardtii* and *Synechocystis sp.* PCC6803. Their study revealed that light-driven photosynthetic metabolism can supply redox equivalents to drive biocatalytic transformations and affect enzyme selectivity. However, they also noted that strong light can repress foreign gene expression or stress the cells, reducing productivity as observed in the current study: lower light intensities in the phytotron favored higher enantiomeric excess, especially in *Leptolyngbya sp.*, suggesting improved expression or stability of endogenous esterases under those conditions. Dong *et al*. [118] also emphasized on strain-specific and condition-dependent stereoselectivity of enantioselective hydrolysis of 1-PEAc using deep-sea *Bacillus* strains. They showed that whole-cell catalysis can reach high enantiomeric excess (up to 96%) under optimized pH and temperature conditions. Moreover, they emphasized the importance of cell membrane permeability and growth phase in determining the reaction rate and selectivity. In our study, the superior selectivity observed in *Leptolyngbya* sp. (compared to *Synechococcus bigranulatus*) could reflect a more favorable membrane composition, improved esterase accessibility, or lower metabolic competition under phototrophic growth.

Bornscheuer [201] offers a detailed classification of microbial esterases and outlines their mechanistic basis for enantioselectivity. He describes how the active site architecture, particularly the arrangement of the catalytic triad and the stereochemical environment, determines substrate binding and enantioselective hydrolysis. This foundational understanding supports the hypothesis that cyanobacterial esterases, although less well studied than those of mesophilic heterotrophs, may possess

inherent or inducible stereoselective activity. The current study investigates this possibility by using whole cyanobacterial cells as the biocatalyst source.

In addition to the desired enantioselective hydrolysis of 1-phenylethyl acetate (1-PEAc), which generated optically enriched 1-phenylethanol, a minor yet consistent was the formation of acetophenone. The likely origin is the oxidation of 1-phenylethanol by alcohol dehydrogenases (ADHs), which convert secondary alcohols to ketones. A detailed enzymatic basis for this reaction is provided by studies on *Azoarcus sp.* strain EbN1, a denitrifying ethylbenzene-degrading bacterium [202] . Kniemeyer and Heider [202] reported the isolation and characterization of a (*S*)-1-phenylethanol dehydrogenase (PED) that catalyzes the NAD^+-dependent oxidation of (*S*)-1-phenylethanol to acetophenone [202]. The enzyme was shown to be strictly stereoselective for the (*S*)-enantiomer, and its activity was linked to redox metabolism in anaerobic aromatic hydrocarbon degradation. This mechanistic detail directly supports the notion that acetophenone formation in our study is not a non-specific oxidative artifact, but rather the outcome of a highly specific enzymatic pathway conserved across multiple bacterial lineages.

Further structural and biochemical analysis by Höffken *et al*. [203] revealed the high-resolution crystal structure of this PED, confirming the positioning of substrate and cofactor in a catalytic triad consistent with other short-chain dehydrogenase/reductase (SDR) family members. This work demonstrated the stereoelectronic complementarity between (*S*)-1-phenylethanol and the enzyme active site, thereby explaining its enantiospecific oxidation. The authors also observed that PED expression in *Azoarcus* is environmentally regulated and tied to metabolic demand for NADH regeneration, a feature potentially mirrored in cyanobacteria under redox stress or prolonged light exposure.

Table 14. Bioconversion of 1-phenylethyl acetate (7 days culture) in phytotron

Biocatalyst	Time (h)	Conversion (%)	e.e. 1-phenyl ethanol (%)	e.e. 1-phenylethyl acetate (%)
Leptolyngbya sp.	2	39.89 ± 1.15	0.36 ± 0.16	0.99 ± 0.04
	4	45.89 ± 0.56	1.11 ± 0.16	1.02 ± 0.09
	6	69.00 ± 8.08	1.57 ± 0.56	0.94 ± 0.18
	8	74.68 ± 7.85	1.58 ± 0.06	0.97 ± 0.11
	24	91.88 ± 6.58	7.98 ± 1.76	3.16 ± 0.22
Synechococcus sp.	2	31.85 ± 11.89	5.33 ± 0.16	3.98 ± 1.45
	4	45.51 ± 6.59	5.09 ± 4.93	5.24 ± 3.31
	6	63.56 ± 1.40	3.54 ± 0.34	7.73 ± 0.21
	8	71.38 ± 1.29	10.47 ± 0.35	29.05 ± 3.02
	24	99.13 ± 0.87	0.33 ± 0.34	57.79 ± 59.69

Table 14 reports results obtained with 7-day-old cultures at ~47 μmol photons·m^{-2}·s^{-1}, whereas Table 15 presents data from 14-day-old cultures exposed either to standard light intensity (~47 μmol photons·m^{-2}·s^{-1}) or reduced intensity (~22 μmol photons·m^{-2}·s^{-1}, indicated by *), provided by 30% cool white (CW). Values are expressed as mean ± standard deviation (SD) from triplicate experiments. Reported parameters include the degree of substrate conversion (%) and the enantiomeric excess (e.e.%) of both the product (1-phenylethanol) and the residual substrate (1-PEAc). Comparison of Tables 1 and 2 shows the influence of biomass age and light intensity on biotransformation kinetics and stereoselectivity, with older cultures and lower light intensities generally favouring higher enantioselectivity, particularly in *L. foveolarum*. However, *Synechococcus* sp. (Table 14) exhibited a rapid increase in bioconversion efficiency over 24 hours, achieving near-complete transformation by 24 hours. *Leptolyngbya* sp. displayed a slower conversion rate, requiring up to 48 hours to reach comparable conversion efficiencies (Table 15) using two weeks old cultures.

Table 15. Bioconversion of 1-phenylethyl acetate (14 days culture) in phytotron

Biocatalyst	Time (h)	Conversion (%)	e.e. 1-phenyl ethanol (%)	e.e. 1-phenylethyl acetate (%)
Leptolyngbya sp.	2	23.25 ± 9.53	8.41 ± 8.75	1.85 ± 1.33
	4	29.64 ± 8.61	3.21 ± 0.20	0.99 ± 0.08
	6	30.29 ± 0.46	2.91 ± 0.52	1.07 ± 0.10
	8	51.81 ± 37.50	5.78 ± 1.13	1.38 ± 0.40
	24	91.70 ± 7.51	41.73 ± 9.09	68.08 ± 41.57
	24*	96.70 ± 0.76	33.59 ± 7.71	2.15 ± 1.56
	48*	99.37 ± 0.51	45.39 ± 20.60	2.36 ± 0.83
	72*	87.13 ± 10.96	34.86 ± 7.88	27.49 ± 27.56
Synechococcus sp.	2	27.02 ± 5.07	3.51 ± 0.45	2.28 ± 0.13
	4	40.72 ± 10.36	4.19 ± 1.23	3.31 ± 0.37
	6	68.08 ± 4.62	3.37 ± 1.63	7.32 ± 0.71
	8	54.70 ± 3.56	8.88 ± 2.45	12.31 ± 1.70
	24	99.17 ± 0.51	0.75 ± 0.34	74.67 ± 12.00
	24*	80.20 ± 15.90	41.34 ± 29.18	32.55 ± 38.70
	48*	97.02 ± 3.65	21.50 ± 14.68	54.63 ± 64.16
	72*	99.96 ± 0.06	19.92 ± 6.25	50.00 ± 70.71

Note: Asterisk-marked entries (*) indicate phytotron settings at reduced light intensity (22 μmol photons m^{-2} s^{-1}), while unmarked values reflect approximately 47 μmol photons m^{-2} s^{-1}.

Table 16 compares biotransformation performance in an automated phytotron chamber versus a manually constructed growth chamber. The primary distinction between the phytotron and manually constructed growth chambers lie in the spectral quality and intensity of the applied light. These photonic variables critically modulate the efficiency and stereoselectivity of photo-biocatalytic processes. Although both systems maintained comparable environmental conditions such as temperature and humidity, the divergent light regimes, characterized by differences in wavelength distribution, irradiance, and photoperiodicity, were likely the primary determinants of the observed disparities in bioconversion outcomes observed between the systems.

The results indicate high conversion degrees and enantiomeric selectivity in both growth chambers. Notably, *Leptolyngbya* sp. achieved over 70% enantiomeric excess towards (*R*)-phenylethanol after seven days, demonstrating its strong enantioselectivity potential.

Table 16. Comparative bioconversion by *Leptolyngbya* sp. (14 days culture) in phytotron vs. manual chamber

Chamber	Time (day)	Conversion (%)	e.e. 1-phenyl ethanol (%)	e.e. 1-phenylethyl acetate (%)
Manual	1	80.49 ± 8.70	14.55 ± 12.74	3.47 ± 0.92
	3	98.40 ± 1.60	36.01 ± 6.13	21.01 ± 5.62
	7	>99.99 ± 0.02	83.48 ± 1.63	0.00 ± 0.00
Phytotron	2	98.70 ± 1.74	17.11 ± 6.30	2.78 ± 2.80
	3	99.52 ± 0.83	38.82 ± 3.77	2.30 ± 3.98
	4	99.97 ± 0.05	42.93 ± 1.71	0.70 ± 1.22
	5	99.83 ± 0.30	55.61 ± 10.63	8.05 ± 13.94
	6	99.65 ± 0.61	47.52 ± 18.39	0.00 ± 0.00
	7	>99.99 ± 0.00	72.51 ± 1.78	0.00 ± 0.00

The optimization process for the bioconversion of 1-phenylethyl acetate aimed to enhance the enantiomeric excess (e.e.) of the final product, phenylethanol. Key parameters assessed include the comparison between automatic and manual growth chambers, the duration of biomass production, photobiocatalysis time, optimization of light exposure, and the selection of a suitable cyanobacterial strain. Through these evaluations, *Leptolyngbya foveolarum* CCALA 76 was identified as the most bioactive strain under the phytotron growth chamber. The biomass of this strain was subsequently utilized for the bioaccumulation of rare earth elements (REEs), yielding promising results (section 4.3). In comparison with the research published by

Śliżewska *et al*. [140], specifically in terms of reproducibility, the findings aligns with the obtained results especially with the *Leptolyngbya foveolarum* CCALA 76.

Figure 7 presents GC chromatograms confirming successful enantioselective bioconversion. The emergence of distinct peaks for (*R*)- and (*S*)-1-phenylethanol supports enzymatic activity favouring selective hydrolysis of 1-phenylethyl acetate. The enantioselectivity data indicate that *Leptolyngbya* sp. outperformed other strains in producing (*R*)-1-phenylethanol with e.e. values exceeding 70% under phytotron conditions.

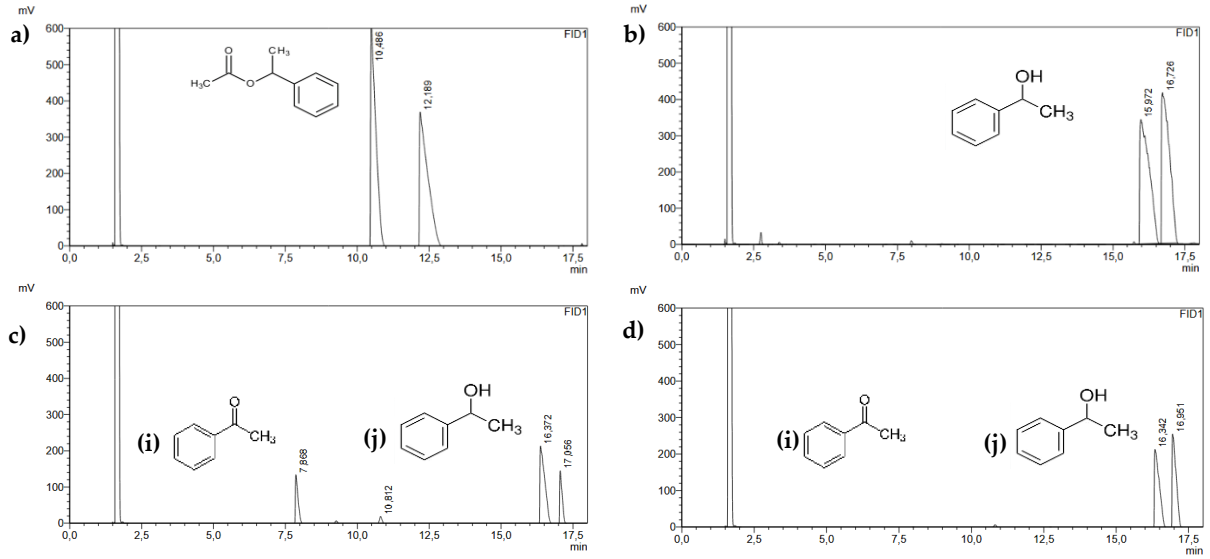

Figure 7. GC analysis of 1-phenylethyl acetate bioconversion. **a**) Chromatogram of the standard starting material – 1-phenylethyl acetate); **b**) Chromatogram of the standard (*R*)-and (*S*)- 1-phenyl ethanol; **c**) Chromatogram of the products: acetophenone (**i**) and (*R*)-and (*S*)- phenyl ethanol (**j**) biocatalyzed by *Leptolyngbya* sp.; **d**) Chromatogram of the products: acetophenone (**i**) and (*R*)-and (*S*)- phenyl ethanol (**j**) biocatalyzed by *Synechococcus* sp.

The GC chromatograms also confirm the formation of acetophenone (Figure 7 c & d), which arises via oxidation of 1-phenylethanol by endogenous alcohol dehydrogenases (ADHs). This oxidation has been documented in various microbial systems, as seen in Höffken *et al*. [203], who characterized NAD^+-dependent oxidation of 1-phenylethanol to acetophenone in *Azoarcus* sp.. Similarly, this observation is consistent with the enzymatic oxidation of 1-phenylethanol to acetophenone, a reaction catalyzed by

NAD^+-dependent alcohol dehydrogenases (ADHs) as demonstrated in the earlier study by Śliżewska *et al*. [140]. In this study, the oxidation pathway was observed as a side reaction during cyanobacteria-mediated enantioselective hydrolysis. Their data revealed that *Leptolyngbya* sp. exhibited both esterase and ADH activities, leading to the formation of acetophenone alongside excess (*R*)-1-phenylethanol. The detection of acetophenone in this study supports the hypothesis that endogenous ADHs in cyanobacteria can facilitate such oxidation under photoautotrophic conditions.

The chiral alcohol products, particularly (*S*)-1-phenylethanol, are valuable intermediates in the synthesis of pharmaceuticals, including β-blockers and antihistamines, as well as in fragrances and agrochemicals [118,201]. From a green chemistry perspective, achieving this transformation under mild, aqueous, and energy-efficient conditions is both scientifically and industrially significant.

4.2.4. Bioconversion of epoxymethyl dimethyl phosphonate

This section investigates the bioconversion of epoxymethyl dimethyl phosphonate by cyanobacterial strains, with emphasis on substrate specificity, enzymatic activity towards substrate, and structural confirmation of the resulting product.

EMDP exhibited very good susceptibility to bioconversion under photoautotrophic conditions. The selective bioconversion of EMDP to dimethyl (1*E*)-3-hydroxyprop-1-enylphosphonate by *Synechococcus bigranulatus* CCALA 187 and *Limnospira sp*. is likely attributable to the presence of epoxide hydrolases, which catalyze the nucleophilic attack on the strained three-membered epoxide ring [204]. This functional group is absent in the other tested organophosphonates, which could explain their inertness under photoautotrophic conditions. EMDP's physicochemical properties, such as its water solubility, moderate lipophilicity, and electrophilic center, further enhance its accessibility to enzymatic systems. These observations highlight a structure - activity relationship governed primarily by functional group compatibility with native cyanobacterial enzymatic machinery. However, *Nostoc cf-muscorum* CCALA 129

demonstrated limited capability due to the shift of their large portions of metabolic resources toward nitrogen fixation rather than photobiocatalysis as expatiated by Herrero *et al*. [205,206]. This strain-specific activity suggests a distinct distribution of epoxide hydrolase enzymes across cyanobacterial taxa.

The transformation of epoxymethyl dimethyl phosphonate into dimethyl (1*E*)-3-hydroxyprop-1-enylphosphonate by cyanobacterial strains is, as we can presume, a two-step biochemical process: epoxide ring opening, yielding a vicinal diol intermediate (β-hydroxyphosphonate), and a subsequent isomerization (dehydration/elimination), resulting in the conjugated vinyl phosphonate product. The ability of certain cyanobacterial strains to catalyze this reaction, while others cannot, points toward species-specific differences in enzymatic equipment, gene regulation, and metabolic prioritization.

The first step, epoxide hydrolysis, is most plausibly catalyzed by epoxide hydrolases (EHs), enzymes that catalyze nucleophilic attack on the strained epoxide ring, converting it to a trans-1,2-diol. The enzymatic basis for this activity in microbes has been extensively reviewed by Hult and Berglund [207], who emphasize that microbial EHs are widespread in both prokaryotic and eukaryotic organisms and can act on a variety of substrates, including terminal epoxides like EMDP. Their work shows that EHs possess a conserved catalytic triad (Asp-His-Asp/Glu) and often function under mild conditions, making them likely candidates for spontaneous or constitutive expression in cyanobacteria. This directly supports the idea that the cyanobacterial conversion of EMDP begins via EH-mediated ring opening, a reaction broadly feasible in microbial hosts [207]. Similarly, Archelas and Furstoss [208] demonstrate that microbial EHs exhibit significant substrate promiscuity and stereoselectivity, suggesting that naturally occurring cyanobacterial EHs (even if not specialized) could process the EMDP substrate, especially due to the electron-withdrawing effect of the phosphonate group, which increases epoxide ring susceptibility. Their work further

supports the view that such transformations can proceed in wild-type, non-engineered strains under standard cultivation [208].

The second step of the bioconversion, conversion of the diol to a conjugated hydroxyalkenyl phosphonate, likely proceeds via isomerization (specifically dehydration of the hydroxyl intermediate), mechanisms previously observed in microbial phosphonate-processing pathways. According to Ruffolo *et al*. [209], microbial phosphonate metabolism encompasses not only C–P bond cleavage but also diverse transformations of phosphonate side chains, including oxidative, hydrolytic, and elimination reactions. Their review highlights multifunctional enzymes, particularly those involved in synthetic phosphonate degradation, capable of coordinating sequential reactions like diol dehydration or rearrangement [209]. This provides mechanistic precedent for the second phase of EMDP transformation in our system.

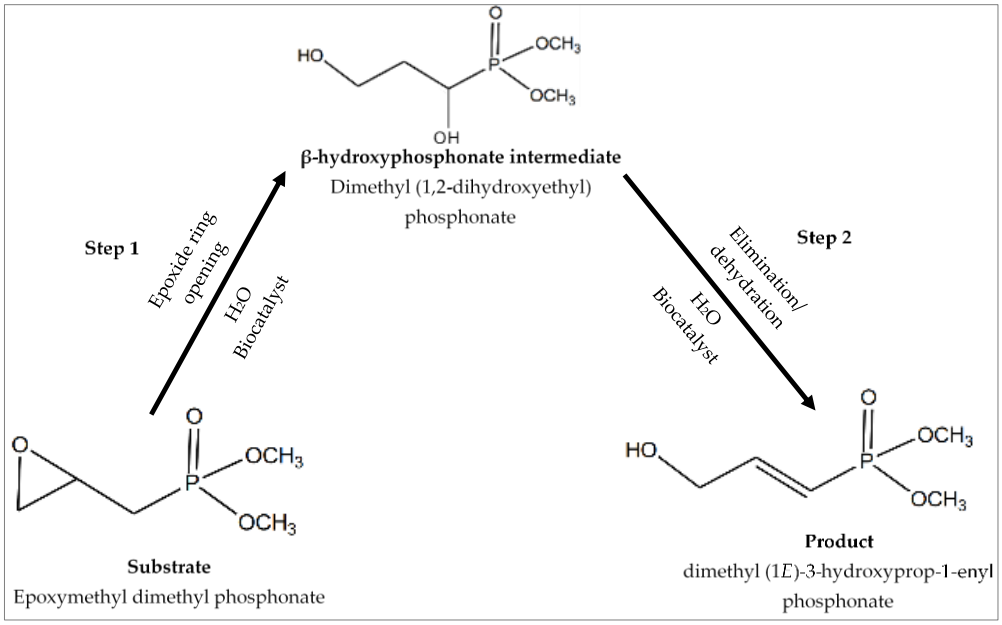

Figure 8. Possible two-step bioconversion of epoxymethyl dimethyl phosphonate by biocatalysts (*Synechococcus* sp. and *Limnospira* sp.).

The EMDP projected to undergo enzymatic ring-opening reactions mediated by the biocatalysts (Figure 8), could result in the formation of β-hydroxyphosphonate, specifically dimethyl (1,2-dihydroxyethyl) phosphonate as the intermediate product

(step 1). While Step 2 involves elimination or isomerization to form the (E)-alkenylphosphonate product, dimethyl (1*E*)-3-hydroxyprop-1-enylphosphonate. β-hydroxyphosphonates possess distinct physicochemical properties and biological activities that are relevant in various biotechnological applications. For example as key building blocks in the synthesis of nucleoside analogs and other bioactive compounds [210].

The biotransformation of epoxymethyl dimethyl phosphonate was systematically investigated using advanced spectroscopic methodologies, including mass spectrometry (MS); nuclear magnetic resonance spectroscopy (^{1}H, ^{13}C, ^{31}P, and 2D NMR); and infrared (IR) spectroscopy. The obtained product from the bioconversion of epoxymethyl dimethyl phosphonate were analysed as follow – MS (TOF MS ES+) Calcd for $C_5H_{11}O_4P$ [M + H]+ 167.0473; found: 167.0481; IR: 3362 (OH), 1638 (CH=CH) cm^{-1}; ^{31}P NMR ($CDCl_3$, δ, ppm): 22.64; ^{1}H NMR ($CDCl_3$, δ, ppm): 3.69 (d, *J* = 11 Hz, 6H, 2×P(O)OC*H*$_3$), 4.26–4.31 (m, 2H, C*H*$_2$OH), 5.96 (ddt, *J* = 2, 17, 21 Hz, 1H, P-CH=C*H*), 6.86 (ddt, *J* = 3, 17, 23 Hz, 1H, P-C*H*=CH); ^{13}C NMR ($CDCl_3$, δ, ppm): 52.58 (d, *J* = 6 Hz, 1C, PO*C*H$_3$), 62.36 (d, *J* = 22 Hz, 1C, HO*C*H$_2$CH=CH), 113.22 (d, *J* = 191 Hz, 1C, P-*C*H=CH), 153.69 (d, *J* = 5 Hz, 1C, P-CH=*C*H) [167]. The assignment of signals on ^{1}H and ^{13}C NMR were further confirmed by ^{1}-^{1}H COSY, ^{1}H-^{13}C HMQC, and ^{1}H-^{13}C HMBC spectra.

Key spectral outcomes derived from ^{31}P NMR and IR analyses are depicted in Figure 9. Figure 10 presents a comparative assessment of six cyanobacterial strains, *Synechococcus bigranulatus* CCALA 187, *Nostoc cf-muscorum* CCALA 129, *Limnospira indica* PCC 8005, *Limnospira maxima* CCALA 27, *Leptolyngbya foveolarum* CCALA 76, and *Nodularia moravica* CCALA 114, for their catalytic efficacy in converting EMDPP into dimethyl (1*E*)-3-hydroxyprop-1-enylphosphonate. All strains demonstrated progressive conversion over a 7-day period, though significant differences in efficiency were observed. The *Limnospira* sp. and *Synechococcus* sp. strains exhibited the most rapid and complete bioconversion, achieving 99% transformation within 24

h for *Limnospira* sp., and 72 h for *Synechococcus* sp., and maintaining this level of efficiency throughout the experimental period. This high performance is likely attributable to their advanced photosynthetic apparatus and their compatibility with the experimental photonic conditions, facilitating enhanced photobiocatalytic activity.

By contrast, *Leptolyngbya foveolarum* CCALA 76 and *Nodularia moravica* CCALA 114 display moderate conversion efficiencies, attaining 96% and 75% conversion respectively by day seven. *Nostoc cf-muscorum* CCALA 129 was the least effective, with only 14% conversion over the same period, potentially due to intrinsic physiological constraints such as lower substrate permeability or limited enzymatic repertoire relevant to EMDP metabolism.

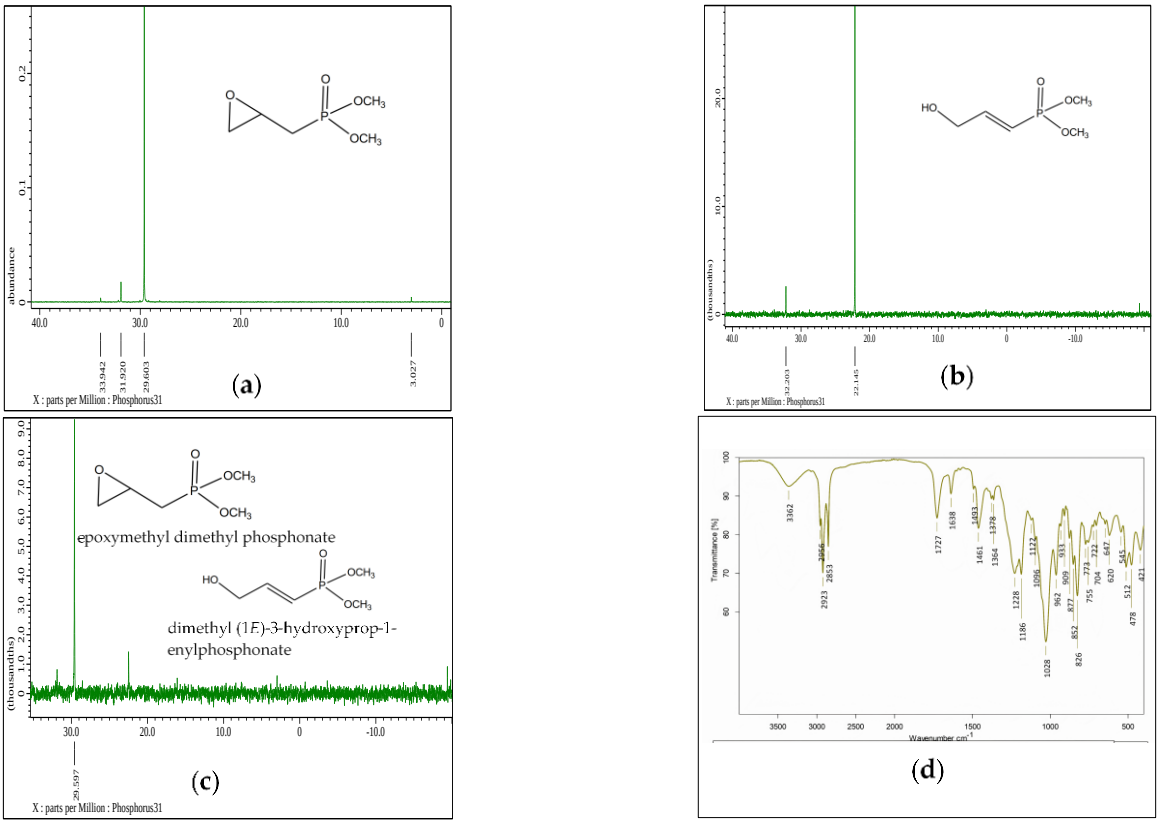

Figure 9. Spectral analysis of the biotransformation process: (**a**) ^{31}P NMR spectrum of the substrate, EMDP; (**b**) ^{31}P NMR spectrum of the complete transformed substrate, EMDP to product, DMHPP; (**c**) ^{31}P NMR spectrum showing partial substrate, EMDP conversion; (**d**) IR spectrum of the complete transformed substrate, EMDP to product, DMHPP [139].

Spectroscopic characterization, as shown in Figure 9, substantiates the molecular transformation of EMDP. The ^{31}P NMR spectrum of the unconverted substrate (Figure 9a) exhibited chemical shifts typical of phosphonate groups. Following complete bioconversion (Figure 9b), notable spectral shifts in the phosphorus environment indicated the formation of product. The partially converted intermediate (Figure 9c) displayed mixed spectral features, confirming simultaneous presence of substrate and product, and thereby offering insights into reaction kinetics. The IR spectrum of the fully transformed product (Figure 9d) corroborated these findings by confirming vibrational bands associated with unsaturated C=C and hydroxyl groups, consistent with the molecular structure of dimethyl (1*E*)-3-hydroxyprop-1-enylphosphonate [211–213].

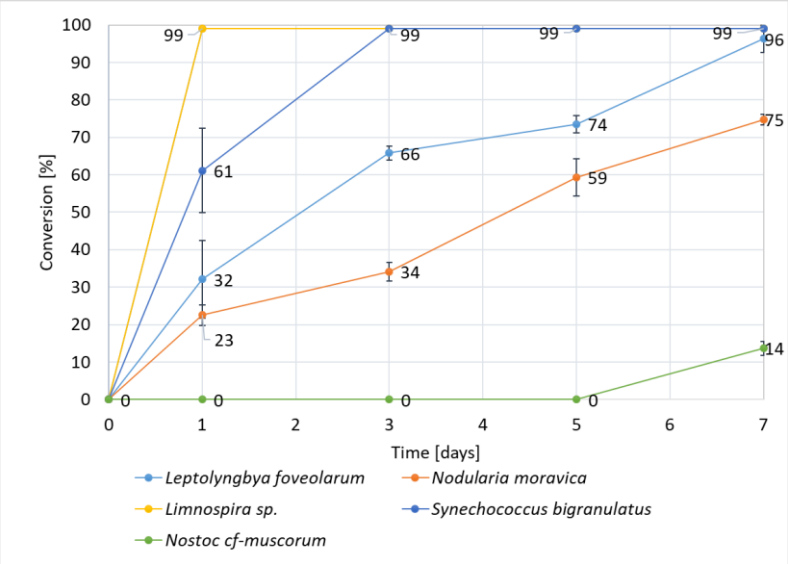

Figure 10. Comparative analysis of the bioconversion percentages by cyanobacterial biocatalysts [139].

The differential transformation ability among cyanobacterial strains, complete conversion of EMDP in *Limnospira* sp. and *Synechococcus bigranulatus* CCALA 187, but minimal activity in *Nostoc sp.*, raises the question of species-specific enzymatic capacity. These differences can be attributed to genomic content, metabolic regulation, and ecophysiological adaptations. In support of this, Herrero *et al*. [205,206] describe how *Nostoc* sp. allocates large portions of their metabolic resources toward nitrogen

fixation and heterocyst maintenance, which can downregulate generalist catabolic enzymes, especially under nutrient-limiting or diazotrophic conditions. This might suppress secondary metabolic functions like xenobiotic processing, leading to low or no EMDP transformation in *Nostoc* cultures. In contrast, Shih *et al*. [214] sequenced diverse cyanobacterial genomes and found that strains like *Synechococcus* sp. exhibit expanded gene clusters encoding oxidoreductases, hydrolases, and stress-response elements, enzymes often associated with xenobiotic degradation [214]. Their work confirms that genomic plasticity in *Limnospira* sp. and *Synechococcus bigranulatus* CCALA 187 correlates with enhanced catalytic versatility, supporting their ability to carry out both steps in the EMDP conversion.

Lipid composition and membrane permeability could also play a role in substrate accessibility and enzyme activity. Guschina and Harwood [180] highlight that cyanobacterial membrane lipid profiles are species-specific and modulated by environmental cues such as light and temperature. In *Limnospira*, for instance, a high degree of unsaturation in membrane fatty acids could enhance substrate diffusion or improve the fluid microenvironment necessary for whole-cell catalysis, thus facilitating better access of EMDP to intracellular or membrane-bound enzymes. Beyond physiology, Huang *et al*. [215] present compelling metagenomic evidence for the horizontal acquisition of phosphonate utilization genes, including those involved in epoxide, diol, and alkylphosphonate transformation. Their analysis of marine microbial communities revealed frequent lateral gene transfer of phosphonate metabolic modules, especially in environments exposed to anthropogenic compounds [215]. This evolutionary mechanism could explain why only some cyanobacteria in this study possess the enzymatic machinery required for EMDP transformation-*Synechococcus* and *Limnospira*, both known for adaptability, could have acquired or retained such functions, while *Nostoc* did not.

4.2.5. DMHPP–membrane interactions as a factor in apparent yield discrepancy

The biotransformation product dimethyl (1*E*)-3-hydroxyprop-1-enylphosphonate, formed from epoxymethyl dimethyl phosphonate, exhibits amphipathic properties that could promote its interaction with or retention in the plasma membrane. Its molecular structure, featuring a hydrophobic alkene chain and a negatively charged phosphonate headgroup, is reminiscent of undecaprenyl phosphate (C_{55}-P), a lipid carrier known to integrate into prokaryotic cell membranes and undergo active translocation via specific flippase systems. Notably, C_{55}-P is recycled across the membrane by the UptA–PopT translocase complex as elucidated by Oluwole *et al*. [216], suggesting that structurally analogous compounds such as DMHPP could similarly associate with or engage membrane-related mechanisms.

In cyanobacteria, several transport systems are known to facilitate the uptake of phosphate and phosphonate compounds, including the ABC-type phosphonate transporter PhnCDE, high- and low-affinity phosphate systems such as Pst and Pit, and phn operons that encode both transport and enzymatic processing components. These systems are typically upregulated under phosphate-limiting conditions [190,217], as applied in the current study. Thus, DMHPP could not merely diffuse passively into cells but could be sequestered through transporter-mediated uptake or become embedded within the lipid bilayer due to its chemical similarity to natural substrates.

In addition to active transport, membrane retention of phosphonate analogues has been demonstrated in pharmacokinetic studies, where compounds of moderate lipophilicity display enhanced membrane partitioning. Specifically, Wiemer and Wiemer [218] and Hecker and Erion [219] reported that phosphonate esters can insert asymmetrically into lipid bilayers, leading to increased retention and altered distribution. This characteristic provides a compelling rationale for the experimentally observed low yield of DMHPP from the supernatant, despite near-complete EMDP

conversion (Table 17). These insights could also justify the bioaccumulation potential of cyanobacterial strains.

Table 17. Percentage yield of DMHPP from EMDP by *Synechococcus* sp. and *Limnospira* sp. at different substrate concentrations (mM).

	Yield (%)		
Day	***Synechococcus* sp. (1 mM)**	***Limnospira* sp. (1 mM)**	***Synechococcus* sp. (4 mM)**
1	9.95 ± 1.08	8.42 ± 2.53	6.46 ± 1.20
3	7.14 ± 0.72	5.87 ± 0.36	6.50 ± 1.20
5	2.63 ± 0.42	0.69 ± 0.01	3.19 ± 0.46
7	1.00 ± 0.40	0.00 ± 0.00	2.93 ± 0.20

DMHPP = Dimethyl (1E)-3-hydroxyprop-1-enylphosphonate; EMDP = Epoxymethyl dimethylphosphonate.

The data presented in Table (17) demonstrated the percentage yield in both *Synechococcus* sp. and *Limnospira* sp.; however, *Synechococcus* sp. consistently outperformed *Limnospira* sp. across the time frame. At 1 mM EMDP, *Synechococcus* sp. achieved a peak yield of 9.95 ± 1.08 % of the product on day 1, which steadily declined to 1.00 ± 0.40 % by day 7. In contrast, *Limnospira* sp. began with a comparable initial product yield of 8.42 ± 2.53 % but declined precipitously, reaching zero by day 7. This sharper decline suggests that *Limnospira* sp. either expresses the relevant phosphonate-hydrolyzing enzymes less effectively or possesses lower metabolic affinity for EMDP. Given these results, *Synechococcus* sp. was selected for optimization under a higher substrate concentration of 4 mM, where a maximum product yield of 6.50 ± 1.20 % was observed by day 3, similar to the day 1 value of 6.46 ± 1.20 %, with a gradual reduction to 2.93 ± 0.20 % by day 7. These outcomes could suggest product metabolism and integration within the cell membrane, a common limitation in whole-cell catalysis [220,221].

4.2.6. Antibacterial plate test

The rationale for testing epoxymethyl dimethyl phosphonate and its bioconversion product, dimethyl (1*E*)-3-hydroxyprop-1-enylphosphonate, for antibacterial activity (Figure 11) lies in the established bioactivity of organophosphorus compounds, particularly those bearing C–P bonds, vinyl, or epoxide moieties. Such structures are frequently found in synthetic phosphonates with reported antimicrobial or inhibitory effects due to their structural mimicry of phosphate esters and their potential to disrupt microbial metabolism [222]. This evaluation aimed to determine whether either compound exhibited inherent antibacterial effects and to assess any biosafety concerns relevant to scale-up or environmental deployment. Although no significant antimicrobial activity was observed, the testing contributes to defining the bioactivity boundaries of these compounds and supports their suitability for biocatalytic applications where non-toxicity is essential.

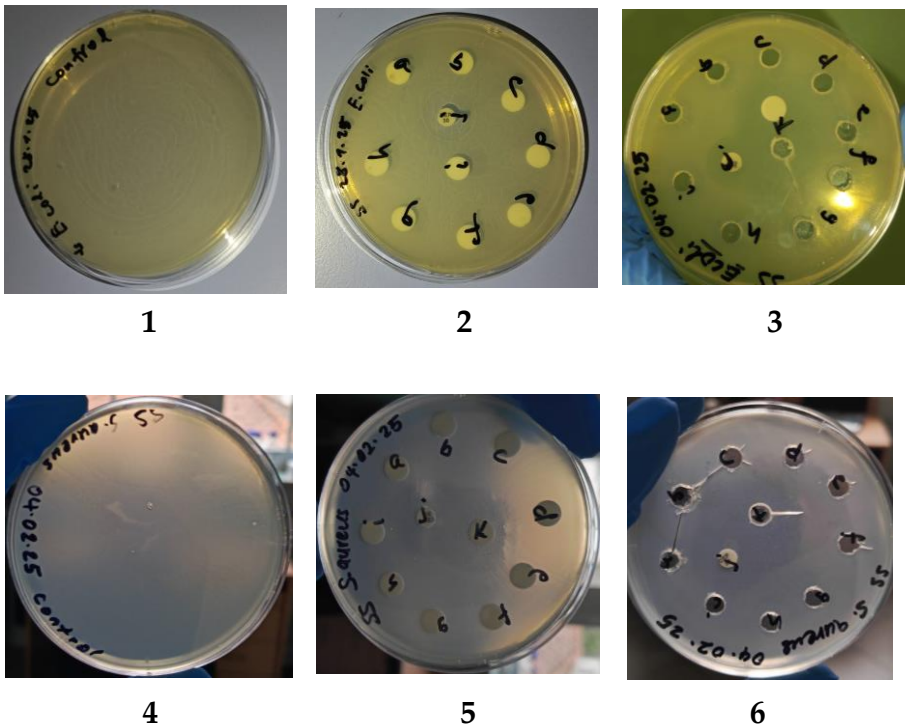

1 **2** **3**

4 **5** **6**

Figure 11. Antimicrobial susceptibility testing using disk diffusion (**Plates 2** and **5**) and agar well diffusion (**Plates 3** and **6**). Plates **1** and **4** are controls with *E. coli* and *S. aureus*. DMHPP (**a – d**) and EMDP (**e – h**) were tested at 15.8, 7.9, 3.95, and 1.98 mg/mL**,** with controls: **i** = DMSO, **j** = cefoperazone 30 μg, **k** = EMDP (24.56 mg for disk diffusion, 85.96 mg for agar well diffusion)**.**

The disk diffusion method (Table 18) showed no antibacterial activity for both the substrate, epoxymethyl dimethyl phosphonate, and the product, dimethyl (1*E*)-3-hydroxyprop-1-enylphosphonate, at concentrations ranging from 0.0396 mg to 0.316 mg per disk. Even at an undiluted concentration equivalent to 24.56 mg per disk, EMDP produced a zone of inhibition of 0.7 cm against *Escherichia coli* and 1.4 cm against *Staphylococcus aureus*. However, DMHPP did not exhibit any inhibitory effect, indicating its ineffectiveness at tested concentrations. Cefoperazone, used as the positive control, showed significantly larger inhibition zones of 0.9 cm for *E. coli* and 1.2 cm for *S. aureus*, demonstrating a strong antibacterial activity.

Table 18. Antimicrobial activity of EMDP and DMHPP using the disk diffusion method

Microbial strain (McFarland standard)	Zone of inhibition (cm)										
	Substrate (EMDP)					Product (DMHPP)				Antibiotic (CEP30)	Solvent (DMSO)
	0.0396 mg	0.079 mg	0.158 mg	0.316 mg	24.56 mg*	0.0396 mg	0.079 mg	0.158 mg	0.316 mg	30 µg	22 mg
Escherichia coli	0.00	0.00	0.00	0.00	0.7 ± 0.00E+00	0.00	0.00	0.00	0.00	0.9 ± 0.00E+00	0.00
Staphylococcus aureus	0.00	0.00	0.00	0.00	1.4 ± 1.41E-01	0.00	0.00	0.00	0.00	1.2 ± 0.00E+00	0.00

Note: Volume of each sample applied to the disk = 20 µL. Equal concentrations of substrate and product were applied, except where indicated by *.

The agar well diffusion method (Table 19) produced similar results, where EMDP exhibited no inhibition at concentrations up to 1.106 mg per well. However, at 85.96 mg, EMDP produced an inhibition zone of 1.65 cm against *E. coli* and 1.55 cm against *S. aureus*, confirming its antibacterial potential at a high concentration. DMHPP exhibited no antibacterial activity at tested concentrations, confirming its inert nature in antimicrobial contexts. The positive control, cefoperazone, produced inhibition zones of 0.9 cm for *E. coli* and 1.2 cm for *S. aureus*, consistent with the disk diffusion method. The lack of antibacterial activity in DMHPP, even at high concentrations, suggests the need for structural modifications or its use in combination with other antimicrobial agents to enhance its potential efficacy in future applications.

Table 19. Antimicrobial activity of EMDP and DMHPP using the agar well diffusion method

Microbial strain (McFarland standard)	Zone of inhibition (cm)										
	Substrate (EMDP)					Product (DMHPP)				Antibiotic (CEP30)	Solvent (DMSO)
	0.1386 mg	0.2765 mg	0.553 mg	1.106 mg	85.96 mg*	0.1386 mg	0.2765 mg	0.553 mg	1.106 mg	30 µg	77 mg
Escherichia coli	0.00	0.00	0.00	0.00	1.65 ± 7.07E-02	0.00	0.00	0.00	0.00	0.9 ± 0.00E+00	0.00
Staphylococcus aureus	0.00	0.00	0.00	0.00	1.55 ± 7.07E-02	0.00	0.00	0.00	0.00	1.2 ± 0.00E+00	0.00

Note: Volume of each sample applied to the well = 70 µL. Equal concentrations of substrate and product were applied, except where indicated by *.

4.3. Bioaccumulation

Following the photobiocatalytic conversion of selected substrates, the secondary aim of this research was to evaluate the potential of cyanobacterial biomass for rare earth element (REE) uptake, specifically gadolinium (Gd) and europium (Eu). Bioaccumulation of REEs by cyanobacteria offers a feasible approach to metal recovery from aqueous environments, aligning with global efforts in green bioremediation and circular economy strategies [130,223,224]. The integration of biotransformation and bioaccumulation studies presents a complete framework for evaluating the dual functional potential of cyanobacterial strains, both as biocatalysts and biosorbents.

4.3.1. Microscopic examination of pre- and post- bioconversion biomass

To assess the physiological integrity of cyanobacterial cells prior to and following photobiocatalysis, microscopic evaluations were conducted using light microscopy (Figure 12). The observations confirmed conservation of viable cellular morphology in both pre- and post-bioconversion biomass. Cells retained structural integrity with no visible signs of lysis, aggregation, or abnormal pigmentation, indicating that the biotransformation processes did not induce significant cytotoxic effects under the applied conditions. Limited contamination was observed, supporting the reliability of biomass for subsequent ecotoxicological and bioaccumulation assessments. The absence of significant contamination is critical to ensure the reliability of downstream

ecotoxicological and bioaccumulation assessments, as competing microbial populations can skew uptake profiles or influence the physiological state of the biomass [225].

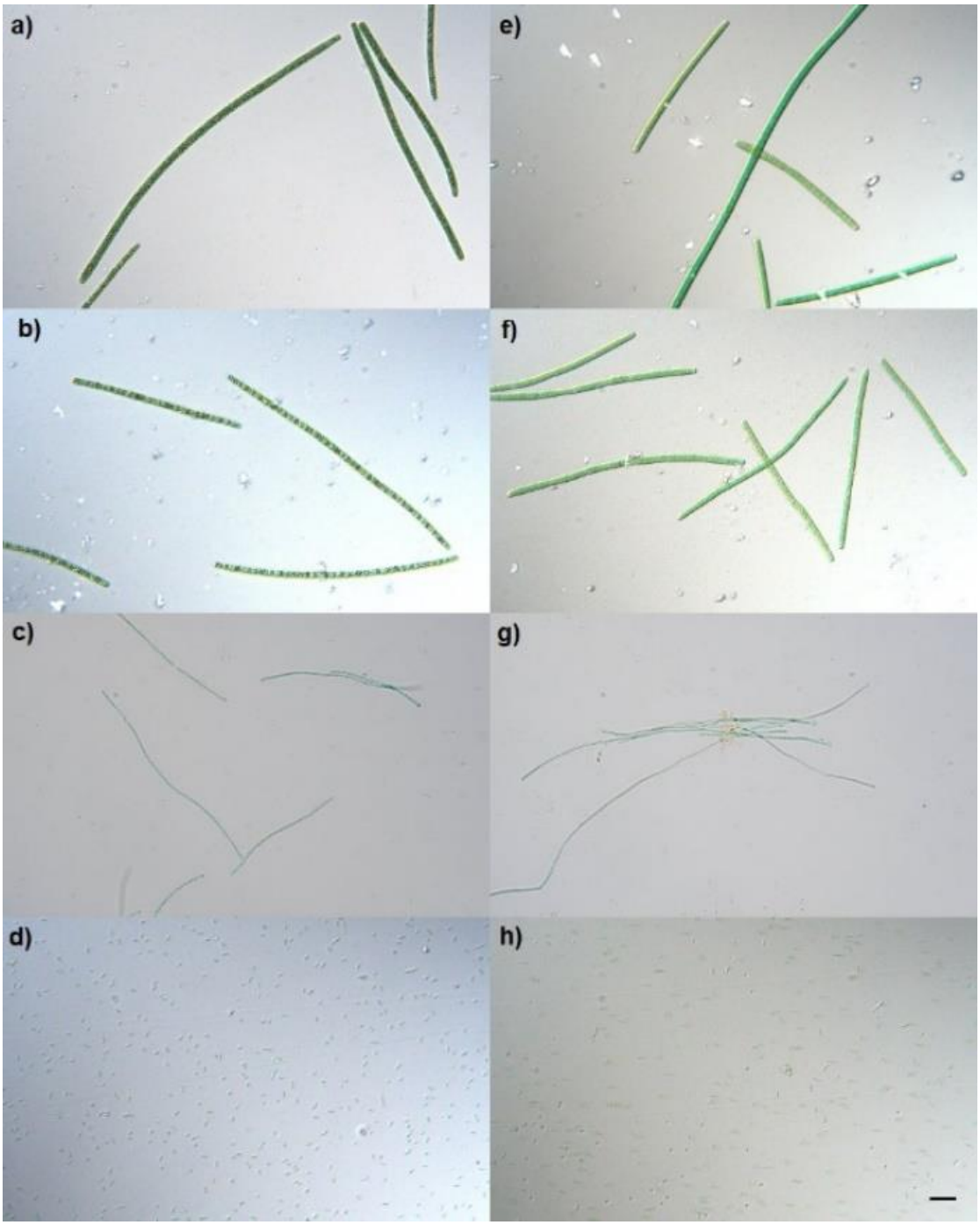

Figure 12. Light microscope images of *Limnospira indica* (a, e), *Limnospira maxima* (b, f), *Leptolyngbya foveolarum* (c, g) and *Synechococcus bigranulatus* (d, h). Pre-bioconversion biomass (**a – d**) and post-bioconversion biomass (**e – h**). Images were captured at 60× magnification (scale bar 20 μm).

4.3.2. Ecotoxicity assessment

Ecotoxicity results revealed significant strain-specific variations in REE tolerance (Figures 13), supporting previous findings that show the adaptive mechanisms of cyanobacteria in response to heavy metals and other stressors [44]. These preliminary assays were conducted at three exposure concentrations (20, 40, and 80 μM). While this design does not yield a full dose-response curve, it allowed for empirical determination of final concentrations for the bioaccumulation phase (Figure 14). Interestingly, in some cases, the lowest concentrations induced stronger inhibitory responses than higher concentrations, a phenomenon (hormesis) previously reported in toxicity studies where stress responses are triggered at sub-lethal levels, resulting in a non-linear response. This aligns with the findings by Gjata *et al*. [45] who showed that several REEs (Ce, Nd, Gd, Dy, Yb, Ho, Lu) in millimolar concentrations produce toxicity (e.g. growth inhibition, oxidative stress) in *Lemna minor*. Whereas in fungi exposed to La, Ce, and Nd, low doses stimulated growth while higher ones were inhibitory [46].

In this research, hormetic-like responses were most evident in *Limnospira* sp. (Figure 13a-d). In the *Limnospira* sp. pre-bioconversion biomass (Figure 13a, c), Gd at the lowest concentration (0.02 mM) caused stronger inhibition than at higher levels. In the post-bioconversion strains (Figure 13b, d), inhibition was most pronounced at 0.04 mM Gd. However, Eu consistently produced strong inhibitory effects at higher concentrations (0.04 and 0.08 mM) in both pre- and post-bioconversion biomass of *Limnospira* sp. A comparable pattern was observed in *L. foveolarum* (Figure 13h), where post-bioconversion biomass growth was more inhibited at low Gd exposure concentrations (0.02 and 0.04 mM) than at 0.08 mM, and Eu at the lowest concentration, 0.02 mM also exerted stronger inhibition. In Figure 13g (pre-bioconversion biomass of *L. foveolarum*), none of the tested REE concentrations produced growth inhibition, indicating a negative response with no detectable adverse effect. By contrast, *S.*

bigranulatus (Figure 13e, f) showed stable growth across exposure levels, indicating higher tolerance.

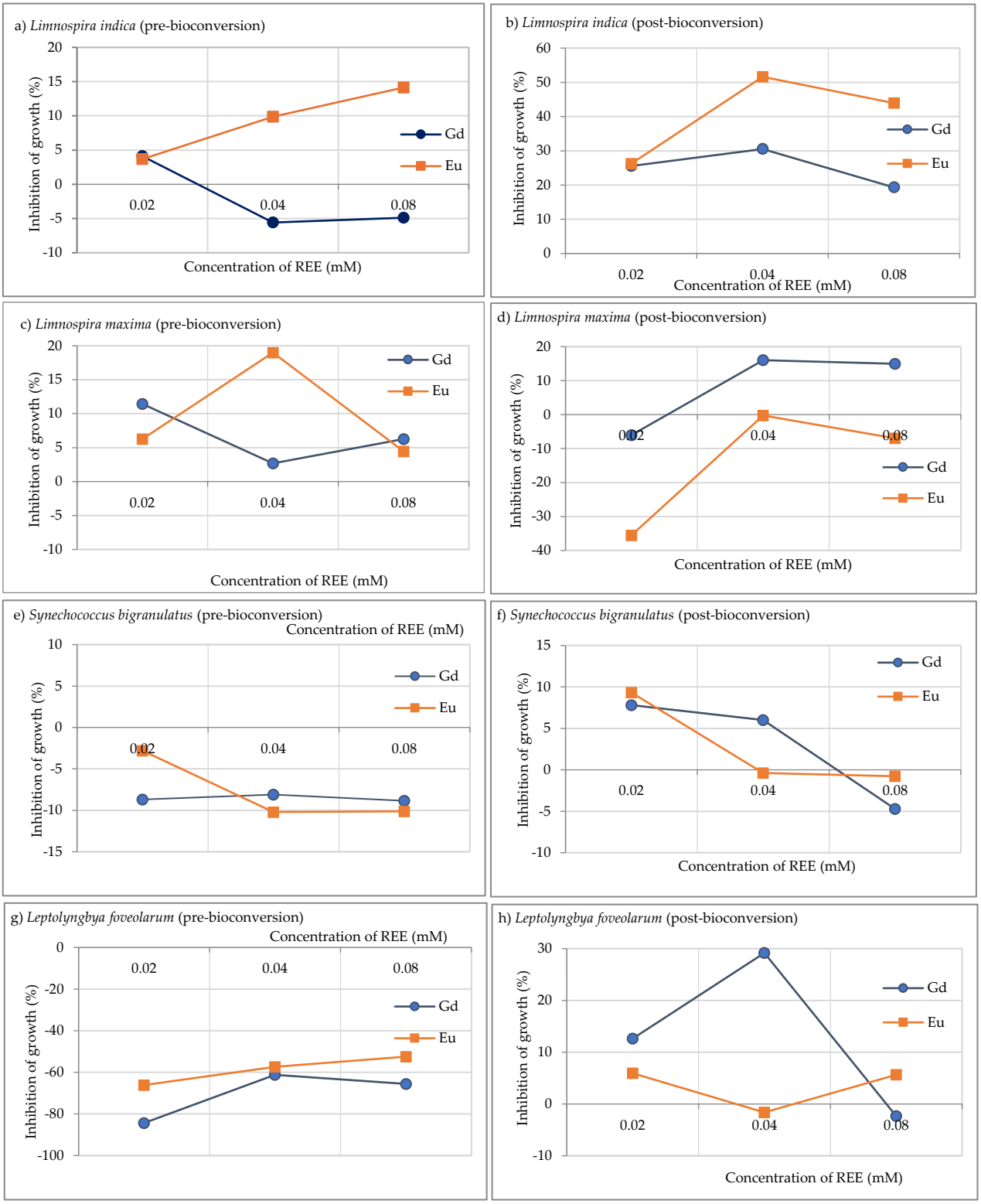

Figure 13. Growth inhibition (%) of four cyanobacterial strains exposed to gadolinium (Gd) and europium (Eu) at three concentrations (data were reported as mean ± standard deviation (SD) from quintuplicate experiments (n=5)).

These hormetic responses to REE treatments as observed in *Limnospira* strains, and increased sensitivity of *Leptolyngbya* sp. post-bioconversion biomass, and the consistent tolerance of *Synechococcus* sp. reveals the existence of clear strain-specific differences in REE response profiles as summarized in Figure 14. However, these disparities could also be attributed to the role of extracellular polymeric substances (EPS), which bind metal ions and limit their intracellular uptake [47]. Limited EPS production in *Limnospira* sp. and *Leptolyngbya* sp. could be responsible for their increased sensitivity. Furthermore, oxidative stress from REE exposure is known to disrupt photosystem II, lowering chlorophyll content and reducing biomass productivity [48]. Notably, post-bioconversion biomass displayed slightly greater resilience at low REE levels, indicating that metabolic adjustments during the biotransformation phase induce protective responses, such as upregulation of stress proteins or efflux systems. This aligns with reports that *Synechococcus* sp. possess efficient heavy-metal efflux systems and strong surface binding capacity due to negatively charged functional groups such as carboxyl, hydroxyl, and phosphate [49–51]. Their metabolic plasticity under stress [52–54], further enhance their effectiveness as a promising candidate for REE bioremediation applications.

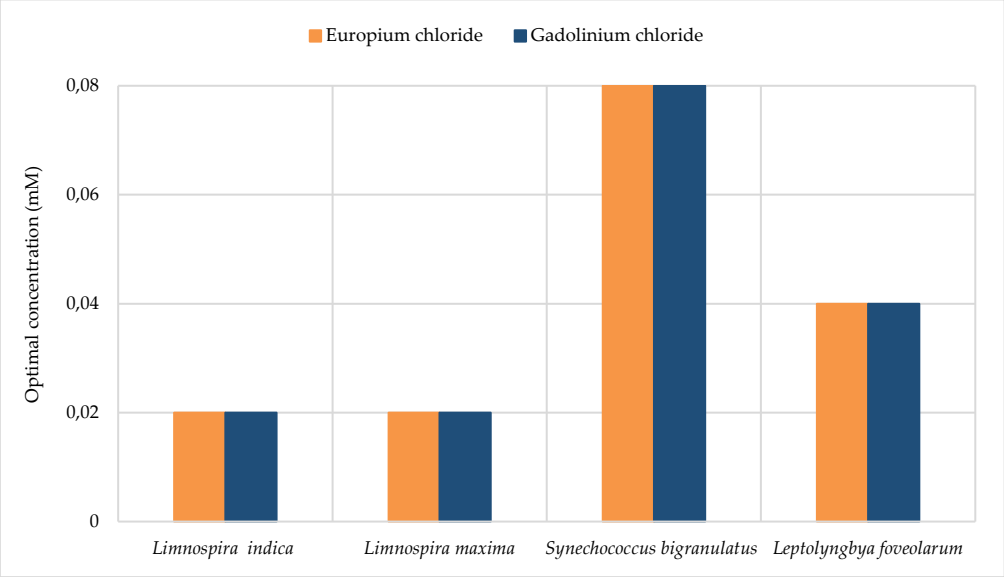

Figure 14. Determination of optimal concentrations of REEs.

4.3.3. Dry mass analysis of bioaccumulated REEs

After 72 h of bioaccumulation experiment, pre-bioconversion cyanobacterial samples treated with REEs exhibited higher increase in biomass weight compared to controls (Figure 4). This trend was observed across all treated samples except for Gd treated *Synechococcus* sp. (Figure 15a). This observation aligns with previous studies that highlight the enhanced resilience and bioaccumulative potential of cyanobacteria when exposed to REEs [223]. In post-bioconversion biomass of *Synechococcus* sp. and *Limnospira maxima*, a decrease in biomass weight was observed, more significant in controls compared to REE treated samples (Figure 15b). This suggests that the response to REE treatment could vary among different cyanobacterial species and REEs could have some beneficial effect on the cyanobacterial growth or induce an accumulation of these specific REEs (Eu and Gd) contributing to increased biomass [135,226,238].

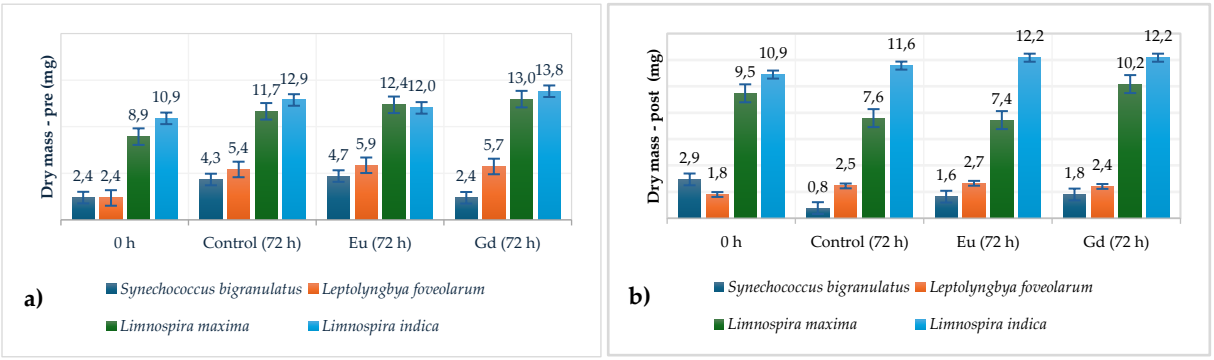

Figure 15. Dry mass assessment of pre- **(a)** and post- **(b)** bioconversion cyanobacterial biomasses after 3 days of bioaccumulation. **Control** = pre-bioconversion **(a)** and post-bioconversion **(b)** biomass without REE treatment; **Eu** = biomass treated by Europium chloride at defined concentrations; **Gd** = biomass treated by Gadolinium chloride at defined concentrations.

4.3.4. Inductively coupled plasma mass spectrometry (ICP-MS) analysis of bioaccumulated REEs

The presented Table 20 – 23 and graphical illustrations in Figure 16 showed the bioaccumulation of rare earth elements (REEs) by cyanobacteria, comparing pre-bioconversion and post-bioconversion biomass. The four cyanobacterial strains examined, *Limnospira indica* PCC 8005, *Limnospira maxima* CCALA 27, *Synechococcus*

bigranulatus CCALA 187, and *Leptolyngbya foveolarum* CCALA 76, demonstrated substantial variations in REE uptake, with a consistent trend of increased bioaccumulation following bioconversion. The observed patterns support the findings that cyanobacteria offer biologically selective and efficient platforms for the sequestration of critical elements such as Eu and Gd from aqueous environments, a concept corroborated in recent literature exploring microbe-mediated REE recovery strategies [223,239].

Table 20. Analysis of bioaccumulated REEs by *Limnospira indica*

Limnospira indica	**Pre-bioconversion (μg/g) ± SD**	**Post-bioconversion (μg/g) ± SD**
Control Biomass	8.6 ± 2.7	14.3 ± 11.1
Eu-Treated Biomass	7495 ± 634.04	12749 ± 654.09
Gd-Treated Biomass	9125 ± 728.53	13963 ± 171.75

Table 21. Analysis of bioaccumulated REEs by *Limnospira maxima*

Limnospira maxima	**Pre-bioconversion (μg/g) ± SD**	**Post-bioconversion (μg/g) ± SD**
Control Biomass	4.3 ± 2.1	4.7 ± 1.6
Eu-Treated Biomass	6934 ± 827.23	38332 ± 5999.61
Gd-Treated Biomass	6433 ± 343.31	30348 ± 3619.25

Table 22. Analysis of bioaccumulated REEs by *Synechococcus bigranulatus*

Synechococcus bigranulatus	**Pre-bioconversion (μg/g) ± SD**	**Post-bioconversion (μg/g) ± SD**
Control Biomass	0.1 ± 0.1	8.3 ± 2.7
Eu-Treated Biomass	32257 ± 1114.91	53599 ± 1619.53
Gd-Treated Biomass	34978 ± 3270.74	54197 ± 2753.11

Table 23. Analysis of bioaccumulated REEs by *Leptolyngbya foveolarum*

Leptolyngbya foveolarum	**Pre-bioconversion (μg/g) ± SD**	**Post-bioconversion (μg/g) ± SD**
Control Biomass	2.2 ± 2.3	1.6 ± 1.1
Eu-Treated Biomass	15157 ± 929.71	40138 ± 1389.97
Gd-Treated Biomass	16021 ± 1838.40	38798 ± 1350.67

The ICP-MS data (Figure 16) illustrate that bioconversion significantly enhances the ability of cyanobacterial biomass to accumulate REEs, supporting the hypothesis

that structural and biochemical modifications in the biomass contribute to improved metal sequestration. For instance, a study on biochar, a form of biomass, highlights that its properties, such as surface area, porosity, pH, surface charge, functional groups, and mineral components, can be tailored to enhance metal sorption. These modifications can significantly improve the biochar's capacity to adsorb various metals from contaminated environments [240]. In another development, research on biomodification in mineral processing demonstrates that microbial-induced changes to mineral surfaces can enhance metal recovery. Microorganisms can alter the surface properties of minerals through biochemical interactions, leading to improved metal sequestration [241].

ICP-MS data (Figure 16a) reveals that pre-bioconversion biomass of *L. indica* exhibited Eu bioaccumulation capacity of 7,495.0 ± 634.0 μg/g and Gd accumulation of 9,125.0 ± 728.5 μg/g. After bioconversion (i.e., post-bioconversion biomass), these values increased to 12,749.0 ± 654.1 μg/g and 13,963.0 ± 171.8 μg/g respectively. *L. maxima* (Figure 16b) followed a similar trend, with Eu accumulation increasing from 6,934.0 ± 827.2 μg/g pre-bioconversion to 38,332.0 ± 5,999.6 μg/g post-bioconversion. The corresponding increase for Gd was from 6,433.0 ± 343.3 μg/g to 30,348.0 ± 3,619.2 μg/g. The most pronounced increases were observed in *S. bigranulatus* (Figure 16c), where Eu accumulation surged from 32,257.0 ± 1,114.9 μg/g to 53,599.0 ± 1,619.5 μg/g post-bioconversion. Gd accumulation increased from 34,978.0 ± 3,270.7 μg/g to 54,197.0 ± 2,753.1 μg/g. *L. foveolarum* (Figure 16d) also exhibited significant increases, with Eu bioaccumulation rising from 15,157.0 ± 929.7 μg/g to 40,138.0 ± 1,390.0 μg/g. Gd increased from 16,021.0 ± 1,838.4 μg/g to 38,798.0 ± 1,350.7 μg/g.

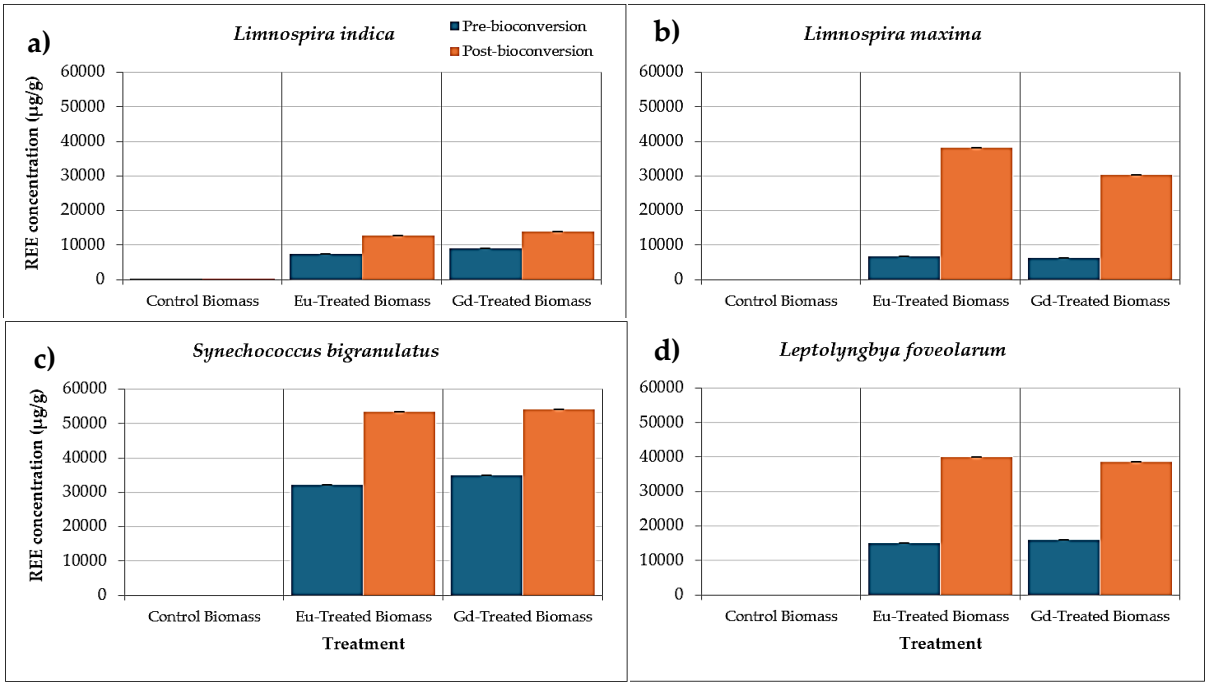

Figure 16. Graphical illustration of ICP-MS analysis of bioaccumulated REEs

These values clearly indicate that bioconversion plays a crucial role in improving REE sequestration across all tested strains. The observed enhancements in REE bioaccumulation post-bioconversion are consistent with findings from previous studies. Research by Paper *et al*. [242] on *Nostoc* sp. *20.02* reported maximum adsorption capacities ranging from 84.2 to 91.5 mg/g for cerium, neodymium, terbium, and lanthanum [243]. The post-bioconversion bioaccumulation values observed in the present study, particularly for *L. maxima* and *S. bigranulatus*, approach or exceed these values, which suggest that bioconversion enhances cyanobacterial metal uptake to levels comparable with the most efficient biosorption strains reported in literature. Similarly, in previous investigation by Yushin *et al*. [244], *Arthrospira platensis* demonstrated a maximum biosorption capacity of 101 mg/g for gadolinium at pH 3.0 and 20°C [244]. The increases observed in *S. bigranulatus* and *L. foveolarum* post-bioconversion align with these findings, reinforcing the efficacy of these strains as viable candidates for large-scale REE biorecovery [243–245].

These strains' high uptake efficiency is consistent with findings by Rastogi and Sinha [246], who identified *Synechococcus* sp. as having robust metal-binding

properties due to their dense exopolysaccharide (EPS) layers and high surface area-to-volume ratios. Additionally, it aligns with the work of Calderón *et al*. [247]; Volesky & Holan [248], where enhanced biosorption in microbial biomass was attributed to the abundance of functional groups (e.g., carboxyl, phosphate) on cell surfaces that form stable complexes with trivalent metal ions [247], resulting to maximum biosorption capacities of 200 - 300 mg/g for heavy metals in brown algae [248].

Additionally, prior studies have shown that the biosorption of europium, samarium, and neodymium by *Anabaena cylindrica* is both rapid and nearly complete within minutes of exposure [135]. The substantial increases in europium and gadolinium bioaccumulation post-bioconversion, particularly in *L. maxima*, *S. bigranulatus*, and *L. foveolarum* suggests that modifications made to the biomass, such as biotransformation with organic compounds, could optimize biosorption kinetics, possibly through increased binding site availability or enhanced metabolic activity [249].

The observed increases in europium and gadolinium accumulation align with existing literatures, confirming the efficiency of post-bioconversion biomass in metal sequestration. The results emphasize the potential of bioconversion as a tool to optimize cyanobacterial bioaccumulation capacity, with applications in bioremediation and resource recovery. For instance, a pertinent study by Pandhal *et al*. [250] investigated the harvesting of environmental microalgal blooms for remediation and resource recovery, assessing economic and microbial community impacts. The research highlights the feasibility of utilizing microalgae for environmental clean-up and the recovery of valuable resources [250].

CHAPTER FIVE

Conclusion

5.1. Summary of major findings

This dissertation explored the biotechnological potential of cyanobacterial biomass in two interconnected domains: biocatalysis and bioaccumulation. Utilizing diverse cyanobacterial strains, including *Synechococcus bigranulatus* CCALA 187, *Nostoc cf-muscorum* CCALA 129, *Limnospira indica* PCC 8005, *Limnospira maxima* CCALA 27, *Leptolyngbya foveolarum* CCALA 76, and *Kamptonema animale* CCALA 138, the study systematically evaluated their ability to perform photobiocatalytic transformations of industrially relevant substrates and accumulate critical rare earth elements (REEs), particularly gadolinium (Gd) and europium (Eu). These features align with emerging goals in industrial biotechnology, particularly within the areas of green chemistry, circular bioeconomy, and low- impact mining technologies.

Key major findings include:

- **Photobiocatalysis**: The cyanobacterial strains demonstrated differential abilities to catalyze the transformation of vinylphosphonates, epoxyphosphonate, and ester compounds. Among the tested strains, *S. bigranulatus* and *Limnospira* sp. consistently showed the highest photobiocatalytic efficiency, especially in the conversion of EMDP to DMHPP. Complete biotransformation was achieved within 72 hours for *S. bigranulatus* and 24 hours for *Limnospira* sp.
- **Selectivity**: The cyanobacterial biomass showed pronounced selectivity, resulting in the bioconversion of epoxymethyl dimethylphosphonate into a pure isomer of dimethyl (1*E*)-3-hydroxyprop-1-enylphosphonate and catalyzing the enantioselective hydrolysis of 1-phenylethyl acetate to optically enriched 1-phenylethanol. This stereoselective behaviour shows the potential of cyanobacteria

as efficient biocatalysts in pharmaceutical synthesis, where enantioselectivity is a critical feature.

- **Bioaccumulation**: All tested strains demonstrated the capacity to bioaccumulate REEs, with notable increases in uptake in post- biotransformation biomass. This suggests that the structural and metabolic changes induced by substrate exposure could enhance cell wall affinity or internalization mechanisms for metal ions.

5.2. Validation of research hypotheses

1. Cyanobacterial strains selectively catalyzed the biotransformation of epoxymethyl dimethyl phosphonate to dimethyl (1*E*)-3-hydroxyprop-1-enylphosphonate and hydrolyzed 1-phenylethyl acetate to its optically enriched alcohol. No biotransformation was observed with vinyl phosphonates or unsaturated fatty acids, confirming substrate specificity.
2. The chemical composition of growth media significantly influenced both the stability of organophosphorus substrates and the metabolic performance of cyanobacterial strains during photobiocatalysis. Optimized media enhanced catalytic outcomes and minimized substrate degradation.
3. Cyanobacterial strains demonstrated enantioselective hydrolysis of 1-phenylethyl acetate, producing optically enriched products with potential pharmaceutical relevance. This confirms their stereoselective biocatalytic potential.
4. Comparative experiments between phytotron and manual growth chambers revealed no observable differences in catalytic performance or enantioselectivity. However, the phytotron offered improved environmental reproducibility.
5. Post-biotransformation cyanobacterial biomass retained or improved its capacity for rare earth element (REE) bioaccumulation (Gd and Eu), demonstrating functional integrity and biotechnological potential after catalytic use.
6. Among all tested strains, *S. bigranulatus* exhibited the highest biocatalytic efficiency, enantioselectivity, substrate tolerance, and REE bioaccumulation

capacity. This strain is therefore well-suited for further process optimization and industrial scale-up.

5.3. Scientific and technological implications

This research reinforces cyanobacteria as viable photoautotrophic framework for synthetic applications and resource recovery. The dual utility of these organisms in catalyzing organic transformations and binding toxic or valuable elements represents a significant advancement in integrated bioprocessing. Notably, the use of light as an energy input reduces the carbon footprint of biocatalytic processes. Cyanobacterial cultures require minimal nutritional input and can thrive in non-arable water systems, enhancing ecological compatibility. The high selectivity and stereospecificity demonstrated in certain biotransformations suggest applicability in the production of chiral pharmaceutical intermediates.

This dissertation has demonstrated that cyanobacterial biomass is a multifunctional biological resource capable of catalyzing structurally diverse chemical substrates while simultaneously offering a biotechnological avenue for rare earth element recovery. The integration of photobiocatalysis and bioaccumulation into a single microbial framework exemplifies a green alternative to conventional chemical and metallurgical processes.

References

1. Sheldon, R.A.; Woodley, J.M. Role of Biocatalysis in Sustainable Chemistry. *Chem. Rev.* **2018**, *118*, 801–838, doi:10.1021/ACS.CHEMREV.7B00203/ASSET/IMAGES/LARGE/CR-2017-002034_0025.JPEG.

2. Faber, K. Biotransformations in Organic Chemistry. *Biotransformations Org. Chem.* **2018**, doi:10.1007/978-3-319-61590-5.

3. Bornscheuer, U.T.; Huisman, G.W.; Kazlauskas, R.J.; Lutz, S.; Moore, J.C.; Robins, K. Engineering the Third Wave of Biocatalysis. *Nat. 2012 4857397* **2012**, *485*, 185–194, doi:10.1038/nature11117.

4. Bornscheuer, U.T.; Kazlauskas, R.J. Hydrolases in Organic Synthesis: Regio- and Stereoselective Biotransformations: Second Edition. *Hydrolases Org. Synth. Regio- Stereoselective Biotransformations Second Ed.* **2006**, 1–355, doi:10.1002/3527607544;CSUBTYPE:STRING:MONOGRAPH;WEBSITE:WEBSITE:PERICLES;ISPURCHASABLE:BOOLEAN:TRUE;PAGE:STRING:BOOK.

5. Liese, A.; Seelbach, K.; Wandrey, C. Industrial Biotransformations: Second, Completely Revised and Extended Edition. *Ind. Biotransformations Second. Complet. Revis. Ext. Ed.* **2006**, 1–556, doi:10.1002/3527608184.

6. Sheldon, R.A.; Brady, D. The Limits to Biocatalysis: Pushing the Envelope. *Chem. Commun.* **2018**, *54*, 6088–6104, doi:10.1039/C8CC02463D.

7. Wu, S.; Snajdrova, R.; Moore, J.C.; Baldenius, K.; Bornscheuer, U.T. Biocatalysis: Enzymatic Synthesis for Industrial Applications. *Angew. Chemie - Int. Ed.* **2021**, *60*, 88–119, doi:10.1002/ANIE.202006648,.

8. Singh, R.S.; Singh, T.; Pandey, A. Microbial Enzymes—An Overview. *Adv. Enzym. Technol. First Ed.* **2019**, 1–40, doi:10.1016/B978-0-444-64114-4.00001-7.

9. Liese, A.; Hilterhaus, L. Evaluation of Immobilized Enzymes for Industrial Applications. *Chem. Soc. Rev.* **2013**, *42*, 6236–6249, doi:10.1039/C3CS35511J.

10. Zhao, H.; Van Der Donk, W.A. Regeneration of Cofactors for Use in Biocatalysis. *Curr. Opin. Biotechnol.* **2003**, *14*, 583–589, doi:10.1016/j.copbio.2003.09.007.

11. Sheldon, R.A. Green Chemistry and Resource Efficiency: Towards a Green Economy. *Green Chem.* **2016**, *18*, 3180–3183, doi:10.1039/C6GC90040B.

12. Tripathi, P.; Sinha, S. Industrial Biocatalysis: An Insight into Trends and Future Directions., doi:10.1007/s40518-020-00150-8.

13. Savile, C.K.; Janey, J.M.; Mundorff, E.C.; Moore, J.C.; Tam, S.; Jarvis, W.R.; Colbeck, J.C.; Krebber, A.; Fleitz, F.J.; Brands, J.; et al. Biocatalytic Asymmetric Synthesis of Chiral Amines from Ketones Applied to Sitagliptin Manufacture. *Science (80-.).* **2010**, *329*, 305–309, doi:10.1126/SCIENCE.1188934,.

14. Arnold, F.H. Directed Evolution: Bringing New Chemistry to Life. *Angew. Chemie Int. Ed.* **2018**, *57*, 4143–4148, doi:10.1002/ANIE.201708408.

15. Coelho, P.S.; Brustad, E.M.; Kannan, A.; Arnold, F.H. Olefin Cyclopropanation via Carbene Transfer Catalyzed by Engineered Cytochrome P450 Enzymes. *Science (80-.).* **2013**, *339*, 307–310, doi:10.1126/SCIENCE.1231434,.

16. Cravens, A.; Payne, J.; Smolke, C.D. Synthetic Biology Strategies for Microbial Biosynthesis of Plant Natural Products. *Nat. Commun.* **2019**, *10*, 1–12, doi:10.1038/S41467-019-09848-W;TECHMETA=140,58;SUBJMETA=252,318,61,631;KWRD=METABOLIC+ENGINEERING.

17. Malihan-Yap, L.; Grimm, H.C.; Kourist, R. Recent Advances in Cyanobacterial Biotransformations. *Chemie-Ingenieur-Technik* **2022**, *94*, 1628–1644, doi:10.1002/CITE.202200077;WGROUP:STRING:PUBLICATION.

18. Wijffels, R.H.; Kruse, O.; Hellingwerf, K.J. Potential of Industrial Biotechnology with Cyanobacteria and Eukaryotic Microalgae. *Curr. Opin. Biotechnol.* **2013**, *24*, 405–413, doi:10.1016/J.COPBIO.2013.04.004.

19. Straathof, A.J.J.; Panke, S.; Schmid, A. The Production of Fine Chemicals by Biotransformations. *Curr. Opin. Biotechnol.* **2002**, *13*, 548–556, doi:10.1016/S0958-1669(02)00360-9.

20. Lish, M.P.; Ashjari, M.; Yousefi, M.; Mohammadi, M.; Ramazani, A. Immobilized Candida Antarctica Lipase B (CALB) for Biodiesel Production from Rapeseed Oil; Evaluation of the Effect of Immobilization Protocol. *Int. J. Biol. Macromol.* **2025**, *297*, doi:10.1016/j.ijbiomac.2025.139814.

21. Schoemaker, H.E.; Mink, D.L.; WubboLts, M.G. Dispelling the Myths - Biocatalysis in Industrial Synthesis. *Science (80-.).* **2003**, *299*, 1694–1697, doi:10.1126/SCIENCE.1079237,.

22. Stepankova, V.; Bidmanova, S.; Koudelakova, T.; Prokop, Z.; Chaloupkova, R.; Damborsky, J. Strategies for Stabilization of Enzymes in Organic Solvents. *ACS Catal.* **2013**, *3*, 2823–2836, doi:10.1021/CS400684X.

23. Fontanille, P.; Gros, J.-B.; Larroche, C. Biotransformations with Crude Enzymes and Whole Cells. *Enzym. Technol.* **2006**, 123–155, doi:10.1007/978-0-387-35141-4_7.

24. Alissandratos, A. In Vitro Multi-Enzymatic Cascades Using Recombinant Lysates of E. Coli: An Emerging Biocatalysis Platform. *Biophys. Rev.* **2020**, *12*, 175, doi:10.1007/S12551-020-00618-3.

25. Bergquist, P.L.; Siddiqui, S.; Sunna, A. Cell-Free Biocatalysis for the Production of Platform Chemicals. *Front. Energy Res.* **2020**, *8*, 572701, doi:10.3389/FENRG.2020.00193/XML.

26. Alcántara, A.R.; Domínguez de María, P.; Littlechild, J.A.; Schürmann, M.; Sheldon, R.A.; Wohlgemuth, R. Biocatalysis as Key to Sustainable Industrial Chemistry. *ChemSusChem* **2022**, *15*, e202102709, doi:10.1002/CSSC.202102709.

27. Bornscheuer, U.T.; Pohl, M. Improved Biocatalysts by Directed Evolution and Rational Protein Design. *Curr. Opin. Chem. Biol.* **2001**, *5*, 137–143, doi:10.1016/S1367-5931(00)00182-4.

28. Keasling, J.D. Synthetic Biology for Synthetic Chemistry. *ACS Chem. Biol.* **2008**, *3*, 64–76, doi:10.1021/CB7002434,.

29. Guo, D.; Zhang, L.; Kong, S.; Liu, Z.; Li, X.; Pan, H. Metabolic Engineering of Escherichia Coli for Production of 2-Phenylethanol and 2-Phenylethyl Acetate from Glucose. *J. Agric. Food Chem.* **2018**, *66*, 5886–5891, doi:10.1021/ACS.JAFC.8B01594,.

30. Garzón-Posse, F.; Becerra-Figueroa, L.; Hernández-Arias, J.; Gamba-Sánchez, D. Whole Cells as Biocatalysts in Organic Transformations. *Mol. 2018, Vol. 23, Page 1265* **2018**, *23*, 1265, doi:10.3390/MOLECULES23061265.

31. Maciel Ferreira, I.; Coutinho Rocha, L.; Akinobo Yoshioka, S.; Nitschke, M.; Jeller, A.H.; Pizzuti, L.; Seleghim, M.H.R.; Porto, A.L.M. Chemoselective Reduction of Chalcones by Whole Hyphae of Marine Fungus Penicillium Citrinum CBMAI 1186, Free and Immobilized on Biopolymers. *Biocatal. Agric. Biotechnol.* **2014**, *3*, 358–364, doi:10.1016/J.BCAB.2014.04.001.

32. Serafin-Lewańczuk, M.; Brzezińska-Rodak, M.; Lubiak-Kozłowska, K.; Majewska, P.; Klimek-Ochab, M.; Olszewski, T.K.; Żymańczyk-Duda, E. Phosphonates Enantiomers Receiving with Fungal Enzymatic Systems. *Microb. Cell Fact.* 2021, *20*.

33. Lubiak-Kozłowska, K.; Brzezińska-Rodak, M.; Klimek-Ochab, M.; Olszewski,

T.K.; Serafin-Lewańczuk, M.; Żymańczyk-Duda, E. (*S*)-Thienyl and (*R*)-Pirydyl Phosphonate Derivatives Synthesized by Stereoselective Resolution of Their Racemic Mixtures With Rhodotorula Mucilaginosa (DSM 70403) - Scaling Approaches. *Front. Chem.* **2020**, *8*, 589720, doi:10.3389/FCHEM.2020.589720.

34. Seppälä, S.; Wilken, S.E.; Knop, D.; Solomon, K. V.; O'Malley, M.A. The Importance of Sourcing Enzymes from Non-Conventional Fungi for Metabolic Engineering and Biomass Breakdown. *Metab. Eng.* **2017**, *44*, 45–59, doi:10.1016/J.YMBEN.2017.09.008.

35. Gruninger, R.J.; Puniya, A.K.; Callaghan, T.M.; Edwards, J.E.; Youssef, N.; Dagar, S.S.; Fliegerova, K.; Griffith, G.W.; Forster, R.; Tsang, A.; et al. Anaerobic Fungi (Phylum Neocallimastigomycota): Advances in Understanding Their Taxonomy, Life Cycle, Ecology, Role and Biotechnological Potential. *FEMS Microbiol. Ecol.* **2014**, *90*, 1–17, doi:10.1111/1574-6941.12383.

36. Hibbett, D.S.; Binder, M.; Bischoff, J.F.; Blackwell, M.; Cannon, P.F.; Eriksson, O.E.; Huhndorf, S.; James, T.; Kirk, P.M.; Lücking, R.; et al. A Higher-Level Phylogenetic Classification of the Fungi. *Mycol. Res.* **2007**, *111*, 509–547, doi:10.1016/J.MYCRES.2007.03.004.

37. Zymańczyk-Duda, E.; Lejczak, B.; Kafarski, P.; Grimaud, J.; Fischer, P. Enantioselective Reduction of Diethyl 2-Oxoalkylphosphonates by Baker's Yeast. *Tetrahedron* **1995**, *51*, 11809–11814, doi:10.1016/0040-4020(95)00742-Q.

38. Orfanidou, M.; Panagiotidou, E.; Makris, A.M.; Theodosiou, E. Engineering Novel Yarrowia Lipolytica Whole-Cell Biocatalysts by Cell Surface Display of the Native Lip2 Lipase for Biodiesel Production. *Biotechnol. Environ. 2025 21* **2025**, *2*, 1–17, doi:10.1186/S44314-025-00021-W.

39. Takoi, K.; Koie, K.; Itoga, Y.; Katayama, Y.; Shimase, M.; Nakayama, Y.; Watari, J. Biotransformation of Hop-Derived Monoterpene Alcohols by Lager Yeast and

Their Contribution to the Flavor of Hopped Beer. *J. Agric. Food Chem.* **2010**, *58*, 5050–5058, doi:10.1021/JF1000524.

40. Serra Colomer, M.; Funch, B.; Solodovnikova, N.; Hobley, T.J.; Förster, J. Biotransformation of Hop Derived Compounds by Brettanomyces Yeast Strains. *J. Inst. Brew.* **2020**, *126*, 280–288, doi:10.1002/JIB.610.

41. Saiman, M.Z.; Miettinen, K.; Mustafa, N.R.; Choi, Y.H.; Verpoorte, R.; Schulte, A.E. Metabolic Alteration of Catharanthus Roseus Cell Suspension Cultures Overexpressing Geraniol Synthase in the Plastids or Cytosol. *Plant Cell. Tissue Organ Cult.* **2018**, *134*, 41–53, doi:10.1007/S11240-018-1398-5/FIGURES/6.

42. Ishihara, K.; Hamada, H.; Hirata, T.; Nakajima, N. Biotransformation Using Plant Cultured Cells. *J. Mol. Catal. B Enzym.* **2003**, *23*, 145–170, doi:10.1016/S1381-1177(03)00080-8.

43. Shimoda, K.; Yamane, S. ya; Hirakawa, H.; Ohta, S.; Hirata, T. Biotransformation of Phenolic Compounds by the Cultured Cells of Catharanthus Roseus. *J. Mol. Catal. B Enzym.* **2002**, *16*, 275–281, doi:10.1016/S1381-1177(01)00073-X.

44. Górak, M.; Zymańczyk-Duda, E. Application of Cyanobacteria for Chiral Phosphonate Synthesis. *Green Chem.* **2015**, *17*, 4570–4578, doi:10.1039/c5gc01195g.

45. Knoot, C.J.; Ungerer, J.; Wangikar, P.P.; Pakrasi, H.B. Cyanobacteria: Promising Biocatalysts for Sustainable Chemical Production. *J. Biol. Chem.* **2018**, *293*, 5044–5052, doi:10.1074/JBC.R117.815886.

46. Knoot, C.J.; Khatri, Y.; Hohlman, R.M.; Sherman, D.H.; Pakrasi, H.B. Engineered Production of Hapalindole Alkaloids in the Cyanobacterium Synechococcus Sp. UTEX 2973. *ACS Synth Biol.* **2019**, *8*, 1941–1951, doi:10.1021/ACSSYNBIO.9B00229.

47. Nielsen, J.; Keasling, J.D. Engineering Cellular Metabolism. *Cell* **2016**, *164*, 1185–1197, doi:10.1016/j.cell.2016.02.004.

48. Tamborini, L.; Fernandes, P.; Paradisi, F.; Molinari, F. Flow Bioreactors as Complementary Tools for Biocatalytic Process Intensification. *Trends Biotechnol.* **2018**, *36*, 73–88, doi:10.1016/j.tibtech.2017.09.005.

49. Castro, G.R.; Knubovets, T. Homogeneous Biocatalysis in Organic Solvents and Water-Organic Mixtures. *Crit. Rev. Biotechnol.* **2003**, *23*, 195–231, doi:10.1080/BTY.23.3.195.

50. Datta, S.; Christena, L.R.; Rajaram, Y.R.S. Enzyme Immobilization: An Overview on Techniques and Support Materials. *3 Biotech* **2013**, *3*, 1–9, doi:10.1007/S13205-012-0071-7,.

51. Fernandes, P.; Cabral, J.M.S. Biotransformations. *Basic Biotechnol. Third Ed.* **2006**, 579–626, doi:10.1017/CBO9780511802409.026.

52. Blaser, H.U. Enantioselective Catalysis in Fine Chemicals Production. *Chem. Commun.* **2003**, *3*, 293–296, doi:10.1039/B209968N.

53. de María, P.D.; Hollmann, F. On the (Un)Greenness of Biocatalysis: Some Challenging Figures and Some Promising Options. *Front. Microbiol.* **2015**, *6*, 164250, doi:10.3389/FMICB.2015.01257/BIBTEX.

54. Anastas, P.T.; Warner, J.C. Green Chemistry: Theory and Practice. **2000**, doi:10.1093/OSO/9780198506980.001.0001.

55. Sperl, J.M.; Sieber, V. Multienzyme Cascade Reactions - Status and Recent Advances. *ACS Catal.* **2018**, *8*, 2385–2396, doi:10.1021/ACSCATAL.7B03440/ASSET/IMAGES/LARGE/CS-2017-03440Y_0020.JPEG.

56. Huffman, M.A.; Fryszkowska, A.; Alvizo, O.; Borra-Garske, M.; Campos, K.R.; Canada, K.A.; Devine, P.N.; Duan, D.; Forstater, J.H.; Grosser, S.T.; et al. Design of an in Vitro Biocatalytic Cascade for the Manufacture of Islatravir. *Science (80-.).* **2019**, *366*, 1255–1259, doi:10.1126/SCIENCE.AAY8484/SUPPL_FILE/AAY8484-HUFFMAN-SM.PDF.

57. Cipolatti, E.P.; Cerqueira Pinto, M.C.; Henriques, R.O.; da Silva Pinto, J.C.C.; de Castro, A.M.; Freire, D.M.G.; Manoel, E.A. Enzymes in Green Chemistry: The State of the Art in Chemical Transformations. *Adv. Enzym. Technol. First Ed.* **2019**, 137–151, doi:10.1016/B978-0-444-64114-4.00005-4.

58. Kries, H.; Trottmann, F.; Hertweck, C. Novel Biocatalysts from Specialized Metabolism. *Angew. Chemie Int. Ed.* **2024**, *63*, e202309284, doi:10.1002/ANIE.202309284.

59. Méndez-Sánchez, D.; López-Iglesias, M.; Gotor-Fernández, V. Hydrolases in Organic Chemistry. Recent Achievements in the Synthesis of Pharmaceuticals. *Curr. Org. Chem.* **2015**, *20*, 1186–1203, doi:10.2174/1385272819666150819190956.

60. Bachosz, K.; Zdarta, J.; Bilal, M.; Meyer, A.S.; Jesionowski, T. Enzymatic Cofactor Regeneration Systems: A New Perspective on Efficiency Assessment. *Sci. Total Environ.* **2023**, *868*, doi:10.1016/J.SCITOTENV.2023.161630.

61. Wichmann, R.; Vasic-Racki, D. Cofactor Regeneration at the Lab Scale. *Adv. Biochem. Eng. Biotechnol.* **2005**, *92*, 225–260, doi:10.1007/B98911.

62. Chaillou, L.L.; Boeris, V.; Spelzini, D.; Nazareno, M.A. Enzymes in Biocatalysis: Characteristics, Kinetic Approach, Production, and Uses. *Adv. Pharm.* **2023**, 83–107, doi:10.2174/9789815049428123010007.

63. Paul, C.; Hanefeld, U.; Hollmann, F.; Qu, G.; Yuan, B.; Sun, Z. Enzyme Engineering for Biocatalysis. *Mol. Catal.* **2024**, *555*, 113874,

doi:10.1016/J.MCAT.2024.113874.

64. Wachtmeister, J.; Rother, D. Recent Advances in Whole Cell Biocatalysis Techniques Bridging from Investigative to Industrial Scale. *Curr. Opin. Biotechnol.* **2016**, *42*, 169–177, doi:10.1016/J.COPBIO.2016.05.005.

65. (PDF) Strategies for Improving Enzymes for Efficient Biocatalysis Available online: https://www.researchgate.net/publication/229052820_Strategies_for_Improving_Enzymes_for_Efficient_Biocatalysis (accessed on 16 July 2025).

66. Faber, K. Biotransformations in Organic Chemistry. *Biotransformations Org. Chem.* **2000**, doi:10.1007/978-3-642-98071-8.

67. Schmid, A.; Dordick, J.S.; Hauer, B.; Kiener, A.; Wubbolts, M.; Witholt, B. Industrial Biocatalysis Today and Tomorrow. *Nat. 2001 4096817* **2001**, *409*, 258–268, doi:10.1038/35051736.

68. Nguyen, L.A.; He, H.; Pham-Huy, C. Chiral Drugs: An Overview. *Int. J. Biomed. Sci.* **2006**, *2*, 85, doi:10.59566/ijbs.2006.2085.

69. McConathy, J.; Owens, M.J. Stereochemistry in Drug Action. *Prim. Care Companion J. Clin. Psychiatry* **2003**, *5*, 70, doi:10.4088/PCC.V05N0202.

70. Weckbecker, A.; Hummel, W. Glucose Dehydrogenase for the Regeneration of NADPH and NADH. *Microb. Enzym. Biotransformations* **2005**, 225–238, doi:10.1385/1-59259-846-3:225.

71. Koszelewski, D.; Grischek, B.; Glueck, S.M.; Kroutil, W.; Faber, K. Enzymatic Racemization of Amines Catalyzed by Enantiocomplementary ω-Transaminases. *Chem. – A Eur. J.* **2011**, *17*, 378–383, doi:10.1002/CHEM.201001602.

72. Kim, Y.; Park, J.; Kim, M.J. Dynamic Kinetic Resolution of Amines and Amino Acids by Enzyme–Metal Cocatalysis. *ChemCatChem* **2011**, *3*, 271–277, doi:10.1002/CCTC.201000330.

73. De Miranda, A.S.; De Silva, M.V.M.; Dias, F.C.; De Souza, S.P.; Leão, R.A.C.; De Souza, R.O.M.A. Continuous Flow Dynamic Kinetic Resolution of Rac-1-Phenylethanol Using a Single Packed-Bed Containing Immobilized CAL-B Lipase and VOSO4 as Racemization Catalysts. *React. Chem. Eng.* **2017**, *2*, 375–381, doi:10.1039/C7RE00003K.

74. Bogár, K.; Martín-Matute, B.; Bäckvall, J.E. Large-Scale Ruthenium- and Enzyme-Catalyzed Dynamic Kinetic Resolution of (Rac)-1-Phenylethanol. *Beilstein J. Org. Chem.* **2007**, *3*, doi:10.1186/1860-5397-3-50.

75. Mu, X.Q.; Xu, Y.; Yang, M.; Sun, Z.H. New Kinetic and Thermodynamic Approach of One-Pot Synthesis of Chiral Alcohol by Oxidoreductase from Candida Parapsilosis. *Process Biochem.* **2011**, *46*, 233–239, doi:10.1016/J.PROCBIO.2010.08.012.

76. Ni, Y.; Xu, J.H. Biocatalytic Ketone Reduction: A Green and Efficient Access to Enantiopure Alcohols. *Biotechnol. Adv.* **2012**, *30*, 1279–1288, doi:10.1016/J.BIOTECHADV.2011.10.007.

77. Ji, Y.; Shi, L.; Chen, M.W.; Feng, G.S.; Zhou, Y.G. Concise Redox Deracemization of Secondary and Tertiary Amines with a Tetrahydroisoquinoline Core via a Nonenzymatic Process. *J. Am. Chem. Soc.* **2015**, *137*, 10496–10499, doi:10.1021/JACS.5B06659/SUPPL_FILE/JA5B06659_SI_001.PDF.

78. Schrittwieser, J.H.; Groenendaal, B.; Resch, V.; Ghislieri, D.; Wallner, S.; Fischereder, E.M.; Fuchs, E.; Grischek, B.; Sattler, J.H.; MacHeroux, P.; et al. Deracemization By Simultaneous Bio-Oxidative Kinetic Resolution and Stereoinversion. *Angew. Chem. Int. Ed. Engl.* **2014**, *53*, 3731,

doi:10.1002/ANIE.201400027.

79. San Mateo California, J. Ketoreductase Polypeptides for the Reduction of Acetophenones. **2008**.

80. Gyarmati, Z.C.; Liljeblad, A.; Rintola, M.; Bernáth, G.; Kanerva, L.T. Lipase-Catalyzed Kinetic Resolution of 7-, 8- and 12-Membered Alicyclic β-Amino Esters and N-Hydroxymethyl-β-Lactam Enantiomers. *Tetrahedron Asymmetry* **2003**, *14*, 3805–3814, doi:10.1016/J.TETASY.2003.08.028.

81. Van Loo, B.; Spelberg, J.H.L.; Kingma, J.; Sonke, T.; Wubbolts, M.G.; Janssen, D.B. Directed Evolution of Epoxide Hydrolase from A. Radiobacter toward Higher Enantioselectivity by Error-Prone PCR and DNA Shuffling. *Chem. Biol.* **2004**, *11*, 981–990, doi:10.1016/J.CHEMBIOL.2004.04.019.

82. Genzel, Y.; Archelas, A.; Lutje Spelberg, J.H.; Janssen, D.B.; Furstoss, R. Microbiological Transformations. Part 48: Enantioselective Biohydrolysis of 2-, 3- and 4-Pyridyloxirane at High Substrate Concentration Using the Agrobacterium Radiobacter AD1 Epoxide Hydrolase and Its Tyr215Phe Mutant. *Tetrahedron* **2001**, *57*, 2775–2779, doi:10.1016/S0040-4020(01)00146-6.

83. Maggio, E.T.; Kenyon, G.L.; Mildvan, A.S.; Hegeman, G.D. Mandelate Racemase from Pseudomonas Putida. Magnetic Resonance and Kinetic Studies of the Mechanism of Catalysis. *Biochemistry* **1975**, *14*, 1131–1139, doi:10.1021/BI00677A006.

84. Roengpithya, C.; Patterson, D.A.; Livingston, A.G.; Taylor, P.C.; Irwin, J.L.; Parrett, M.R. Towards a Continuous Dynamic Kinetic Resolution of 1-Phenylethylamine Using a Membrane Assisted, Two Vessel Process. *Chem. Commun.* **2007**, 3462–3463, doi:10.1039/B709035H.

85. Baxter, S.; Royer, S.; Grogan, G.; Brown, F.; Holt-Tiffin, K.E.; Taylor, I.N.;

Fotheringham, I.G.; Campopiano, D.J. An Improved Racemase/Acylase Biotransformation for the Preparation of Enantiomerically Pure Amino Acids. *J. Am. Chem. Soc.* **2012**, *134*, 19310–19313, doi:10.1021/JA305438Y.

86. Yamanaka, R.; Nakamura, K.; Murakami, M.; Murakami, A. Selective Synthesis of Cinnamyl Alcohol by Cyanobacterial Photobiocatalysts. *Tetrahedron Lett.* **2015**, *56*, 1089–1091, doi:10.1016/j.tetlet.2015.01.092.

87. Lim, K.J.H.; Hartono, Y.D.; Xue, B.; Go, M.K.; Fan, H.; Yew, W.S. Structure-Guided Engineering of Prenyltransferase NphB for High-Yield and Regioselective Cannabinoid Production. *ACS Catal.* **2022**, *12*, 4628–4639, doi:10.1021/ACSCATAL.2C00786/ASSET/IMAGES/LARGE/CS2C00786_0011.JPEG.

88. Park, Y.S.; Kim, M.; Na, C.Y.; Ham, H.W.; Cho, J.Y.; Park, B.; Jung, C.; Park, D.; Yoo, T.H. A Highly Active and Regioselective Cannabigerolic Acid Synthase Engineered from a Promiscuous Prenyltransferase NphB. *Catal. Sci. Technol.* **2025**, *15*, 3363–3371, doi:10.1039/D4CY01367K.

89. Eggbauer, B.; Schrittwieser, J.H.; Kerschbaumer, B.; Macheroux, P.; Kroutil, W. Regioselective Biocatalytic C4-Prenylation of Unprotected Tryptophan Derivatives. *Chembiochem* **2022**, *23*, e202200311, doi:10.1002/CBIC.202200311.

90. Pellissier, H. Recent Developments in Dynamic Kinetic Resolution. *Tetrahedron* **2008**, *64*, 1563–1601, doi:10.1016/J.TET.2007.10.080.

91. Reetz, M.T. Lipases as Practical Biocatalysts. *Curr. Opin. Chem. Biol.* **2002**, *6*, 145–150, doi:10.1016/S1367-5931(02)00297-1.

92. Patel, R.N. Biocatalytic Synthesis of Chiral Alcohols and Amino Acids for Development of Pharmaceuticals. *Biomolecules* **2013**, *3*, 741–777, doi:10.3390/BIOM3040741.

93. Mishra, S.; Kumari, N.; Singh, V.K.; Sinha, R.P. Cyanobacterial Biofuel: A Platform for Green Energy. *Adv. Environ. Eng. Res.* **2023**, *04*, 1–42, doi:10.21926/AEER.2303041.

94. Welker, M.; Von Döhren, H. Cyanobacterial Peptides — Nature's Own Combinatorial Biosynthesis. *FEMS Microbiol. Rev.* **2006**, *30*, 530–563, doi:10.1111/J.1574-6976.2006.00022.X.

95. Mazard, S.; Penesyan, A.; Ostrowski, M.; Paulsen, I.T.; Egan, S. Tiny Microbes with a Big Impact: The Role of Cyanobacteria and Their Metabolites in Shaping Our Future. **2016**, *14*, 97, doi:10.3390/MD14050097.

96. Ng, H.-S.; Chew, L.-L. Valuable Compounds Produced by Microalgae. *Handb. Biorefinery Res. Technol.* **2022**, 1–23, doi:10.1007/978-94-007-6724-9_13-1.

97. Orona-Navar, A.; Aguilar-Hernández, I.; Nigam, K.D.P.; Cerdán-Pasarán, A.; Ornelas-Soto, N. Alternative Sources of Natural Pigments for Dye-Sensitized Solar Cells: Algae, Cyanobacteria, Bacteria, Archaea and Fungi. *J. Biotechnol.* **2021**, *332*, 29–53, doi:10.1016/J.JBIOTEC.2021.03.013.

98. Chittora, D.; Meena, M.; Barupal, T.; Swapnil, P. Cyanobacteria as a Source of Biofertilizers for Sustainable Agriculture. *Biochem. Biophys. Reports* **2020**, *22*, 100737, doi:10.1016/J.BBREP.2020.100737.

99. Nicoletti, M. The Nutraceutical Potential of Cyanobacteria. *Pharmacol. Potential Cyanobacteria* **2022**, 287–330, doi:10.1016/B978-0-12-821491-6.00010-7.

100. Agarwal, P.; Soni, R.; Kaur, P.; Madan, A.; Mishra, R.; Pandey, J.; Singh, S.; Singh, G. Cyanobacteria as a Promising Alternative for Sustainable Environment: Synthesis of Biofuel and Biodegradable Plastics. *Front. Microbiol.* **2022**, *13*, 939347, doi:10.3389/FMICB.2022.939347.

101. Böttger, A.; Vothknecht, U.; Bolle, C.; Wolf, A. Plant Secondary Metabolites and

Their General Function in Plants. **2018**, 3–17, doi:10.1007/978-3-319-99546-5_1.

102. Chomel, M.; Guittonny-Larchevêque, M.; Fernandez, C.; Gallet, C.; DesRochers, A.; Paré, D.; Jackson, B.G.; Baldy, V. Plant Secondary Metabolites: A Key Driver of Litter Decomposition and Soil Nutrient Cycling. *J. Ecol.* **2016**, *104*, 1527–1541, doi:10.1111/1365-2745.12644.

103. Baselga-Cervera, B.; Balboa, C.G.; Costas, E.; Lopez-Rodas, victoria Why Cyanobacteria Produce Toxins? Evolutionary Game Theory Suggests the Key. *Int. J. Biol.* **2014**, *7*, p64, doi:10.5539/IJB.V7N1P64.

104. Singh, D.P.; Prabha, R.; Verma, S.; Meena, K.K.; Yandigeri, M. Antioxidant Properties and Polyphenolic Content in Terrestrial Cyanobacteria. *3 Biotech* **2017**, *7*, doi:10.1007/S13205-017-0786-6.

105. Formighieri, C.; Melis, A. Cyanobacterial Production of Plant Essential Oils. *Planta 2018 2484* **2018**, *248*, 933–946, doi:10.1007/S00425-018-2948-0.

106. Khalifa, S.A.M.; Shedid, E.S.; Saied, E.M.; Jassbi, A.R.; Jamebozorgi, F.H.; Rateb, M.E.; Du, M.; Abdel-Daim, M.M.; Kai, G.Y.; Al-Hammady, M.A.M.; et al. Cyanobacteria—From the Oceans to the Potential Biotechnological and Biomedical Applications. **2021**, *19*, 241, doi:10.3390/MD19050241.

107. Dong, Q.; Dong, R.; Xing, X.; Li, Y. A New Antibiotic Produced by the Cyanobacterium-Symbiotic Fungus Simplicillium Lanosoniveum. *https://doi.org/10.1080/14786419.2017.1343320* **2017**, *32*, 1348–1352, doi:10.1080/14786419.2017.1343320.

108. Sunday, O.S.; Emmanuel, E.; Cornelius, A.O. In-Vitro Assessment of Antibacterial Activity of Crude Methanolic and Aqueous Extracts of Mitracarpus Villosus. *African J. Microbiol. Res.* **2021**, *15*, 62–68, doi:10.5897/AJMR2020.9416.

109. Zahra, Z.; Choo, D.H.; Lee, H.; Parveen, A. Cyanobacteria: Review of Current Potentials and Applications. *Environ. - MDPI* 2020, *7*.

110. Rachedi, R.; Foglino, M.; Latifi, A. Stress Signaling in Cyanobacteria: A Mechanistic Overview. *Life* **2020**, *10*, 1–24, doi:10.3390/LIFE10120312.

111. Chen, B.; Wan, C.; Mehmood, M.A.; Chang, J.S.; Bai, F.; Zhao, X. Manipulating Environmental Stresses and Stress Tolerance of Microalgae for Enhanced Production of Lipids and Value-Added Products–A Review. *Bioresour. Technol.* **2017**, *244*, 1198–1206, doi:10.1016/J.BIORTECH.2017.05.170.

112. Ge, S.; Champagne, P.; Plaxton, W.C.; Leite, G.B.; Marazzi, F. Microalgal Cultivation with Waste Streams and Metabolic Constraints to Triacylglycerides Accumulation for Biofuel Production. *Biofuels, Bioprod. Biorefining* **2017**, *11*, 325–343, doi:10.1002/BBB.1726.

113. Singh, R.; Parihar, P.; Singh, M.; Bajguz, A.; Kumar, J.; Singh, S.; Singh, V.P.; Prasad, S.M. Uncovering Potential Applications of Cyanobacteria and Algal Metabolites in Biology, Agriculture and Medicine: Current Status and Future Prospects. *Front. Microbiol.* **2017**, *8*, 515, doi:10.3389/FMICB.2017.00515/BIBTEX.

114. El-Baz, F.K.; El-Senousy, W.M.; El-Sayed, A.B.; Kamel, M.M. In Vitro Antiviral and Antimicrobial Activities of Spirulina Platensis Extract. **2013**.

115. Singh, D.P.; Prabha, R.; Meena, K.K.; Sharma, L.; Sharma, A.K.; Singh, D.P.; Prabha, R.; Meena, K.K.; Sharma, L.; Sharma, A.K. Induced Accumulation of Polyphenolics and Flavonoids in Cyanobacteria under Salt Stress Protects Organisms through Enhanced Antioxidant Activity. *Am. J. Plant Sci.* **2014**, *5*, 726–735, doi:10.4236/AJPS.2014.55087.

116. Patipong, T.; Hibino, T.; Waditee-Sirisattha, R.; Kageyama, H. Induction of Antioxidative Activity and Antioxidant Molecules in the Halotolerant

Cyanobacterium Halothece Sp. PCC7418 by Temperature Shift. *Nat. Prod. Commun.* **2019**, *14*, 1–6, doi:10.1177/1934578X19865680/ASSET/IMAGES/LARGE/10.1177_1934578X19865680-FIG2.JPEG.

117. Park, H.J.; Cho, J.H.; Hong, S.H.; Kim, D.H.; Jung, H.Y.; Kang, I.K.; Cho, Y.J. Whitening and Anti-Wrinkle Activities of Ferulic Acid Isolated from Tetragonia Tetragonioides in B16F10 Melanoma and CCD-986sk Fibroblast Cells. *J. Nat. Med.* **2018**, *72*, 127–135, doi:10.1007/S11418-017-1120-7.

118. Dong, L.; Xu, Y.; Zhang, Y.; Sun, A.; Hu, Y. Enantioselective Resolution of (±)-1-Phenylethyl Acetate by Using the Whole Cells of Deep-Sea Bacterium Bacillus Sp. DL-2. *Chem. Res. Chinese Univ.* **2019**, *35*, 792–798, doi:10.1007/S40242-019-9126-1/METRICS.

119. Helliwell, K.E.; Lawrence, A.D.; Holzer, A.; Kudahl, U.J.; Sasso, S.; Kräutler, B.; Scanlan, D.J.; Warren, M.J.; Smith, A.G. Cyanobacteria and Eukaryotic Algae Use Different Chemical Variants of Vitamin B12. *Curr. Biol.* **2016**, *26*, 999–1008, doi:10.1016/J.CUB.2016.02.041.

120. Grosshagauer, S.; Kraemer, K.; Somoza, V. The True Value of Spirulina. *J. Agric. Food Chem.* **2020**, *68*, 4109–4115, doi:10.1021/ACS.JAFC.9B08251/ASSET/IMAGES/LARGE/JF9B08251_0001.JPEG.

121. Ljubic, A.; Jacobsen, C.; Holdt, S.L.; Jakobsen, J. Microalgae Nannochloropsis Oceanica as a Future New Natural Source of Vitamin D 3. *Food Chem.* **2020**, *320*, doi:10.1016/J.FOODCHEM.2020.126627.

122. Wang, H.; Fewer, D.P.; Holm, L.; Rouhiainen, L.; Sivonen, K. Atlas of Nonribosomal Peptide and Polyketide Biosynthetic Pathways Reveals Common Occurrence of Nonmodular Enzymes. *Proc. Natl. Acad. Sci. U. S. A.* **2014**, *111*,

9259–9264,
doi:10.1073/PNAS.1401734111/SUPPL_FILE/PNAS.1401734111.SD01.XLS.

123. Scheidler, C.M.; Kick, L.M.; Schneider, S. Ribosomal Peptides and Small Proteins on the Rise. *ChemBioChem* **2019**, *20*, 1479–1486, doi:10.1002/CBIC.201800715.

124. Jahnke, L.L.; Embaye, T.; Hope, J.; Turk, K.A.; Zuilen, M. Van; Marais, D.J. Des; Farmer, J.D.; Summons, R.E. Lipid Biomarker and Carbon Isotopic Signatures for Stromatolite-Forming, Microbial Mat Communities and Phormidium Cultures from Yellowstone National Park. *Geobiology* **2004**, *2*, 31–47, doi:10.1111/J.1472-4677.2004.00021.X.

125. Kusama, Y.; Inoue, S.; Jimbo, H.; Takaichi, S.; Sonoike, K.; Hihara, Y.; Nishiyama, Y. Zeaxanthin and Echinenone Protect the Repair of Photosystem II from Inhibition by Singlet Oxygen in Synechocystis Sp. PCC 6803. *Plant Cell Physiol.* **2015**, *56*, 906–916, doi:10.1093/PCP/PCV018.

126. Mo, S.; Krunic, A.; Pegan, S.D.; Franzblau, S.G.; Orjala, J. An Antimicrobial Guanidine-Bearing Sesterterpene from the Cultured Cyanobacterium Scytonema Sp. *J. Nat. Prod.* **2009**, *72*, 2043–2045, doi:10.1021/NP900288X/SUPPL_FILE/NP900288X_SI_001.PDF.

127. Haque, N.; Hughes, A.; Lim, S.; Vernon, C. Rare Earth Elements: Overview of Mining, Mineralogy, Uses, Sustainability and Environmental Impact. *Resour. 2014, Vol. 3, Pages 614-635* **2014**, *3*, 614–635, doi:10.3390/RESOURCES3040614.

128. Schulze, R. Reducing Environmental Impacts of the Global Rare Earth Production for Use in Nd-Fe-B Magnets How Much Can Recycling Contribute? **2018**, doi:10.01.2018.

129. How Do We Use the Rare-Earth Elements?, doi:10.3133/fs20143078.

130. Paper, M.; Koch, M.; Jung, P.; Lakatos, M.; Nilges, T.; Brück, T.B. Rare Earths

Stick to Rare Cyanobacteria: Future Potential for Bioremediation and Recovery of Rare Earth Elements. *Front. Bioeng. Biotechnol.* **2023**, *11*, doi:10.3389/FBIOE.2023.1130939/FULL.

131. Dell'Aversano, C.; Eaglesham, G.K.; Quilliam, M.A. Analysis of Cyanobacterial Toxins by Hydrophilic Interaction Liquid Chromatography-Mass Spectrometry. *J. Chromatogr. A* **2004**, *1028*, 155–164, doi:10.1016/j.chroma.2003.11.083.

132. Barros, Ó.; Costa, L.; Costa, F.; Lago, A.; Rocha, V.; Vipotnik, Z.; Silva, B.; Tavares, T. Recovery of Rare Earth Elements from Wastewater Towards a Circular Economy. *Mol. 2019, Vol. 24, Page 1005* **2019**, *24*, 1005, doi:10.3390/MOLECULES24061005.

133. Gardea-Torresdey, J.L.; Arenas, J.L.; Webb, R.; Tiemann, K.J.; Gonzalez, J.H. Uptake of Metal Ions from Solution by Inactivated Cells of Cyanobacteria.

134. Paper, M.; Jung, P.; Koch, M.; Lakatos, M.; Nilges, T.; Brück, T.B. Stripped: Contribution of Cyanobacterial Extracellular Polymeric Substances to the Adsorption of Rare Earth Elements from Aqueous Solutions. *Front. Bioeng. Biotechnol.* **2023**, *11*, 1299349, doi:10.3389/FBIOE.2023.1299349/BIBTEX.

135. Fischer, C.B.; Körsten, S.; Rösken, L.M.; Cappel, F.; Beresko, C.; Ankerhold, G.; Schönleber, A.; Geimer, S.; Ecker, D.; Wehner, S. Cyanobacterial Promoted Enrichment of Rare Earth Elements Europium, Samarium and Neodymium and Intracellular Europium Particle Formation. *RSC Adv.* **2019**, *9*, 32581–32593, doi:10.1039/C9RA06570A.

136. Telgmann, L.; Lindner, U.; Lingott, J.; Jakubowski, N. Analysis and Speciation of Lanthanoides by ICP-MS. *Phys. Sci. Rev.* **2019**, *1*, doi:10.1515/PSR-2016-0058/ASSET/GRAPHIC/PSR-2016-0058_FIG_005.JPG.

137. Breuker, A.; Ritter, S.F.; Schippers, A. Biosorption of Rare Earth Elements by

Different Microorganisms in Acidic Solutions. *Met. 2020, Vol. 10, Page 954* **2020**, *10*, 954, doi:10.3390/MET10070954.

138. Analysis of Rare Earth Elements by ICP-OES and ICP-MS − Potentials and Limitations - Analytik Jena Available online: https://www.analytik-jena.com/knowledge/applications/application-teasers/analysis-of-rare-earth-elements-by-icp-oes-and-icp-ms-potentials-and-limitations/ (accessed on 4 June 2025).

139. Samson, S.O.; Serafin-Lewańczuk, M.; Brzezińska-Rodak, M.; Klimek-Ochab, M.; Żymańczyk-Duda, E. Complete Epoxy Phosphonate Conversion to Dimethyl (1*E*)-3-Hydroxyprop-1-Enylphosphonate with Photobiocatalysts' Assistance. *Symmetry 2024, Vol. 16, Page 1676* **2024**, *16*, 1676, doi:10.3390/SYM16121676.

140. Śliżewska, A.; Majewska, P.; Żymańczyk-Duda, E. Biotransformations with Photobiocatalysts for Enantioselective Ester Hydrolysis. *Mol. 2025, Vol. 30, Page 2767* **2025**, *30*, 2767, doi:10.3390/MOLECULES30132767.

141. Lotufo, G.R.; Biedenbach, J.M.; Farrar, J.D.; Chanov, M.K.; Hester, B.W.; Warbritton, C.R.; Steevens, J.A.; Netchaev, J.M.; Bednar, A.J.; Moore, D.W. Interlaboratory Comparison of Three Sediment Bioaccumulation Tests. *Environ. Toxicol. Chem.* **2022**, *41*, 1260–1275, doi:10.1002/ETC.5300.

142. Iversen, P.W.; Beck, B.; Chen, Y.-F.; Dere, W.; Devanarayan, V.; Eastwood, B.J.; Farmen, M.W.; Iturria, S.J.; Montrose, C.; Moore, R.A.; et al. HTS Assay Validation. **2012**, 1–20.

143. Zhu, T.; Li, N.; Zhao, C.; Liu, J.; Liu, Y.; Chen, J.; Dong, Y.; Tian, Y.; Hong, X.; Xiong, H. Comprehensive Characterization and Identification of Chemical Constituents of Pingwei Powder by Ultra High Performance Liquid Chromatography Tandem Quadrupole-Time-of-Flight Tandem Mass

Spectrometry. *J. Chromatogr. Open* **2025**, *7*, doi:10.1016/J.JCOA.2025.100203.

144. Snow, N. From Detector to Decision Part IV: Demystifying Peak Integration. *LCGC Int.* **2024**, 24–26, doi:10.56530/LCGC.INT.HH5984I5.

145. Deem, M.C.; Hein, J.E. A Method for Converting HPLC Peak Area from Online Reaction Monitoring to Concentration Using Nonlinear Regression. *J. Org. Chem.* **2023**, *88*, 1292–1297, doi:10.1021/ACS.JOC.2C02737/SUPPL_FILE/JO2C02737_SI_001.PDF.

146. Głąb, A.; Szmigiel-Merena, B.; Brzezińska-Rodak, M.; Żymańczyk-Duda, E. Biotransformation of 1- and 2-Phenylethanol to Products of High Value via Redox Reactions. *Biotechnologia* **2016**, *97*, 203–210, doi:10.5114/bta.2016.62358.

147. Cai, H.; Chuang, W.G.; Cui, X.; Cheng, R.H.; Chiu, K.; Chen, Z.; Ding, S. High Resolution 31P NMR Spectroscopy Generates a Quantitative Evolution Profile of Phosphorous Translocation in Germinating Sesame Seed. *Sci. Reports 2018 81* **2018**, *8*, 1–10, doi:10.1038/s41598-017-18722-y.

148. Barekatain, Y.; Khadka, S.; Harris, K.; Delacerda, J.; Yan, V.C.; Chen, K.C.; Pham, C.D.; Uddin, M.N.; Avritcher, R.; Eisenberg, E.J.; et al. Quantification of Phosphonate Drugs by 1H-31P HSQC Shows That Rats Are Better Models of Primate Drug Exposure than Mice. *Anal. Chem.* **2022**, *94*, 10045–10053, doi:10.1021/ACS.ANALCHEM.2C00553/ASSET/IMAGES/MEDIUM/AC2C00553_M002.GIF.

149. Sotirhos, N.; Herslof, B.; Kenne, L. Quantitative Analysis of Phospholipids by 31P-NMR. *J. Lipid Res.* **1988**, *27*, 386–392, doi:10.1016/S0022-2275(20)38816-7.

150. Carter, S.G.; Karl, D.W. Inorganic Phosphate Assay with Malachite Green: An Improvement and Evaluation. *J. Biochem. Biophys. Methods* **1982**, *7*, 7–13, doi:10.1016/0165-022X(82)90031-8.

151. Ohno, T.; Zibilske, L.M. Determination of Low Concentrations of Phosphorus in Soil Extracts Using Malachite Green. *Soil Sci. Soc. Am. J.* **1991**, *55*, 892–895, doi:10.2136/SSSAJ1991.03615995005500030046X.

152. Motomizu, S.; Wakimoto, T.; Tôei, K. Spectrophotometric Determination of Phosphate in River Waters with Molybdate and Malachite Green. *Analyst* **1983**, *108*, 361–367, doi:10.1039/AN9830800361.

153. Liu, Y.; Gao, L.; Yu, Z. Quantitative 31P NMR Spectroscopy: Principles, Methodologies, and Applications in Phosphorus-Containing Compound Analysis. *Appl. Sci. 2025, Vol. 15, Page 323* **2024**, *15*, 323, doi:10.3390/APP15010323.

154. Weber, M.; Hellriegel, C.; Rueck, A.; Wuethrich, J.; Jenks, P.; Obkircher, M. Method Development in Quantitative NMR towards Metrologically Traceable Organic Certified Reference Materials Used as (31)P QNMR Standards. *Anal. Bioanal. Chem.* **2015**, *407*, 3115–3123, doi:10.1007/S00216-014-8306-6.

155. Oromí-Farrús, M.; Minguell, J.M.; Oromi, N.; Canela-Garayoa, R. A Reliable Method for Quantification of Phosphonates and Their Impurities by 31P NMR. *Anal. Lett.* **2013**, *46*, 1910–1921, doi:10.1080/00032719.2013.780239.

156. Rippka, E.; Deruelles, J.; Waterbury, N.B. *Generic Assignments, Strain Histories and Properties of Pure Cultures of Cyanobacteria*; 1979; Vol. 111;.

157. El-fayoumy, E.A.; Shanab, S.M.; Hassan, O.M.A.; Shalaby, E.A. Enhancement of Active Ingredients and Biological Activities of Nostoc Linckia Biomass Cultivated under Modified BG-110 Medium Composition. *Biomass Convers. Biorefinery* **2023**, *13*, 6049, doi:10.1007/S13399-021-01509-7.

158. Johnson, E.M.; Kumar, K.; Das, D. Physicochemical Parameters Optimization, and Purification of Phycobiliproteins from the Isolated Nostoc Sp. *Bioresour.*

Technol. **2014**, *166*, 541–547, doi:10.1016/J.BIORTECH.2014.05.097.

159. Nayak, M.; Suh, W.I.; Chang, Y.K.; Lee, B. Exploration of Two-Stage Cultivation Strategies Using Nitrogen Starvation to Maximize the Lipid Productivity in Chlorella Sp. HS2. *Bioresour. Technol.* **2019**, *276*, 110–118, doi:10.1016/J.BIORTECH.2018.12.111.

160. McGrath, J.W.; Chin, J.P.; Quinn, J.P. Organophosphonates Revealed: New Insights into the Microbial Metabolism of Ancient Molecules. *Nat. Rev. Microbiol. 2013 116* **2013**, *11*, 412–419, doi:10.1038/nrmicro3011.

161. Hermosilla, D.; Cortijo, M.; Huang, C.P. The Role of Iron on the Degradation and Mineralization of Organic Compounds Using Conventional Fenton and Photo-Fenton Processes. *Chem. Eng. J.* **2009**, *155*, 637–646, doi:10.1016/J.CEJ.2009.08.020.

162. Qiang, H.; Guterman, H.; Richmond, A. PHYSIOLOGICAL CHARACTERISTICS OF SPIRULINA PLATENSIS (CYANOBACTERIA) CULTURED AT ULTRAHIGH CELL DENSITIES1. *J. Phycol.* **1996**, *32*, 1066–1073, doi:10.1111/J.0022-3646.1996.01066.X.

163. Croft, M.T.; Lawrence, A.D.; Raux-Deery, E.; Warren, M.J.; Smith, A.G. Algae Acquire Vitamin B12 through a Symbiotic Relationship with Bacteria. *Nat. 2005 4387064* **2005**, *438*, 90–93, doi:10.1038/nature04056.

164. Hamouda, R.A.; El-Boraey, N.G.; El Bialy, B.E.; Alrdahe, S.S.; Darwish, D.B.E. Vitamin Supplements Enhance Spirulina Platensis Biomass and Phytochemical Contents. *Green Process. Synth.* **2022**, *11*, 266–274, doi:10.1515/GPS-2022-0028/ASSET/GRAPHIC/J_GPS-2022-0028_FIG_003.JPG.

165. Martens, J.H.; Barg, H.; Warren, M.; Jahn, D. Microbial Production of Vitamin B12. *Appl. Microbiol. Biotechnol.* **2002**, *58*, 275–285, doi:10.1007/S00253-001-0902-7.

166. Rippka, R.; Deruelles, J.; Waterbury, J.B. Generic Assignments, Strain Histories

and Properties of Pure Cultures of Cyanobacteria. *J. Gen. Microbiol.* **1979**, *111*, 1–61, doi:10.1099/00221287-111-1-1/CITE/REFWORKS.

167. Just, G.; Potvin, P.; Hakimelahi, G.H. *3-Diethylphosphonoacrolein Diethylthioacetal Anion (6*), a Reagent for the Conversion of Aldehydes to u,p-Unsaturated Ketene Dithioacetals and Three-Carbon Homologated u ,p-Unsaturated Aldehydes*;

168. Malachite Green Phosphate Assay Kit | Cayman Chemical Available online: https://www.caymanchem.com/product/10009325 (accessed on 17 March 2025).

169. Gupta, S.D.; Song, D.G.; Lee, S.; Lee, J.W.; Park, J.S.; Prodromou, C.; Pan, C.H. Malachite Green Assay for the Discovery of Heat-Shock Protein 90 Inhibitors. *JoVE (Journal Vis. Exp.* **2023**, *2023*, e64693, doi:10.3791/64693.

170. Malachite Green Phosphate Assay Kit | BioAssay Systems Available online: https://bioassaysys.com/malachite-green-phosphate-assay-kit/ (accessed on 17 March 2025).

171. Van Veldhoven, R. 1; Mannaerts, G.P. Malachite Green Phosphate Detection Kit Catalog Number: DY996 INTENDED USE. *Anal. Biochem* **1987**, *161*, 727.

172. Balouiri, M.; Sadiki, M.; Ibnsouda, S.K. Methods for in Vitro Evaluating Antimicrobial Activity: A Review. *J. Pharm. Anal.* **2016**, *6*, 71–79, doi:10.1016/J.JPHA.2015.11.005.

173. Stevenson, K.; McVey, A.F.; Clark, I.B.N.; Swain, P.S.; Pilizota, T. General Calibration of Microbial Growth in Microplate Readers. *Sci. Rep.* **2016**, *6*, doi:10.1038/SREP38828.

174. How to Optimise OD600 Measurements | BMG LABTECH Available online: https://www.bmglabtech.com/en/howto-notes/how-to-optimise-od600-measurements/ (accessed on 17 March 2025).

175. Kõllo, M.; Kudrjašova, M.; Kulp, M.; Aav, R. Methylphosphonic Acid as a 31P-NMR Standard for the Quantitative Determination of Phosphorus in Carbonated Beverages. *Anal. Methods* **2013**, *5*, 4005–4009, doi:10.1039/C3AY40743H.

176. Čížková, M.; Mezricky, P.; Mezricky, D.; Rucki, M.; Zachleder, V.; Vítová, M. Bioaccumulation of Rare Earth Elements from Waste Luminophores in the Red Algae, Galdieria Phlegrea. *Waste and Biomass Valorization* **2021**, *12*, 3137–3146, doi:10.1007/S12649-020-01182-3/METRICS.

177. Singh, A.; Čížková, M.; Náhlík, V.; Mezricky, D.; Schild, D.; Rucki, M.; Vítová, M. Bio-Removal of Rare Earth Elements from Hazardous Industrial Waste of CFL Bulbs by the Extremophile Red Alga Galdieria Sulphuraria. *Front. Microbiol.* **2023**, *14*, 1130848, doi:10.3389/FMICB.2023.1130848/BIBTEX.

178. Mian, M.R.; Wang, X.; Wang, X.; Kirlikovali, K.O.; Xie, H.; Ma, K.; Fahy, K.M.; Chen, H.; Islamoglu, T.; Snurr, R.Q.; et al. Structure-Activity Relationship Insights for Organophosphonate Hydrolysis at Ti(IV) Active Sites in Metal-Organic Frameworks. *J. Am. Chem. Soc.* **2023**, *145*, 7435–7445, doi:10.1021/JACS.2C13887.

179. Callaghan, A. V.; Morris, B.E.L.; Pereira, I.A.C.; McInerney, M.J.; Austin, R.N.; Groves, J.T.; Kukor, J.J.; Suflita, J.M.; Young, L.Y.; Zylstra, G.J.; et al. The Genome Sequence of Desulfatibacillum Alkenivorans AK-01: A Blueprint for Anaerobic Alkane Oxidation. *Environ. Microbiol.* **2012**, *14*, 101–113, doi:10.1111/J.1462-2920.2011.02516.X.

180. Guschina, I.A.; Harwood, J.L. Lipids and Lipid Metabolism in Eukaryotic Algae. *Prog. Lipid Res.* **2006**, *45*, 160–186, doi:10.1016/J.PLIPRES.2006.01.001.

181. Kahn, A.; Oliveira, P.; Cuau, M.; Leão, P.N. Incorporation, Fate, and Turnover of Free Fatty Acids in Cyanobacteria. *FEMS Microbiol. Rev.* **2023**, *47*, doi:10.1093/FEMSRE/FUAD015.

182. Xiaoyuan, C.; Yang, Q.; Zhao, F.; Qin, S.; Yang, Y.; Shen, J.; Lin, H. Comparative Analysis of Fatty Acid Desaturases in Cyanobacterial Genomes. *Int. J. Genomics* **2008**, *2008*, 284508, doi:10.1155/2008/284508.

183. Ruffing, A.M. Improved Free Fatty Acid Production in Cyanobacteria with Synechococcus Sp. PCC 7002 as Host. *Front. Bioeng. Biotechnol.* **2014**, *2*, doi:10.3389/FBIOE.2014.00017.

184. Singh, B.K.; Walker, A. Microbial Degradation of Organophosphorus Compounds. *FEMS Microbiol. Rev.* **2006**, *30*, 428–471, doi:10.1111/J.1574-6976.2006.00018.X.

185. Drzyzga, D.; Lipok, J. Analytical Insight into Degradation Processes of Aminopolyphosphonates as Potential Factors That Induce Cyanobacterial Blooms. *Environ. Sci. Pollut. Res.* **2017**, *24*, 24364–24375, doi:10.1007/S11356-017-0068-1/TABLES/7.

186. Ternan, N.G.; Mc Grath, J.W.; Mc Mullan, G.; Quinn, J.P. Review: Organophosphonates: Occurrence, Synthesis and Biodegradation by Microorganisms. *World J. Microbiol. Biotechnol.* **1998**, *14*, 635–647, doi:10.1023/A:1008848401799/METRICS.

187. Hove-Jensen, B.; Zechel, D.L.; Jochimsen, B. Utilization of Glyphosate as Phosphate Source: Biochemistry and Genetics of Bacterial Carbon-Phosphorus Lyase. *Microbiol. Mol. Biol. Rev.* **2014**, *78*, 176–197, doi:10.1128/MMBR.00040-13.

188. Villarreal-Chiu, J.F.; Quinn, J.P.; McGrath, J.W. The Genes and Enzymes of Phosphonate Metabolism by Bacteria, and Their Distribution in the Marine Environment. *Front. Microbiol.* **2012**, *3*, 20011, doi:10.3389/FMICB.2012.00019/BIBTEX.

189. Ponce-Toledo, R.I.; Deschamps, P.; López-García, P.; Zivanovic, Y.; Benzerara,

K.; Moreira, D. An Early-Branching Freshwater Cyanobacterium at the Origin of Plastids. *Curr. Biol.* **2017**, *27*, 386–391, doi:10.1016/J.CUB.2016.11.056.

190. Sosa, O.A.; Burrell, T.J.; Wilson, S.T.; Foreman, R.K.; Karl, D.M.; Repeta, D.J. Phosphonate Cycling Supports Methane and Ethylene Supersaturation in the Phosphate-Depleted Western North Atlantic Ocean. *Limnol. Oceanogr.* **2020**, *65*, 2443–2459, doi:10.1002/LNO.11463.

191. Schwarzenböck, C.; Vagin, S.I.; Heinz, W.R.; Nelson, P.J.; Rieger, B. Studies on the Biocompatibility of Poly(Diethyl Vinyl-Phosphonate) with a New Fluorescent Marker. *Macromol. Rapid Commun.* **2018**, *39*, 1800259, doi:10.1002/MARC.201800259.

192. Lanzinger, D.; Salzinger, S.; Soller, B.S.; Rieger, B. Poly(Vinylphosphonate)s as Macromolecular Flame Retardants for Polycarbonate. *Ind. Eng. Chem. Res.* **2015**, *54*, 1703–1712, doi:10.1021/IE504084Q.

193. Duke, S.O.; Powles, S.B. Glyphosate: A Once-in-a-Century Herbicide. *Pest Manag. Sci.* **2008**, *64*, 319–325, doi:10.1002/PS.1518.

194. Azema, L.; Baron, R.; Ladame, S. Targeting Enzymes with Phosphonate-Based Inhibitors: Mimics of Tetrahedral Transition States and Stable Isosteric Analogues of Phosphates. *Curr. Enzym. Inhib.* **2006**, *2*, 61–72, doi:10.2174/157340806775473526.

195. Schramm, V.L. Enzymatic Transition States and Drug Design. *Chem. Rev.* **2018**, *118*, 11194, doi:10.1021/ACS.CHEMREV.8B00369.

196. Zhang, Q.; Jia, L.; Chen, Y.; Yan, H.; Chen, Q.; Zhang, J.; Sun, H. Molecular Mechanisms of the Cyanobacterial Response to Different Phosphorus Sources. *Sustain. 2024, Vol. 16, Page 5642* **2024**, *16*, 5642, doi:10.3390/SU16135642.

197. Adams, M.M.; Gómez-García, M.R.; Grossman, A.R.; Bhaya, D. Phosphorus

Deprivation Responses and Phosphonate Utilization in a Thermophilic Synechococcus Sp. from Microbial Mats. *J. Bacteriol.* **2008**, *190*, 8171–8184, doi:10.1128/JB.01011-08/SUPPL_FILE/SUPPLEMENTARY_MATERIAL.DOC.

198. Zhao, L.; Lin, L.Z.; Zeng, Y.; Teng, W.K.; Chen, M.Y.; Brand, J.J.; Zheng, L.L.; Gan, N.Q.; Gong, Y.H.; Li, X.Y.; et al. The Facilitating Role of Phycospheric Heterotrophic Bacteria in Cyanobacterial Phosphonate Availability and Microcystis Bloom Maintenance. *Microbiome* **2023**, *11*, 1–16, doi:10.1186/S40168-023-01582-2/FIGURES/6.

199. Geladopoulos, T.P.; Sotiroudis, T.G.; Evangelopoulos, A.E. A Malachite Green Colorimetric Assay for Protein Phosphatase Activity. *Anal. Biochem.* **1991**, *192*, 112–116, doi:10.1016/0003-2697(91)90194-X.

200. Bartsch, M.; Gassmeyer, S.K.; Köninger, K.; Igarashi, K.; Liauw, P.; Dyczmons-Nowaczyk, N.; Miyamoto, K.; Nowaczyk, M.M.; Kourist, R. Photosynthetic Production of Enantioselective Biocatalysts. *Microb. Cell Fact.* **2015**, *14*, 1–9, doi:10.1186/S12934-015-0233-5/FIGURES/7.

201. Bornscheuer, U.T. Microbial Carboxyl Esterases: Classification, Properties and Application in Biocatalysis. *FEMS Microbiol. Rev.* **2002**, *26*, 73–81, doi:10.1111/J.1574-6976.2002.TB00599.X.

202. Kniemeyer, O.; Heider, J. (*S*)-1-Phenylethanol Dehydrogenase of Azoarcus Sp. Strain EbN1, an Enzyme of Anaerobic Ethylbenzene Catabolism. *Arch. Microbiol.* **2001**, *176*, 129–135, doi:10.1007/S002030100303/METRICS.

203. Höffken, H.W.; Duong, M.; Friedrich, T.; Breuer, M.; Hauer, B.; Reinhardt, R.; Rabus, R.; Heider, J. Crystal Structure and Enzyme Kinetics of the (*S*)-Specific 1-Phenylethanol Dehydrogenase of the Denitrifying Bacterium Strain EbN1. *Biochemistry* **2006**, *45*, 82–93, doi:10.1021/BI051596B.

204. Rui, L.; Cao, L.; Chen, W.; Reardon, K.F.; Wood, T.K. Active Site Engineering of the Epoxide Hydrolase from Agrobacterium Radiobacter AD1 to Enhance Aerobic Mineralization of Cis-1,2-Dichloroethylene in Cells Expressing an Evolved Toluene Ortho-Monooxygenase. *J. Biol. Chem.* **2004**, *279*, 46810–46817, doi:10.1074/jbc.M407466200.

205. Herrero, A.; Muro-Pastor, A.M.; Flores, E. Nitrogen Control in Cyanobacteria. *J. Bacteriol.* **2001**, *183*, 411, doi:10.1128/JB.183.2.411-425.2001.

206. Flores, E.; López-Lozano, A.; Herrero, A. Nitrogen Fixation in the Oxygenic Phototrophic Prokaryotes (Cyanobacteria): The Fight against Oxygen. *Biol. Nitrogen Fixat.* **2015**, *2–2*, 879–890, doi:10.1002/9781119053095.ch86.

207. Hult, K.; Berglund, P. Enzyme Promiscuity: Mechanism and Applications. *Trends Biotechnol.* **2007**, *25*, 231–238, doi:10.1016/j.tibtech.2007.03.002.

208. Archelas, A.; Furstoss, R. Synthetic Applications of Epoxide Hydrolases. *Curr. Opin. Chem. Biol.* **2001**, *5*, 112–119, doi:10.1016/S1367-5931(00)00179-4.

209. Ruffolo, F.; Dinhof, T.; Murray, L.; Zangelmi, E.; Chin, J.P.; Pallitsch, K.; Peracchi, A. The Microbial Degradation of Natural and Anthropogenic Phosphonates. *Mol. 2023, Vol. 28, Page 6863* **2023**, *28*, 6863, doi:10.3390/MOLECULES28196863.

210. Ganesan, M.; Muraleedharan, K.M. Synthesis of β-Hydroxyphosphonate and 1,2-Dihydroxy Acyclic Nucleoside Analogs via 1,3-Dipolar Cycloaddition Strategy. *Nucleosides, Nucleotides and Nucleic Acids* **2010**, *29*, 91–96, doi:10.1080/15257771003597709.

211. Galezowska, J.; Gumienna-Kontecka, E. Phosphonates, Their Complexes and Bio-Applications: A Spectrum of Surprising Diversity. *Coord. Chem. Rev.* **2012**, *256*, 105–124, doi:10.1016/J.CCR.2011.07.002.

212. Thornburg, C.C.; Cowley, E.S.; Sikorska, J.; Shaala, L.A.; Ishmael, J.E.; Youssef,

D.T.A.; McPhail, K.L. Apratoxin H and Apratoxin A Sulfoxide from the Red Sea Cyanobacterium Moorea Producens. *J. Nat. Prod.* **2013**, *76*, 1781, doi:10.1021/NP4004992.

213. H:\chm_51\website\chapters\carey-13.PDF | Enhanced Reader.

214. Shih, P.M.; Wu, D.; Latifi, A.; Axen, S.D.; Fewer, D.P.; Talla, E.; Calteau, A.; Cai, F.; Tandeau De Marsac, N.; Rippka, R.; et al. Improving the Coverage of the Cyanobacterial Phylum Using Diversity-Driven Genome Sequencing. *Proc. Natl. Acad. Sci. U. S. A.* **2013**, *110*, 1053–1058, doi:10.1073/PNAS.1217107110/SUPPL_FILE/SD03.XLSX.

215. Huang, J.; Su, Z.; Xu, Y. The Evolution of Microbial Phosphonate Degradative Pathways., doi:10.1007/s00239-004-0349-4.

216. Oluwole, A.O.; Kalmankar, N. V.; Guida, M.; Bennett, J.L.; Poce, G.; Bolla, J.R.; Robinson, C. V. Lipopeptide Antibiotics Disrupt Interactions of Undecaprenyl Phosphate with UptA. *Proc. Natl. Acad. Sci. U. S. A.* **2024**, *121*, e2408315121, doi:10.1073/PNAS.2408315121/SUPPL_FILE/PNAS.2408315121.SAPP.PDF.

217. Tetu, S.G.; Brahamsha, B.; Johnson, D.A.; Tai, V.; Phillippy, K.; Palenik, B.; Paulsen, I.T. Microarray Analysis of Phosphate Regulation in the Marine Cyanobacterium Synechococcus Sp. WH8102. *ISME J.* **2009**, *3*, 835–849, doi:10.1038/ISMEJ.2009.31.

218. Wiemer, A.J.; Wiemer, D.F. Prodrugs of Phosphonates and Phosphates: Crossing the Membrane Barrier. *Top. Curr. Chem.* **2015**, *360*, 115–160, doi:10.1007/128_2014_561.

219. Hecker, S.J.; Erion, M.D. Prodrugs of Phosphates and Phosphonates. *J. Med. Chem.* **2008**, *51*, 2328–2345, doi:10.1021/JM701260B/ASSET/JM701260B.FP.PNG_V03.

220. Lucius, S.; Hagemann, M. The Primary Carbon Metabolism in Cyanobacteria and Its Regulation. *Front. Plant Sci.* **2024**, *15*, 1417680, doi:10.3389/FPLS.2024.1417680/XML/NLM.

221. Smith, M.R.; Khera, E.; Wen, F. Engineering Novel and Improved Biocatalysts by Cell Surface Display. *Ind. Eng. Chem. Res.* **2015**, *54*, 4021, doi:10.1021/IE504071F.

222. Krečmerová, M.; Majer, P.; Rais, R.; Slusher, B.S. Phosphonates and Phosphonate Prodrugs in Medicinal Chemistry: Past Successes and Future Prospects. *Front. Chem.* **2022**, *10*, 889737, doi:10.3389/FCHEM.2022.889737/BIBTEX.

223. Vítová, M.; Mezricky, D. Microbial Recovery of Rare Earth Elements from Various Waste Sources: A Mini Review with Emphasis on Microalgae. *World J. Microbiol. Biotechnol. 2024 406* **2024**, *40*, 1–13, doi:10.1007/S11274-024-03974-4.

224. Ciani, M.; Adessi, A. Cyanoremediation and Phyconanotechnology: Cyanobacteria for Metal Biosorption toward a Circular Economy. *Front. Microbiol.* **2023**, *14*, 1166612, doi:10.3389/FMICB.2023.1166612/BIBTEX.

225. Hellal, J.; Lise, B.; Annette, B.; Aurelie, C.; Giulia, C.; Simon, C.; Cristiana, C.L.; Caroline, D.C.; Nicolas, G.; Marina, H.; et al. Unlocking Secrets of Microbial Ecotoxicology: Recent Achievements and Future Challenges. *FEMS Microbiol. Ecol.* **2023**, *99*, fiad102, doi:10.1093/FEMSEC/FIAD102.

226. Mahfooz, S.; Shamim, A.; Husain, A.; Hasan, Z.; Farooqui, A. Oxidative Stress Biomarkers in Cyanobacteria Exposed to Heavy Metals. *Contam. Water Heal. Risk Assess. Treat. Strateg.* **2021**, 385–403, doi:10.1016/B978-0-12-824058-8.00007-4.

227. Mota, R.; Rossi, F.; Andrenelli, L.; Pereira, S.B.; De Philippis, R.; Tamagnini, P. Released Polysaccharides (RPS) from Cyanothece Sp. CCY 0110 as Biosorbent for Heavy Metals Bioremediation: Interactions between Metals and RPS Binding

Sites. *Appl. Microbiol. Biotechnol.* **2016**, *100*, 7765–7775, doi:10.1007/S00253-016-7602-9.

228. Banaee, M.; Mossotto, C.; Maganza, A.; Azizi, R.; Prearo, M.; Pastorino, P.; Faggio, C. Rare Earth Elements on Aquatic Organisms: Toxicity, Detoxification, and Ecological Implications. *Emerg. Contam.* **2025**, *11*, 100457, doi:10.1016/J.EMCON.2024.100457.

229. Rastogi, R.P.; Richa; Sinha, R.P.; Singh, S.P.; Häder, D.P. Photoprotective Compounds from Marine Organisms. *J. Ind. Microbiol. Biotechnol.* **2010**, *37*, 537–558, doi:10.1007/S10295-010-0718-5.

230. Liu, Y.; Alessi, D.S.; Owttrim, G.W.; Petrash, D.A.; Mloszewska, A.M.; Lalonde, S. V.; Martinez, R.E.; Zhou, Q.; Konhauser, K.O.; Liu, Y.; et al. Cell Surface Reactivity of Synechococcus Sp. PCC 7002: Implications for Metal Sorption from Seawater. *GeCoA* **2015**, *169*, 30–44, doi:10.1016/J.GCA.2015.07.033.

231. Yu, R.; Chai, H.; Yu, Z.; Wu, X.; Liu, Y.; Shen, L.; Li, J.; Ye, J.; Liu, D.; Ma, T.; et al. Behavior and Mechanism of Cesium Biosorption from Aqueous Solution by Living Synechococcus PCC7002. *Microorg. 2020, Vol. 8, Page 491* **2020**, *8*, 491, doi:10.3390/MICROORGANISMS8040491.

232. Cassier-Chauvat, C.; Chauvat, F. Responses to Oxidative and Heavy Metal Stresses in Cyanobacteria: Recent Advances. *Int. J. Mol. Sci.* **2014**, *16*, 871, doi:10.3390/IJMS16010871.

233. Yang, W.; Wang, F.; Liu, L.N.; Sui, N. Responses of Membranes and the Photosynthetic Apparatus to Salt Stress in Cyanobacteria. *Front. Plant Sci.* **2020**, *11*, 537220, doi:10.3389/FPLS.2020.00713/XML/NLM.

234. Allakhverdiev, S.I.; Sakamoto, A.; Nishiyama, Y.; Murata, N. Inactivation of Photosystems I and II in Response to Osmotic Stress in Synechococcus.

Contribution of Water Channels. *Plant Physiol.* **2000**, *122*, 1201–1208, doi:10.1104/PP.122.4.1201.

235. Callieri, C. Synechococcus Plasticity under Environmental Changes. *FEMS Microbiol. Lett.* **2017**, *364*, doi:10.1093/FEMSLE/FNX229.

236. Lourembam, J.; Haobam, B.; Singh, K.B.; Verma, S.; Rajan, J.P. The Molecular Insights of Cyanobacterial Bioremediations of Heavy Metals: The Current and the Future Challenges. *Front. Microbiol.* **2024**, *15*, 1450992, doi:10.3389/FMICB.2024.1450992/BIBTEX.

237. Khare, D.; Kumar, R.; Acharya, C. Genomic and Functional Insights into the Adaptation and Survival of Chryseobacterium Sp. Strain PMSZPI in Uranium Enriched Environment. *Ecotoxicol. Environ. Saf.* **2020**, *191*, 110217, doi:10.1016/J.ECOENV.2020.110217.

238. Pollmann, K.; Kutschke, S.; Matys, S.; Raff, J.; Hlawacek, G.; Lederer, F.L. Bio-Recycling of Metals: Recycling of Technical Products Using Biological Applications. *Biotechnol. Adv.* **2018**, *36*, 1048–1062, doi:10.1016/J.BIOTECHADV.2018.03.006.

239. Gavrilescu, M. Microbial Recovery of Critical Metals from Secondary Sources. *Bioresour. Technol.* **2022**, *344*, doi:10.1016/J.BIORTECH.2021.126208.

240. Li, H.; Dong, X.; da Silva, E.B.; de Oliveira, L.M.; Chen, Y.; Ma, L.Q. Mechanisms of Metal Sorption by Biochars: Biochar Characteristics and Modifications. *Chemosphere* **2017**, *178*, 466–478, doi:10.1016/J.CHEMOSPHERE.2017.03.072.

241. Kaksonen, A.H.; Sofía Urbieta, M.; Castro, L.; Pawlowska, A.; Sadowski, Z. The Role of Biomodification in Mineral Processing. *Miner. 2023, Vol. 13, Page 1246* **2023**, *13*, 1246, doi:10.3390/MIN13101246.

242. Paper, M.; Koch, M.; Jung, P.; Lakatos, M.; Nilges, T.; Brück, T.B. Rare Earths

Stick to Rare Cyanobacteria: Future Potential for Bioremediation and Recovery of Rare Earth Elements. *Front. Bioeng. Biotechnol.* **2023**, *11*, doi:10.3389/FBIOE.2023.1130939.

243. Paper, M.; Koch, M.; Jung, P.; Lakatos, M.; Nilges, T.; Brück, T.B. Rare Earths Stick to Rare Cyanobacteria: Future Potential for Bioremediation and Recovery of Rare Earth Elements. *Front. Bioeng. Biotechnol.* **2023**, *11*, doi:10.3389/FBIOE.2023.1130939/FULL.

244. Yushin, N.; Zinicovscaia, I.; Cepoi, L.; Chiriac, T.; Rudi, L.; Grozdov, D. Cyanobacteria Arthospira Platensis as an Effective Tool for Gadolinium Removal from Wastewater. *Clean Technol.* **2023**, *5*, 638–651, doi:10.3390/CLEANTECHNOL5020032/S1.

245. Bacteria Found to Collect Rare Earth Elements for Reuse Available online: https://www.innovationnewsnetwork.com/bacteria-found-collect-rare-earth-elements-reuse/30496/?utm_source=chatgpt.com (accessed on 18 March 2025).

246. Rastogi, R.P.; Sinha, R.P. Biotechnological and Industrial Significance of Cyanobacterial Secondary Metabolites. *Biotechnol. Adv.* **2009**, *27*, 521–539, doi:10.1016/J.BIOTECHADV.2009.04.009.

247. Ramírez Calderón, O.A.; Abdeldayem, O.M.; Pugazhendhi, A.; Rene, E.R. Current Updates and Perspectives of Biosorption Technology: An Alternative for the Removal of Heavy Metals from Wastewater. *Curr. Pollut. Reports* **2020**, *6*, 8–27, doi:10.1007/S40726-020-00135-7.

248. Volesky, B.; Holan, Z.R. Biosorption of Heavy Metals. *Biotechnol. Prog.* **1995**, *11*, 235–250, doi:10.1021/BP00033A001.

249. Kazak, E.S.; Kalitina, E.G.; Kharitonova, N.A.; Chelnokov, G.A.; Elovskii, E. V.; Bragin, I. V. Biosorption of Rare-Earth Elements and Yttrium by Heterotrophic

Bacteria in an Aqueous Environment. *Moscow Univ. Geol. Bull.* **2018**, *73*, 287–294, doi:10.3103/S0145875218030043/METRICS.

250. Pandhal, J.; Choon, W.L.; Kapoore, R. V.; Russo, D.A.; Hanotu, J.; Wilson, I.A.G.; Desai, P.; Bailey, M.; Zimmerman, W.J.; Ferguson, A.S. Harvesting Environmental Microalgal Blooms for Remediation and Resource Recovery: A Laboratory Scale Investigation with Economic and Microbial Community Impact Assessment. *Biol. 2018, Vol. 7, Page 4* **2017**, *7*, 4, doi:10.3390/BIOLOGY7010004.